Analyzing the Suppressive Properties of ZNF132 and ZNF154 in Head and Neck Squamous Carcinoma

by Patrick Murray Pearson

A thesis submitted to the School of Graduate

Studies in partial fulfillment of the requirements for the degree of

Master of Science in Medicine (Cancer and Development)

Faculty of Medicine

Memorial University of Newfoundland

May 2025

St. John's Newfoundland and Labrador

Abstract

Head and neck squamous cell carcinoma (HNSCC) is a disease of the head and neck derived from the mucosal epithelium. ZNF154 has been previously shown to have tumour suppressive properties in nasopharynx cancer cell lines. Investigation of the TCGA dataset reveals that patients with low expression of ZNF132 and ZNF154 have statistically significant worse overall survival rate when compared to patients with high expression of each gene. ZNF132 and ZNF154 has been shown to be hypermethylated as well as have reduced gene expression in HNSCC. Overexpression of ZNF154 in the oral cavity cancer cell line UM-SCC1 appears to cause the production of a truncated ZNF154 protein. Additionally, this causes the production of a shortened ZNF154 transcript. Overexpression of ZNF154 in the immortalized kidney cell line HEK293 causes a significant downregulation of both p53 and FOX01. Gene sequencing of ZNF154 overexpressing UM-SCC1 shows a segment of the ZNF154 gene is missing in the coding region of ZNF154. siRNA knockdown of KAP1 in keratinocyte cells causes a significant increase in ZNF154 expression. These results appear to indicate a relationship between KAP1 and ZNF154. We expect that KAP1 is having a regulatory effect on ZNF154 in UM-SCC1 cells, binding downstream in the coding region of ZNF154 causing the production of a shortened transcript. The silencing of ZNF154 likely involves two mechanisms, DNA methylation as well as the KAP1-ZNF complex binding in the coding region of ZNF154**.**

General Summary

Head and neck squamous cell carcinoma are a cancer of the head and neck that are defined by their aggressive nature and molecular heterogeneity. There has been a lack of progress on reliable treatments and biomarkers for the diagnosis of these diseases. Investigation of The Cancer Genome Atlas has revealed two target genes that affect HNSCC survival rate. Low expression of ZNF132 and ZNF154 has been shown to be associated with a reduced survival rate in patients, compared to those who have high expression of each gene. When ZNF154 is overexpressed in the cancer cell line UM-SCC1, it causes the production of a truncated ZNF154 protein. When ZNF154 overexpressing UM-SCC1 samples were sequenced, there was a coding section of the ZNF154 gene missing. KAP1 knockdown in keratinocyte cells affected the expression of ZNF154. We believe that KAP1 is regulating ZNF154 via its coding region, causing a shortened gene to be produced.

Co-Authorship Statement

As the primary author of this thesis, I was responsible for the majority of experiments conducted, analyses completed, and preparing an initial draft. I would like to acknowledge and thank my supervisor, Dr. Tom Belbin, my supervisory committee, Dr. Touati Benoukraf and Michael Leitges, and Dr. Simon Kirby for their invaluable feedback and constructive criticism.

Figures from Chapter 1 were published in Head and Neck Oncology, Cancers, Translational Oncology, Mobile DNA, and PLoS Genetics.

Additionally, a prior researcher, Nilita Sood, conducted preliminary research on the survival analysis of ZNF132 and ZNF154 as seen in Chapter 2.

Kendra Smith and Elizabeth Chia assisted with cell culture and sample collection, genomic sequencing, Western blot, and genomic PCR imagining in Chapter 3 where credited. Elizabeth Chia completed the Western blot as seen in **Figure 3.4A**. Kendra Smith completed the genomic PCR and genomic sequencing as seen in **Figure 3.4B, Figure 3.5, and Figure 3.6B**. I performed all other experiments myself.

Appendix A is a published paper for which I am a primary co-author, using data I completed over the course of my Master's degree. The paper is published in the Journal of Otolaryngology – Head and Neck Surgery, expanding upon some of the topics covered in my thesis and exploring others. Many people contributed to the publication of the paper including, Patrick Pearson[1†], Kendra Smith[1,2†], Nilita Sood[2], Elizabeth Chia[1,2], Alicia Follett[1], Michael B.

Prystowsky[4], Simon Kirby[3] and Thomas J. Belbin[1,2,4*]. † denotes equal contribution and * denotes correspondence.

Acknowledgements

First, I Would like to thank Dr. Tom Belbin for all the indispensable help he has provided throughout my Master's. He has been an excellent mentor, providing new knowledge and techniques for how to best approach academic research. I would also like to thank all my lab members, especially Kendra Smith and Elizabeth Chia for teaching new techniques and answering any questions I have had throughout my degree. Additionally, I would like to thank all of members of the Cancer and Development program for their advice throughout my seminar sessions. I would like to thank J. D. Irving and the School of Graduate Studies at MUN for their gracious contribution of funding, which was extremely helpful over the course of my Master's. I could not have completed my degree without the continuous support of my family who have been there for me at every stage, their encouragement has been tremendous. Finally, I would like to thank my supervisory committee, Dr. Touati Benoukraf and Dr. Michael Leitges, and Dr. Simon Kirby, for their suggestions and advice, which were very helpful in advancing my research.

Table of Contents

List of Figures:

List of Tables:

List of Abbreviations

Computerized tomography – CT

Deoxyribonucleic acid - DNA

Epithelial mesenchymal transition - EMT

Eppstein-Barr Virus - EBV

Human Embryonic Kidney - HEK

Head and neck squamous cell carcinoma - HNSCC

Human papillomavirus – HPV

Krüppel associated box - KRAB

Magnetic resonance imaging - MRI

National Cancer Institute - NCI

National Human Genome Research Institute - NHGRI

Nasopharyngeal carcinoma - NPC

Oropharyngeal squamous cell carcinoma – OSCC

Polymerase chain reaction – PCR

Quantitative polymerase chain reaction- qPCR

P-Lenti-50 – PL50

P-Lenti-100 – PL100

Reads per kilobase per million mapped reads – RPKM

Ribonucleic acid – RNA

Small interfering RNA - siRNA

The Cancer Genome Atlas - TCGA

Zinc finger protein – ZNF

CHAPTER 1: INTRODUCTION

Co-Authorship Statement

As the primary author of this thesis, I was responsible for drafting this chapter. I would like to acknowledge and thank my supervisor, Dr. Tom Belbin, my supervisory committee, Dr. Touati Benoukraf and Michael Leitges, and Dr. Simon Kirby for their invaluable feedback and constructive criticism. They aided in revising the introduction, which served to strengthen my thesis.

Figures from Chapter 1 were published in Head and Neck Oncology, Cancers, Translational Oncology, Mobile DNA, and PLoS Genetics.

Section 1.1: Head and Neck Cancer

Head and neck squamous cell carcinomas (HNSCCs) are a group of cancers that present in the oral cavity, pharynx, and larynx (Alsahafi *et al*., 2019; Johnson *et al*., 2020; **Figure 1.1**). It is an extremely aggressive group of cancers that are characterized by their molecular and genetic heterogeneity. The various subtypes of HNSCCs are molecularly distinct; however, they often receive similar therapies, despite their uniqueness. Survival rates have improved only modestly for HNSCC patients, primarily due to a lack of reliable biomarkers (Alsahafi *et al*., 2019; Johnson *et al*., 2020). Five-year survival rates improved from 55% in the period of 1992-1996, to 66% in 2002-2006 (Johnson *et al*., 2020). Over 830,000 people are diagnosed with HNSCCs worldwide each year, with over 430,000 people dying annually (Cramer, Burtness, & Ferris, 2019; Canadian Cancer Society, 2020). In Canada, it is estimated that there were approximately 6550 cases of HNSCCs, with over 1900 deaths occurring, in 2020.

Chapter one of this thesis will provide an overview on HNSCCs, cancer prognosis, and treatment. Chapter two will examine the Cancer Genome Atlas for the effects of ZNF132 and ZNF154 (zinc finger protein) expression on HNSCC. Chapter three will analyze how overexpressing these genes *in vitro* affects various cell lines. Chapter four will explore the effects of KAP1 knockdown on ZNF132 and ZNF154 in human epithelial keratinocytes. Finally, chapter five will provide a conclusion summarizing the findings of the research.

HNSCCs can be classified into two subtypes, those that are caused by human papillomavirus (HPV) infection and those that are not (Cramer, Burtness, & Ferris, 2019; "Cancer-specific stats 2020"). The majority of HNSCC cases, 75%, are associated with tobacco and alcohol use. A minority, 25%, are associated with HPV infection (Cramer, Burtness, & Ferris, 2019; "Cancer-specific stats 2020"). Current trends indicate that an increasing proportion

of HNSCCs are HPV-driven, due to a decreasing amount of tobacco use and tobacco related cancer in these populations. There are differences between cases that are HPV-driven and non-HPV-driven. For example, men, particularly young men, constitute the majority of diagnoses of oropharyngeal squamous cell carcinoma (OSCC), a subtype of HNSCC (Cramer, Burtness, & Ferris, 2019; "Cancer-specific stats 2020"). The time period between initial HPV infection and the appearance of HPV-driven OPSCC is estimated to range from 10-30 years. Additionally, geographic location is heavily implicated in the prevalence of HPV-driven OPSCC, constituting 70% of oropharyngeal cancers in the USA, whereas low and middle-income countries only account for 10%. Females were identified as having poorer overall survival rates when compared to males with HNSCCs (Mundi *et al*., 2020). This can be attributed to a higher incidence of HPV-driven HNSCCs in men. When controlling for HPV status in a univariate analysis of a TCGA HNSCC cohort detailing overall survival rates for a 5 year period, there was no sex difference (Mundi *et al*., 2020). The high rate of genetic mutations in HNSCCs can cause loss-of-function mutations, activating oncogenes. This has caused the development of effective targeted treatments to develop quite slowly.

The primary options for treating HNSCCs involve radiotherapy, chemotherapy, and surgery (Goel *et al*., 2022). However, all of these options have had mixed success rates and reduce the quality of life of the patient. Many factors can affect the success rate of treatments. For example, the effectiveness of radiation treatment is severely restricted by tumour hypoxia, which signifies an aggressive phenotype (Graham and Unger, 2018). Cancers with biomarkers indicative of tumour hypoxia, hypoxia inducible factors, have shown higher rates of metastasis and disease recurrence (Fares *et al*., 2020). There have been many attempts in recent years to develop new treatments with greater efficacies that are not as impactful on patients' wellbeing

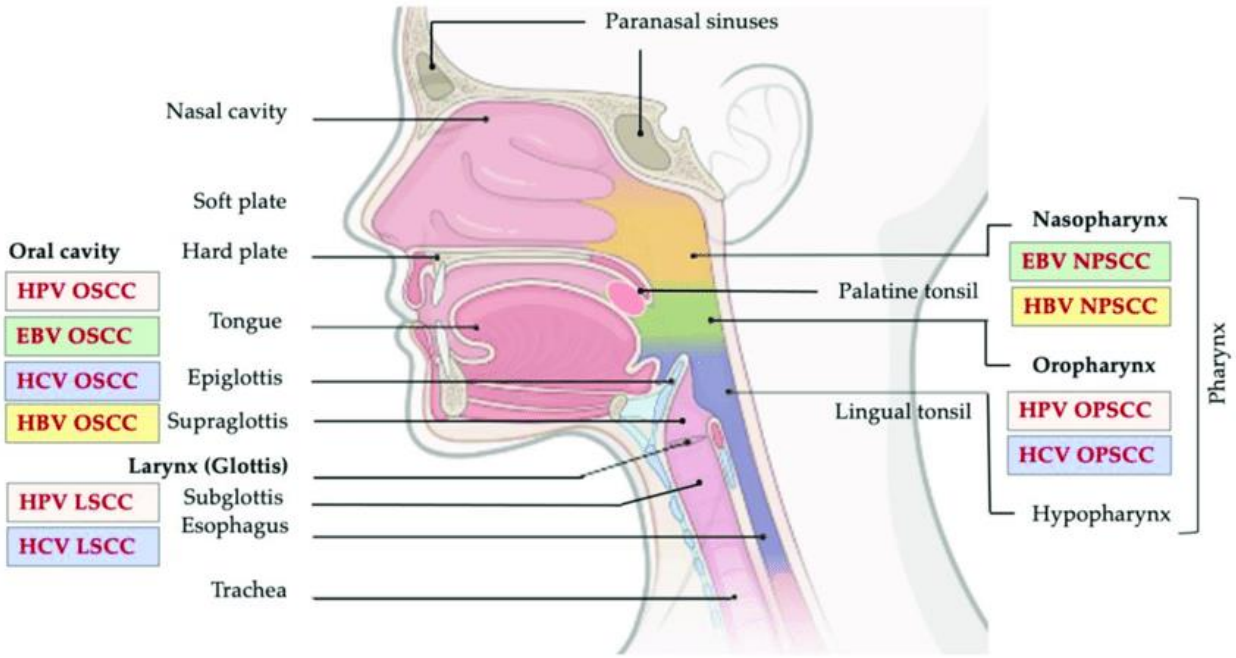

Figure 1.1: Anatomic tumour subsites in HNSCC (Mahmutović *et al*, 2021). Creative commons license.

Common subsites for HNSCC onset and progression include the nasopharynx, oropharynx, larynx, and oral cavity. The occurrence rate of HNSCC at each site varies by region.

(Muzaffar *et al*. 2021). These efforts have had mixed success, demonstrating the continued need for research and development into new and effective treatments, as well as the elucidation of clinical biomarkers.

Section 1.2: Incidence and Risk Factors

HNSCC is one of the most prevalent forms of cancer worldwide, being the sixth most common. Rates of HNSCC are expected to rise significantly in the near future, with an estimated 30% increase in cases by 2030 (Johnson *et al*., 2020). Different regions across the world have varying rates of HNSCCs with unique causes. For example, in areas such as Southeast Asia and Australia, the high frequency of cases of Epstein-Barr Virus (EBV) related nasopharyngeal cancer is related to the significant usage of products containing carcinogens, such as chewing tobacco (Johnson *et al*., 2020). In comparison, oropharyngeal infection and HPV have contributed to increasing cases of HNSCC in the USA and Western Europe.

There are numerous factors that can cause an increased risk for HNSCC. Some of the primary risk factors include alcohol and tobacco consumption, environmental pollutants, and viral infections (Descamps *et al*., 2016; Johnson *et al*., 2020); many of these affect protein p53 (**Figure 1.2**). Notably, significant consumption of both tobacco and alcohol can lead to higher than a 35-fold increased risk of HNSCC. Factors affecting HNSCC, such as these, are greatly influenced by culture and geographical location (Johnson *et al*., 2020; Su *et al*., 2016). For example, oral cavity cancer is of specifically high prevalence among Asia-Pacific populations. This is due to a high rate of chewing areca nut derivatives that contain betel quid (Johnson *et al*., 2020; Su *et al*., 2016). Betel quid is used to describe the combination of areca nut, betel leaf, slaked lime/tobacco, and any spices that may be included. The usage of these mixtures has been

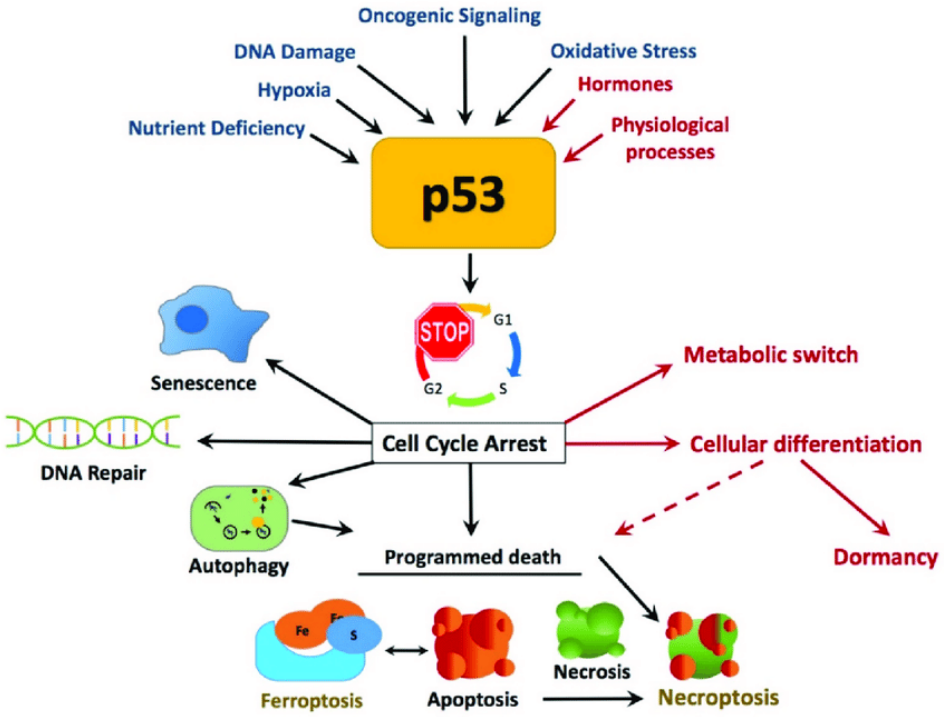

Figure 1.2: Role of p53 in cancer onset (Moulder *et al.*, 2018). Creative commons license.

p53 has a role as a tumour suppressor, which is caused by a variety of stress signals including hypoxic conditions, activations of oncogenes, and DNA damage among others. p53 functions include DNA repair, autophagy, and senescence. Non canonical cell cycle arrest include ferroptosis, necrosis, and necroptosis. Normal bodily processes can lead to p53-induced cell cycle arrest in which it acts as a switch for metabolic processes.

associated with a high prevalence of oral cavity cancer within the Asia-Pacific region, particularly India, Taiwan, and some regions of China. Air pollutants common in the aforementioned regions also contribute to an increased risk of HNSCC.

HPV infection has also contributed to an increased risk of developing HNSCC, especially of the oropharynx and nasopharynx regions (Elrefaey *et al*., 2014). The HPV subtypes responsible for these increased risks are the oncogenic types HPV 16 and 18. Despite similar rates of anogenital HPV infection between men and women, the rate of oropharyngeal HPV infection is much higher in men (Elrefaey *et al*., 2014). This causes the male to female ratio of HPV-positive HNSCC to be as high as three to six times greater. HPV-positive HNSCC are especially prevalent in populations that are unvaccinated for HPV (Elrefaey *et al*., 2014). The rates of HPV induced HNSCC have been increasing in recent years. HPV subtypes, such as HPV 16 and 18, are high risk due to the immortalizing properties of HPV oncoproteins E6 and E7. These target the p53 and pRB tumour suppressor pathways, leading to them having an increased likelihood of mutation and cancer formation.

Genetic risk factors can also contribute to the risk of developing HNSCC (Errazquin *et al*., 2021). Certain inherited genetic conditions or disease can greatly increase the risk of developing HNSCC. For example, Fanconi anaemia is a rare disease in which mutations to the *FANC* genes lead to improper DNA repair (Errazquin *et al*., 2021). It is thought that pathway gene mutations in the FA/BRCA pathway are behind some complications of Fanconi anemia. Cases of HNSCC with this disease have significantly high mortality rates. Polymorphisms in *CTLA4, Il10,* cytochrome P450 1A1, and glutathione *S*-transferase μ1 have all been associated with an increased risk of HNSCC (Johnson *et al*., 2020; Niu *et al*., 2015). Somatic Variants to DNA repair genes, such as *TP53, CDKN2A,* and *PIK3CA* have been associated with the early

onset of HNSCC (Curry *et al*., 2021). Mutations in genes that influence the breakdown of carcinogens and that are involved with immunity can contribute to the risk of developing HNSCC (Johnson *et al*., 2020). These include polymorphisms to cytotoxic T lymphocyte antigen 4, cytochrome P450 1A1, *IL10*, and glutathione S-transferase μ1. The decrease in effective metabolism of carcinogens can weaken immunity and contribute to the onset of HNSCCs (Johnson *et al*., 2020).

Section 1.3: Cancer Staging

Cancer is an incredibly complex group of diseases that requires multiple methodologies to properly diagnose and stage (Journal of Cancer Diagnosis, n.d.; Oral and Oropharyngeal Cancer - Stages and Grades, 2021). Initial suspicion of cancer onset may be due to an abnormal mole, lump, or generalized pain or soreness. Preliminary assessment is usually conducted by physical examination in an attempt to identify the presence of a lump or tumour. Following this, imaging and laboratory tests are common involving techniques such as computerized tomography (CT) scanning, magnetic resonance imaging (MRI), and biopsy examinations by a pathologist.

Diagnosis of cancer occurs through multiple stages, the two primaries being clinical and pathological diagnoses (Journal of Cancer Diagnosis, n.d.; Oral and Oropharyngeal Cancer - Stages and Grades, 2021). A clinical diagnosis involves a physical examination of the tumour and imaging. TNM staging is used to quantify the burden of disease and prognosticate. T represents the size of a tumour, N represents if the cancer has spread to any lymph nodes, and M represents if the cancer has undergone distant metastasis (Oral and Oropharyngeal Cancer - Stages and Grades, 2021). Advancements in imaging technologies have improved the accuracy

of TNM staging, even having the ability to detect metastases in lymph nodes. However, errors in staging can still occur. Pathologic staging requiring surgical resection is a much more accurate methodology that involves a detailed histopathological analysis of tissue. The TNM system is the standardized method for reporting cancer staging (Oral and Oropharyngeal Cancer - Stages and Grades, 2021; UICC, 2021; **Figure 1.3**).

Section 1.4: Treatment

Treating HNSCC patients can present a multitude of problems for doctors due to the variability and diversity of the disease (Johnson *et al*., 2020). Advanced or metastatic cancer can present issues for developing an appropriate treatment plan. HNSCCs can derive themselves from distinct anatomical sites, including the oral cavity, larynx, oropharynx, and hypopharynx. The disease is heterogenous in its genetic composition, leading to complex treatment parameters (Johnson *et al*., 2020). The anatomical location for HNSCC dictates the cell of origin. In these cases, stem or progenitor cells can transform into cancer stem cells. Approximately 40% of HNSCC patients can be categorized as limited or early-stage disease, upon presentation (Lee *et al*., 2020). These patients typically require only a single modality of treatment. However, patients who present with locally advanced HNSCCs often require multidisciplinary treatments.

Many modalities of treatments exist for use against HNSCCs (**Figure 1.4**). Some of these include anticancer drug therapies, cetuximab, and immune checkpoint inhibitors (Kitamura *et al*., 2021). Treatment approaches are dictated by disease site and stage of the disease. Typically, surgery is a first line treatment approach for oral cavity cancer. Conversely, organ preservation approaches, such as surgery and radiation are considered common treatments for laryngeal and oropharyngeal tumours. Anticancer drug therapies involve combining cisplatin and radiation are

	x	1	2	3	4	4a (lip)	4a (oral cavity)	4b
T	The primary tumour cannot be detected.	The tumour measures 2 cm or less in diameter and has a depth of between 5-10 mm. Additionally, the tumour may be between 2-4 cm in diameter and have a depth of less than 10 mm.	The tumour has a diameter of more than 4 cm or a depth greater than 10 mm.	The tumour has a diameter of more than 4 cm or a depth greater than 10 mm.	This stage represents moderate to very advanced local disease.	The tumour originates on the lip, but then spreads to bone or the inferior alveolar nerve if the mouth, the mouth floor, or skin on the face.	The tumour has spread to nearby mouth structures, such as the jaw, sinuses, or skin on the face.	The tumour has spread to the muscles and bones that constitute the mouth or skull base. It may also surround the internal arteries.

	x	0	1	2a	2b	2c
N	The lymph nodes are unable to be evaluated.	Cancer in the regional lymph nodes cannot be detected.	Cancer has spread to only 1 lymph node with the same laterality as the tumour and measures 3 cm or less in diameter. There is no ENE.	Cancer has spread to 1 lymph node and measures 3 cm or less in diameter. There is ENE. Alternatively, the cancer has spread to 1 lymph node with the same laterality as the tumour and measures between 3-6 cm in diameter. There is no ENE.	Cancer has spread to 1 lymph node with the same laterality as the tumour and measures greater than 6 cm in diameter. There is no ENE.	Cancer has spread to 1 lymph node on either side of the body and measures less than 6 cm in diameter. There is no ENE.

	3a	3b
N	Cancer has spread to 1 lymph node on either side of the body and measures greater than 6 cm in diameter. There is no ENE.	There is ENE in 1 lymph node with the same laterality as the primary tumour and measures greater than 3 cm in diameter. Alternatively, cancer has spread to multiple lymph nodes, with at least 1 having ENE; or cancer has spread to 1 lymph node on the side of opposing laterality from the tumor, measures 3 cm or less in diameter, and has ENE.

	0	1
M	Cancer has not spread to other regions of the body.	Cancer has spread to other regions of the body.

	0	I	II	III	IVA	IVB	IVC
Pathologic Stage	Tis, N0, M0	T1, N0, M0	T2, N0, M0	T3, N0, M0 OR T1, T2, T3, N1, M0	T4A, N0 or N1, M0 OR T1, T2, T3 or T4A, M2, N0	Any T, N3, M0 OR T4B, Any N, M0	Any T, Any M, N1

Figure 1.3: Summary of TNM staging and pathologic stage (Oral and Oropharyngeal Cancer - Stages and Grades, 2021; UICC, 2021).

Figure 1.3 summarizes the various levels of TNM staging for oral cabity cancer. Once a patient's TNM staging has been completed, the various stages can be combined to determine a patient's overall pathologic stage (Oral Cavity and Oropharyngeal Cancer Stages, n.d.).

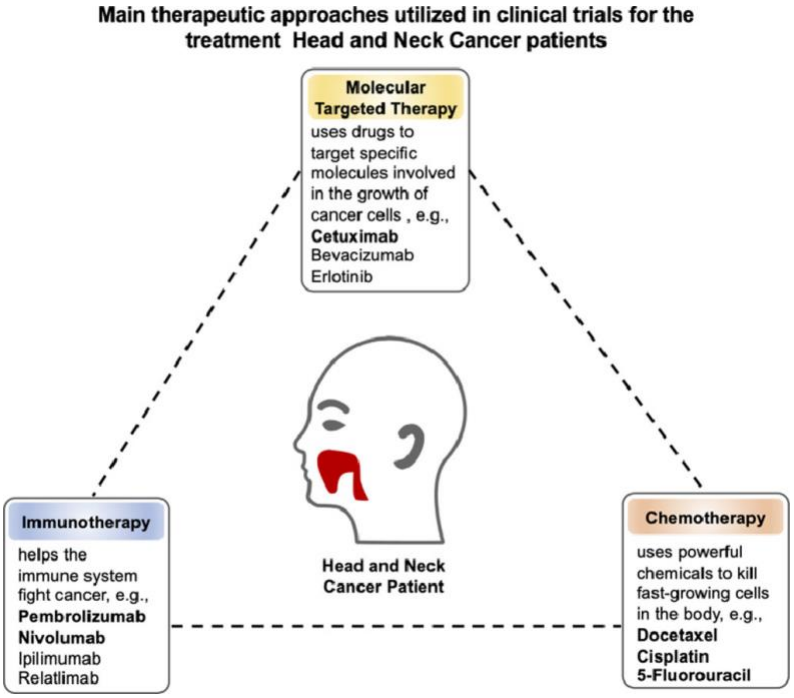

Figure 1.4: Various treatment strategies used for HNSCC patients (Goel *et al.*, 2022). Creative Commons license.

Abstract image representing the main therapeutic approaches that are used in clinical trials to treat HNSCC patients. These approaches can be used on their own or in combination with one another.

one example treatment for locally advanced HNSCC (Plavc & Strojan, 2020). Since 2000, platinum based anticancer drugs are an extremely common choice in therapy, including cisplatin and carboplatin (Baur *et al*., 2002; Caponigro *et al*., 2001; Glisson *et al*., 2002). Additionally, taxane based anticancer drugs such as docetaxel and paclitaxel have begun to be used with success since 2010.

Cetuximab is a chimeric human and mouse monoclonal antibody that targets epidermal growth factor receptors (Kitamura *et al*., 2021). Clinical studies have found that when combined with radiation and chemotherapy, cetuximab has improved locoregional control and reduced mortality (Bonner *et al*., 2006). Cetuximab has been shown to significantly improve survival outcomes, as well as improve local disease control periods. HNSCC is a disease in which the immune system becomes suppressed, noted by a decrease in the number of lymphocytes, a lack of function in natural killer and T cells, and poor antigen presenting function (Ferris, 2015). Immune checkpoint inhibitors function by preventing tumour cells from binding with checkpoint proteins on immune cells, which inhibits an immune response (*NCI dictionary of Cancer TERMS*, n.d.). Immune checkpoint inhibitors allow immune cells to function properly in the presence of tumor cells and destroy them. Immune checkpoint inhibitors displayed higher overall response rate and overall survival than historical controls for second line or beyond in treating recurrent and metastatic HNSCCs (Pestana *et al*., 2020).

HNSCCs are usually treated by first surgically resecting the cancerous tissue, followed by secondary treatments, such as radiation and/or chemotherapy (Head and neck cancer - types of treatment, 2021). Anticancer drug therapies may be used when appropriate. The primary goal of treatment is to remove the tumour, however another extremely important factor is preserving the function of associated tissues and organs. The timeline by which HNSCCs are first identified

can greatly influence the success of treatment and limit any potential negative effects (Head and neck cancer - types of treatment, 2021). Depending on the genotypic and phenotypic characteristics of a tumour, epidermal growth factor inhibitors, such as cetuximab, and immune checkpoint inhibitors, such as nivolumab and pembrolizumab, may also be useful for treatment (Kitamura *et al*., 2021). The frequency of such drugs is increasing in both usage and importance in recent years. The type of treatments used in HNSCC therapy is highly individualized according to the patient receiving treatment (Cohen *et al*., 2019). The progression of disease upon primary diagnosis also has a large impact on both the type and number of treatments that are used. Disease progression at diagnosis can determine whether a singular or multidisciplinary treatment type is required.

A major factor of HNSCC treatments are the potentially devastating side effects treatments can have on a patient's quality of life (Oosting & Haddad, 2019). Some of the potential side effects include partial or complete loss of speech, and difficulty breathing, chewing, and swallowing. New biological agents, such as cetuximab, can have systemic adverse effects. This can include the development of gastrointestinal issues (Eisa & Omer, 2022). Additionally, checkpoint inhibitors can cause symptoms similar to Rheumatoid arthritis (Ghosh *et al.,* 2021). The tumour site may also cause issues with daily activities such as eating, further complicating treatment plans due to potential excessive weight loss. Notably, weight loss that is greater than 5% is an independent factor for worse progression free survival (Oosting & Haddad, 2019). Additionally, some patients with HNSCCs can have obstructed airways requiring a of individuals and can influence the types of treatments pursued (Johnson *et al*., 2020).

Section 1.5: Prognosis

The rate of occurrence of HNSCCs is increasing, and by the year 2030, there is a projected annual new case rate of 1.08 million (Johnson *et al*., 2020). That represents a 30% increase based upon the prior mentioned cases. In a study published by Chang *et al*. (2017), they found that the locoregional rate and incidence rate of HNSCC was 14.44% and 40.73% respectively. The rates of recurrence after disease free intervals of at least one and two years were 60% and 85%, respectively. The age at which recurrence occurred in the study population was less than 65 years for more than 85% of the population (Chang *et al*., 2017). Discovering recurrent disease within a shorter period dramatically increases patient survival. Recurrent early stage HNSCC had a 5-year survival rate of 54.95%. Aggressive treatments have been found to significantly increase the rate of survival in those with recurrent disease.

The HPV status of OPSCC patients has been found to significantly affect the rate of locoregional recurrence (Asheer *et al*., 2020). HPV positive OPSCC positive patients had a 9% recurrence rate, whereas 26% of OPSCC negative patients had locoregional recurrence. The difference in recurrence rate between HPV positive and negative OPSCC patients is possibly due to the biological uniqueness of the disease. The increased survivability related to HPV positive OPSCC cancers may be a result of the sensitivity of viral cancers to radiation and/or chemotherapy (Asheer *et al*., 2020).

Distant metastasis is not common in HNSCCs, but nonetheless is significant due to its severity when it does occur (Van der Kamp *et al*., 2020). Distant metastasis from HNSCCs can severely worsen survival outcomes. A study published in 2020 by Kamp *et al*. displayed that distant metastasis occurred in 9.3% of HNSCC patients. Of this subset, 1.9% were diagnosed simultaneously with a primary tumour, 1.9% were diagnosed synchronously, and 5.4 % were

diagnosed metachronously. The three most common sites of distant metastasis were the lungs, bone and liver, respectively. Notably, age was not found to play a factor in the likelihood of developing a distant metastasis. The state of the lymph node is one of the most important factors when determining HNSCC prognosis (Pisani *et al*., 2020). A single positive lymph node can dramatically decrease survival odds by as much as 50%, as lymphatics facilitate metastasis. Multiple factors can contribute to the risk of lymph node metastasis, including the size and depth of the tumour. Additionally, locoregional recurrence of a tumour increases the risk of lymphatic spread.

HNSCCs are a genetically heterogeneous disease, and a multitude of factors contribute to their onset and development (Cadoni *et al*., 2017). Some of the various subtypes of HNSCCs include cancers of the larynx, hypopharynx, oral cavity, and oropharynx. A dataset from Cadoni *et al*. (2017) shows that when stratified by HNSCC site, median survival time for laryngeal cancer was higher than for the other sites. Smoking and drinking chronically were both associated with an increased risk of developing second primary cancer. The factors that were most important in determining an individuals' overall chance of survival are age of onset and tumour stage.

Section 1.6: Zinc-finger Proteins

Zinc-finger proteins (ZNF) are one of the most numerous subtypes of proteins in cells that have varying functions (Cassandri *et al*., 2017). Among these functions include the ability to interact with other proteins, DNA, and RNA. ZNFs take part in a range of activities, many of which have to do with the cell cycle (Cassandri *et al*., 2017). This includes events such as DNA repair and apoptosis. ZNFs are part of a class of proteins known as transcription factors, and are

suspected to have a role in cancer progression and metastasis (**Figure 1.5**). ZNFs have a significant function in gene regulation, exhibited through the structural motifs by which they bind to DNA, including C2H2 and Gag knuckle (Li *et al*., 2022). One of the main features of some ZNFs is the KRAB domain. These have been shown to have a significant role in transcriptional regulation and silencing. KAP1 has been shown to interact with KRAB ZNFs, including repressing both endogenous retroviruses and ZNFs (Tie *et al*., 2018). KAP1 interacts with the NURD/HDAC repressor complex and histone methyltransferases after being recruited by the KRAB domain (Wolf *et al*., 2015). This causes the removal of H3K9ac and the addition of H3K9me3. DNA methyltransferases cause inheritable silencing via methylation of genomic CpG sites. ZNFs have functions in lipid metabolism, cell differentiation, and immune response (Li *et al*., 2022). ZNFs have been shown to have a role in a variety of cancers such as HNSCC, lung, gastric, colorectal, and more through apoptosis, metastasis, and EMT. ZNFs can play both oncogenic and tumour suppressive roles.

In a genome wide study of differential DNA methylation at different sites in HNSCC, 44 CpG sites showed significantly different DNA methylation in primary tumours compared to matched adjacent normal tissue (Lleras, Belbin, *et al*., 2013). Of these differentially methylated CpG sites there was only a small number that had been previously studied in relation to HNSCC. Of these genes, the most overrepresented were ZNF genes, specifically ZNF132 and ZNF154. Both of these genes' displayed heightened DNA hypermethylation, as well as reduced gene expression in HNSCC tumours, when compared to non-cancerous adjacent tissue (Lleras, Belbin, *et al*., 2013).

Hypermethylation of the ZNF154 CpG island promoter region has been found in 15 different solid epithelial tumour types originating from 13 different organs

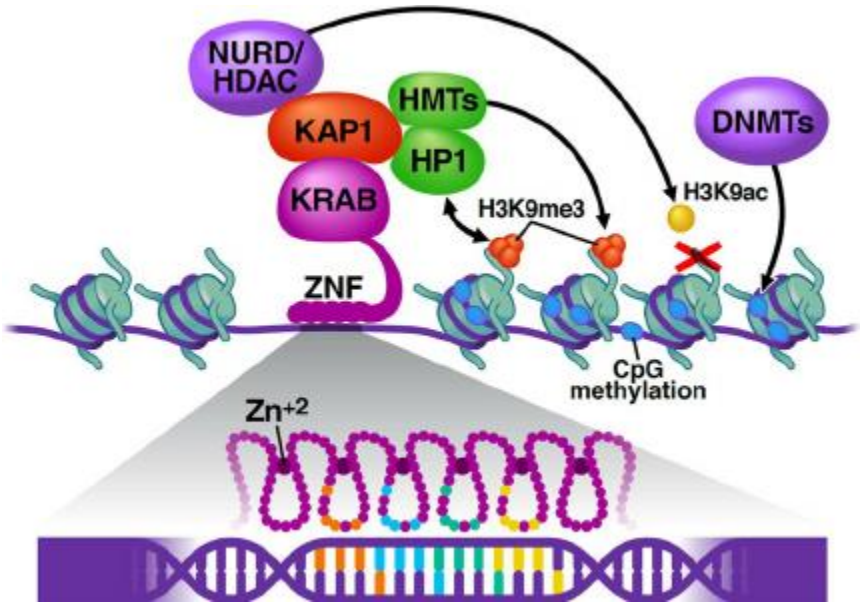

Figure 1.5: KRAB-ZNF complex binding to DNA and introducing inheritable silencing (Wolf *et al.*, 2015). Creative Commons license.

Protein and DNA interactions are primarily medicated by four amino acids. KAP1 interacts with the NURD/HDAC repressor complex and histone methyltransferases after being recruited by the KRAB domain. This causes the removal of H3K9ac and the addition of H3K9me3. DNA methyltransferases cause inheritable silencing via methylation of genomic CpG sites.

(Margolin *et al*., 2016). Differential methylation of this CpG across various tumour subtypes reveals that this CpG island is frequently hypermethylated, when compared to normal tissue. Hypermethylation of the ZNF154 CpG island has shown promise as a solid tumour biomarker, as well as a universal pan-cancer biomarker from the DNA of circulating tumours. Additionally, ZNF154 hypermethylation may have use as an early detection biomarker, as seen from the voided urine of cancer patients (Margolin *et al*., 2016).

A cohort of seventy-four patients with advanced stage nasopharyngeal carcinoma (NPC) were followed up for greater than five years (Hu *et al*., 2017). Individuals with ZNF154 hypermethylation have been found to have significantly poorer disease free and distant metastasis free survival rates when compared to hypomethylation groups in nasopharyngeal cancer patients. Those who had the highest levels of ZNF154 hypermethylation had the shortest survival time (Hu *et al*., 2017). Additionally, when investigating a TCGA cohort of approximately 500 HNSCC patients, we observed that a small subset of patients presents with higher levels of ZNF132 and ZNF154. These individuals who have higher expression of both genes have significantly higher survival rates, when compared to people with low levels of those same genes.

Section 1.7: **Hypothesis**

Through these experiments we expect ZNF132 and ZNF154 to exhibit tumour suppressive properties. Specifically, we hypothesize that these ZNF proteins inhibit the epithelial to mesenchymal transition (EMT) by downregulating mesenchymal markers and upregulating epithelial markers. These ZNFs likely inhibit the transition from an epithelial to a more mesenchymal phenotype, as well as interfere with the motility of these mesenchymal-like cells.

KAP1 is suspected of interfering with ZNF132 and ZNF154 expression in HNSCC cell lines, so knocking down KAP1 is expected to increase these ZNF's expression.

CHAPTER 2: EXPRESSION OF ZNF132 AND ZNF154 IN PATIENT TUMOUR TISSUE AND ADJACENT NON-TUMOUR TISSUE FROM THE CANCER GENOME ATLAS (TCGA)

Co-Authorship Statement

As the primary author of this thesis, I was responsible for drafting this chapter and conducting all analyses. I would like to acknowledge and thank my supervisor, Dr. Tom Belbin and my supervisory committee, Dr. Touati Benoukraf and Michael Leitges. They aided in revising this chapter, which served to strengthen my thesis. Dr. Belbin provided **Table 2.5** and **Table 2.6** to provide background data on the dataset.

Additionally, a prior researcher, Nilita Sood, conducted preliminary research on the survival analysis of ZNF132 and ZNF154.

INTRODUCTION

Section 2.1: Overview of The Cancer Genome Atlas (TCGA) Database

The TCGA database was undertaken as a joint project between National Cancer Institute (NCI) and the National Human Genome Research Institute (NHGRI) in 2006 (The cancer genome atlas, n.d.). To date, the TCGA project has characterized greater than 20,000 primary and matched cancer samples from more than 33 different cancer types. In the years since the project's inception, the TCGA project has produced more than 2.5 petabytes of genomic data comprising genomic, epigenetic, transcriptomic, and even proteomic data. The huge amount of biological data from these patient cohorts has allowed for the examination of associations between ancestry, mRNA and miRNA expression, genomic DNA methylation, and genomic mutations across various cancer types (Carrot-Zhang *et al*., 2020). These analyses are extremely powerful as they allow for the detection of ancestry related molecular features among cancers, as well as identification of molecular targets of interest across a wide population.

In the case of HNSCC patients, the TCGA project has collected data on 528 cases of HNSCC; 279 of these cases were characterized in the initial paper to Nature in 2015 (Perdomo *et al*., 2018; Krishnan *et al*., 2015, Lawrence, Nature 2015 PMID: 25631445). The TCGA-HNSCC dataset contains data on various clinical and molecular variables, including age, sex, alcohol consumption, history of tobacco consumption, HPV status, nodal status, gene methylation status, and differentially expressed genes, among others. The status of HPV infection was characterized from a 2015 TCGA network group classification. HPV status was taken from over 1000 mapped RNA sequencing reads (Sayáns *et al*., 2019). Data collected from these patients have been repeatedly verified, ensuring accuracy.

Section 2.2: Hypothesis

The TCGA-HNSCC RNAseq dataset was used in our investigation of the levels of ZNF132 and ZNF154 expression and DNA methylation in primary tumour and non-tumour tissue samples. Secondly, we utilized the expression data to stratify patients based on ZNF132 and ZNF154 expression in order to test our hypothesis. We hypothesize that low expression of ZNF132 and ZNF154 may be associated with poor patient outcome, specifically overall survival. If true, these ZNFs might represent novel molecular markers for prognosis in this disease.

METHODS

Section 2.3: Analysis of gene expression and DNA methylation from the Cancer Genome Atlas (TCGA) dataset

Data from 530 HNSCC patients were downloaded from the TCGA database. This data was up to date as of December 2020. The dataset included both clinical and molecular data, including gene expression, clinical features, overall survival data, as well as genetic and epigenetic profiles. Overall survival time in this cohort was characterized as the period of time between surgery and date of death or last followup, and the time of surgery. In furtherance of the TCGA dataset, data including DNA methylation and gene expression was analyzed from tissue samples taken from 50 primary HNSCC patients. Data of the samples from the 50 HNSCC patients was also downloaded from the TCGA database. These samples included matched tumour tissue as well as adjacent non-tumour tissue. HNSCC tumours were divided amongst three categories. The oropharynx, larynx, and the oral cavity.

Analysis of data and figure development was completed using OncoLnc, R, and RStudio (version 4.2.1). Data was presented as Mean ± SD, unless otherwise stated. Gene expression and

DNA methylation data were categorized as continuous variables, while most clinical characteristics were considered as categorical variables. Differences in expression and DNA methylation measurements between tumour and matched adjacent non-tumour tissue samples were assessed using a paired two tailed Student's t-test. A p-value of >0.05 was considered to be statistically relevant. Overall survival analysis of HNSCC patients stratified by high and low expression of ZNF132, ZNF154, and ZNF671 were carried out using Kaplan-Meier analysis, while the log-rank test was used to assess statistical significance. ZNF132, ZNF154, and ZNF671 were stratified by multiple expression thresholds to determine statistically significant separations in survival outcomes. Overall survive was characterized as the period of time between surgery and date of death or last followup, and the time of surgery. High expression of ZNF154 was defined as the top 26 percent of patients, high expression of ZNF132 was defined as the top 52 percent of patients, and high expression of ZNF671 was defined as the top 83 percent of patients.

Gene associations were calculated between ZNF132, ZNF154, and ZNF671 to test for correlations. A list of genes correlated with both ZNF132 and ZNF154, as well as ZNF132, ZNF154, and ZNF671 were generated from the TCGA HNSCC dataset. This was achieved by querying cBioPortal for each respective gene and analyzing the list of genes from the co-expression tab. Significantly correlated genes were those that had a q-value < 0.05. These genes were further categorized as having "moderate" and "strong" correlations determined by their respective Spearman correlation. A Spearman correlation greater than 0.200, but less than 0.400 was defined as having a moderate correlation. A Spearman correlation greater than 0.400 was defined as having a strong correlation.

RESULTS

Section 2.4: Overview of the TCGA HNSCC cohort

Tumours from the TCGA-HNSCC cohort come from three primary locations, which are the oral cavity (alveolar ridge, buccal mucosa, floor of mouth, hard palate, and oral tongue), oropharynx (base of tongue, uvula, soft palate, and tonsil), and larynx (hypopharynx and larynx) (Sayáns *et al*., 2019; Krishnan *et al*., 2015). The majority of these tumours are from the oral cavity (n=310), followed by the larynx (n=124), and the oropharynx (n=82), respectively. Most patients from the cohort are male (n=376), compared to female (n=140). 98 patients are HPV positive, while 416 patients are HPV negative. 2 patients are of HPV status indeterminate 384 patients have smoked at some point in their life, while 119 patients have never smoked. The majority of tumours are stage IV (n=367), followed by stage III (n=75), and stage II (n=78), and stage I (n=25). 239 patients had a positive nodal status, while 177 patients had a negative nodal status. 348 patients had a vital status of alive, while 148 patients had a vital status of deceased.

Section 2.5: ZNF132, ZNF154, and ZNF671 appear to be epigenetically downregulated in HNSCC primary tumour tissue compared to matched normal adjacent tissue

We examined expression and DNA methylation data from fifty HNSCC patients from which matched adjacent tumour and non tumour tissue were available. Of these, thirty patients did not have DNA expression or methylation data for both the matched adjacent tumour and non tumour tissue. Our analayses used the remaining twenty matched tumour and non tumour tissue for which data was available. ZNF132, ZNF154, and ZNF671 methylation and DNA expression data was analyzed for the sample. RNA sequencing data showed a significant downregulation of ZNF154 in tumour tissue, compared to matched normal tissue (tumour 11.94±13.59 versus non-

tumour 25.16±20.75, $p<0.05$; **Figure 2.1**). The reduced gene expression in ZNF154 tumour tissue was also seen in ZNF132 expression, with ZNF132 expression also being reduced [(tumour) 31.91±23.26 versus (non-tumour) 88.89±43.65, $p<0.001$]. Finally, this same trend was also seen in another ZNF's (ZNF671) expression, [(tumour) 34.99±28.62 versus (non-tumour) 80.04±63.17, $p<0.001$].

Global measurements of CpG DNA methylation in these same tissue samples was measured using the Illumina Human Methylation450k beadchip. In a study by Lleras and Belbin in 2013, 972 CpG loci were identified as being differntailly methylated in HNSCC. Four of these were of specific interest to ZNF132 and ZNF154: cg08668790, cg21790626, cg13877915, and cg19776201. Two CpG loci within the promoter region of the ZNF154 gene showed significantly increased DNA methylation (M-value) in primary tumour tissue compared to adjacent normal tissue from the same patient [cg08668790: 1.01±0.91 (tumor) versus -2.22±0.90 (non-tumour) $p<0.001$], and [cg21790626: 0.38±0.83 (tumour) versus -3.98±1.50 (non-tumour) $p<0.001$; **Figure 2.2**]. Similarly, for ZNF132, two CpG loci within the promoter region of the ZNF132 gene showed significantly increased DNA methylation in primary tumour tissue when compared to adjacent normal tissue from the same patient [cg13877915: 0.80±1.38 (tumor) versus -1.67±1.21 (non-tumour) $p<0.001$], and [cg19776201: -1.01±1.14 (tumour) versus -3.49±1.39 (non-tumour) $p<0.001$].

The gene expression and methylation data indicate that ZNF132, ZNF154, and ZNF671 appear to be epigenetically downregulated. DNA methylation is associated with downregulated gene expression (Xu *et al*., 2019). ZNF671, along with ZNF132 and ZNF154 are all associated with epigenetic silencing in HNSCC, making them interesting candidates to investigate (Lleras, Belbin, *et al*., 2013).

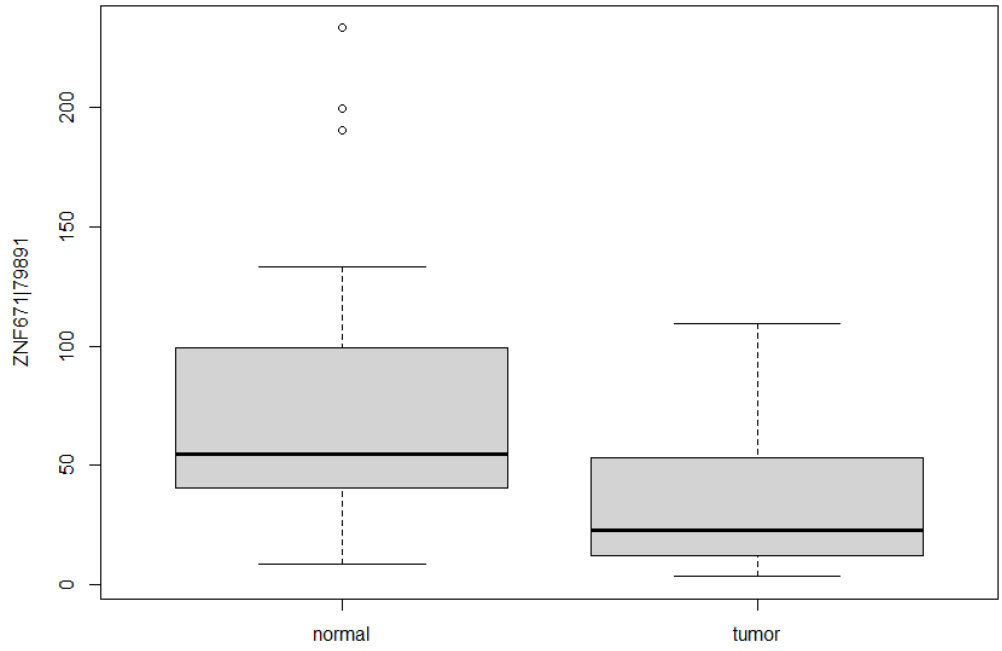
ZNF671|79891
0
50
100
150
200
normal
tumor
Tumour/Normal Tissue

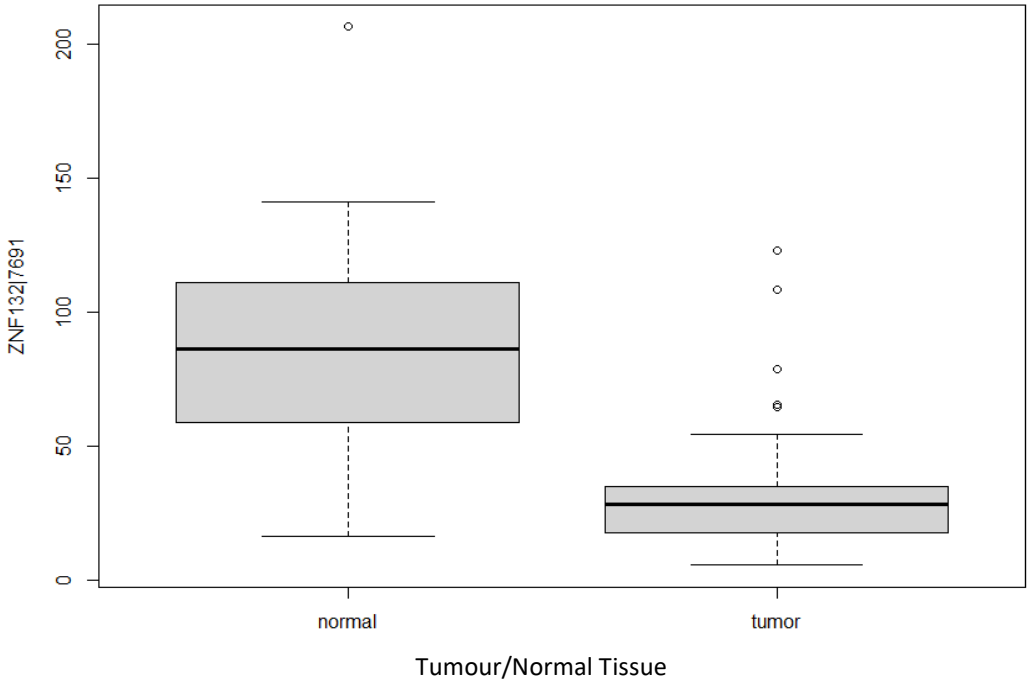
ZNF132|7691
0
50
100
150
200
normal
tumor
Tumour/Normal Tissue

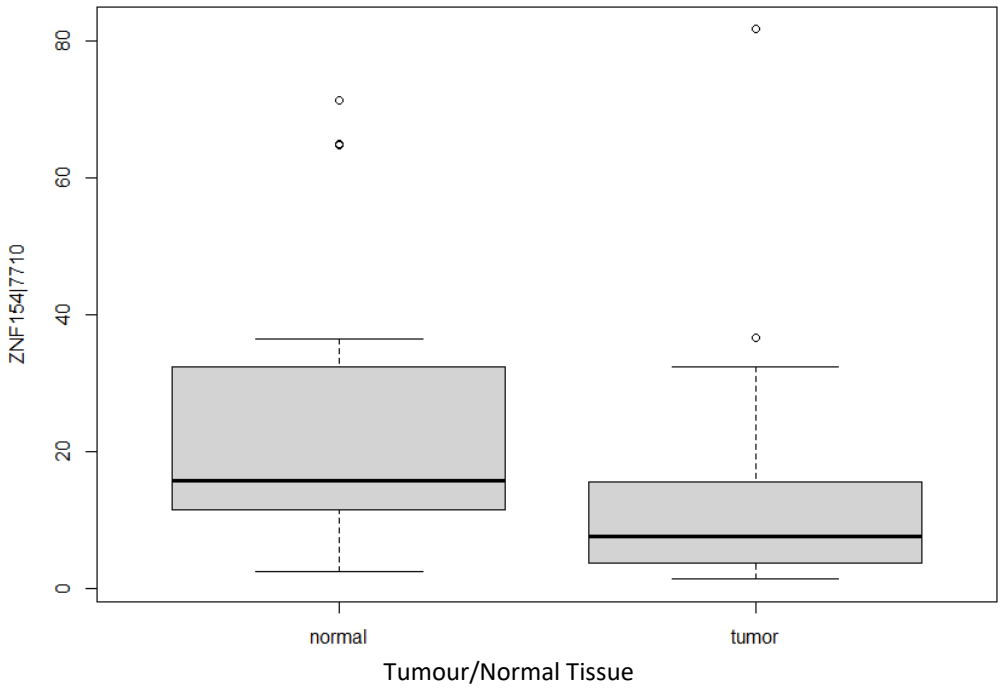

Figure 2.1: Gene expression analysis (RPKM) of ZNF132, ZNF154, and ZNF671 in HNSCC tumor and adjacent non-tumor tissue samples.

Gene expression (RPKM, Y axis) of ZNF132, ZNF154, and ZNF671 was conducted comparing HNSCC tumour and adjacent non tumour tissue (X axis). Data was obtained from the TCGA database containing information from 50 samples.

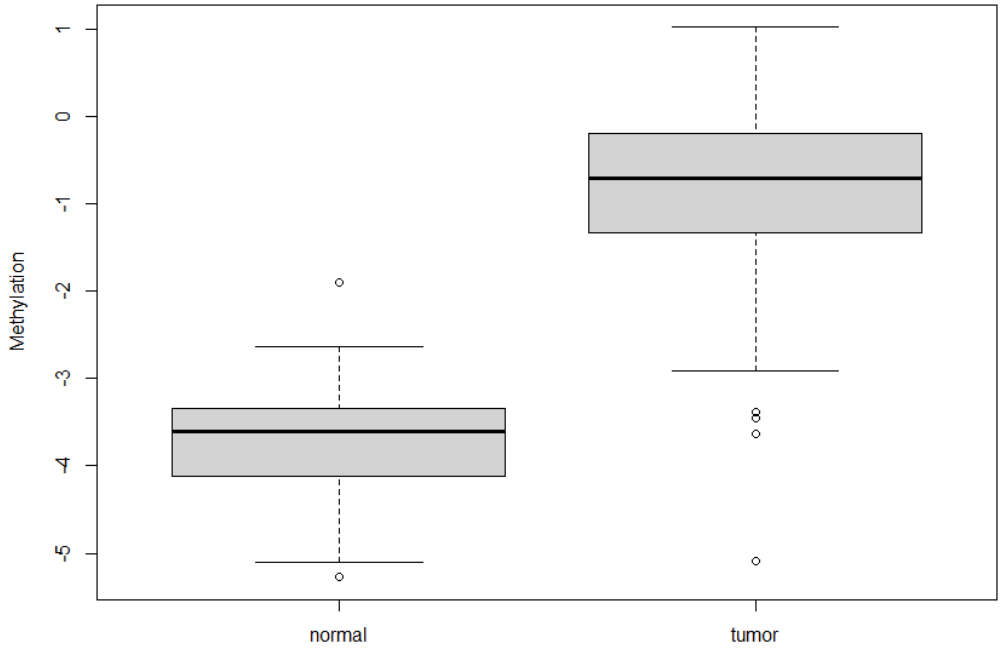

ZNF132 cg19776201

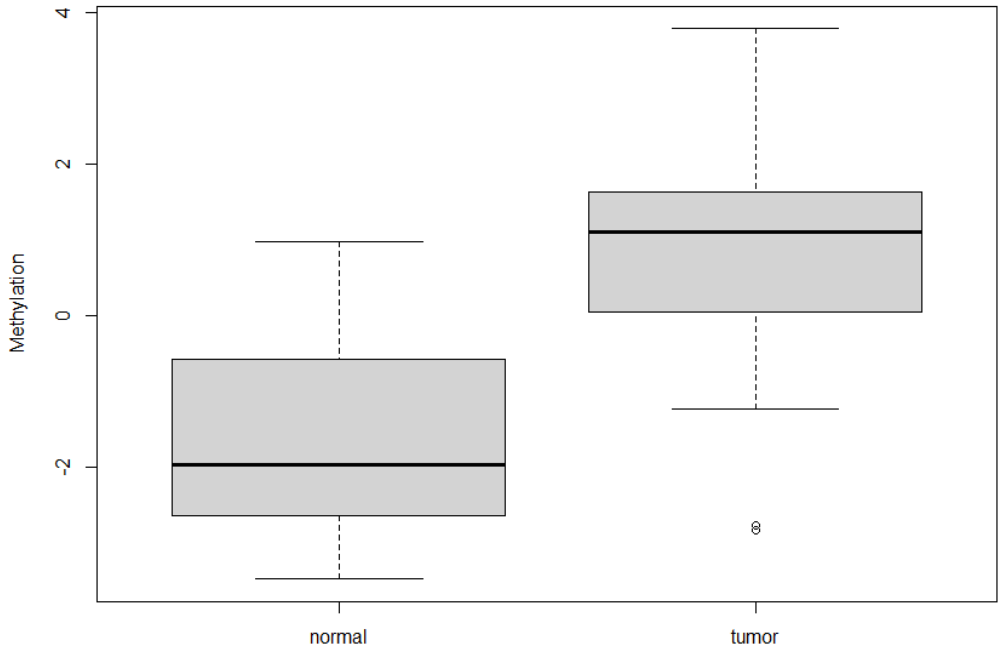

ZNF132 cg13877915

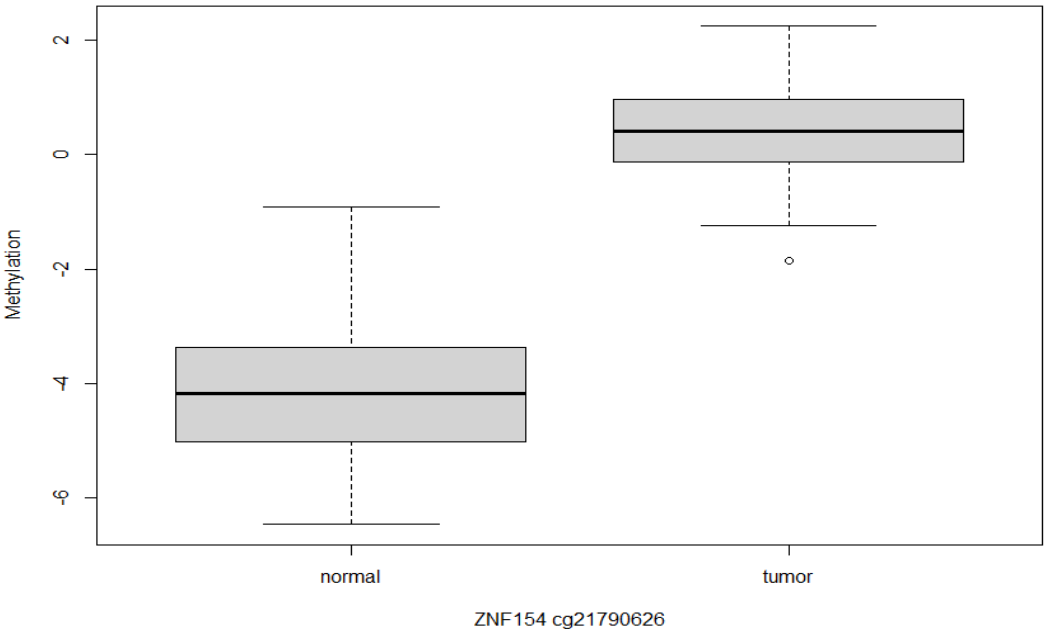

ZNF154 cg21790626

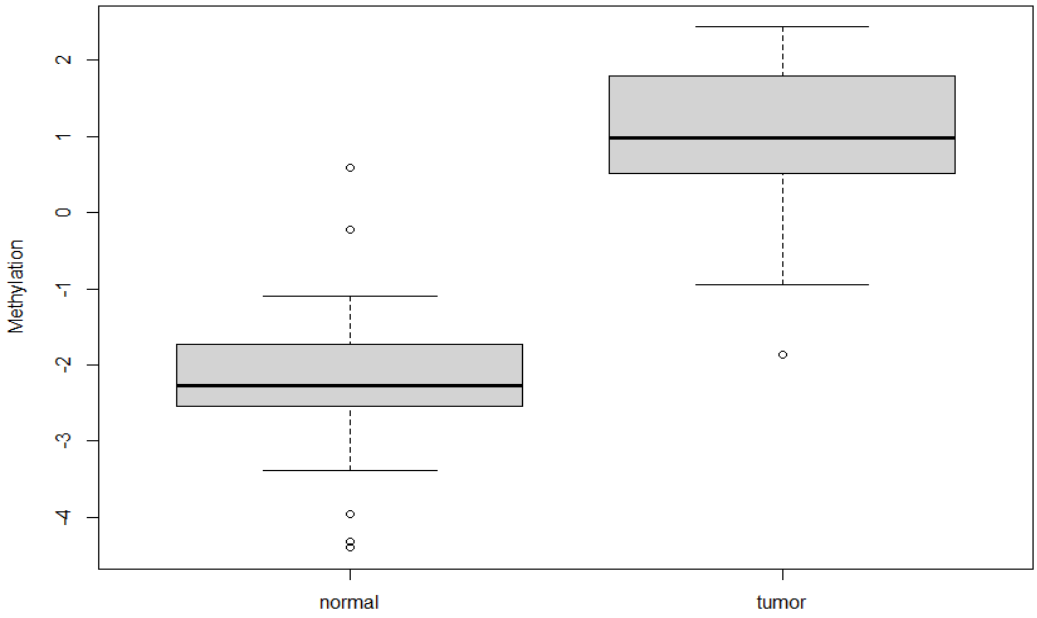

ZNF154 cg08668790

Figure 2.2: DNA methylation (M-score) analysis of ZNF132 and ZNF154 in HNSCC tumor and adjacent non-tumor tissue samples. Specific CpG loci corresponding to each ZNF gene are shown on the x-axis label.

DNA methylation (M-score, Y axis) of ZNF132 and ZNF154 was conducted comparing HNSCC tumour and adjacent non tumour tissue (X axis). Data was obtained from the TCGA database containing information from 50 samples. ZNF132 and ZNF154 each have two CpG loci being analyzed from the dataset.

Section 2.6: ZNF132, ZNF154, and ZNF671 downregulation was significantly associated with poor overall survival in HNSCC patients

While the majority of HNSCC tumours display decreased ZNF132, ZNF154, and ZNF671 expression, not all patients' tumours showed this genotype. We therefore hypothesized that expression levels of these ZNFs may have a significant association with disease prognosis. Using data from the cohort of 530 primary HNSCC patients, we determined cutoff points for the expression levels of the ZNFs through a percentile-based stratification. Log-rank tests were conducted for various stratifications to determine a statistically significant cutoff point. In the case of ZNF154, a subset of patients (n=124, top 25%) showed ZNF154 expression that was similar to that observed in non-tumor tissue. Kaplan-Meier survival analysis stratifying patients based on ZNF154 expression showed that those HNSCC patients who had higher expression of ZNF154 in primary tumour tissue also had a significantly improved overall survival when compared to the remaining patient cohort (Log-rank, $p<0.05$; **Figure 2.3**). The patient cohort in the TCGA dataset displayed a wider range of expression for ZNF132. We identified 258 patients as having high expression levels of ZNF132 (n=258, top 52%). Kaplan-Meier survival analysis stratifying HNSCC patients based on expression of ZNF132 showed that, like ZNF154, those with higher expression of ZNF132 in primary tumour tissue had significantly improved overall survival when compared to the remaining patient cohort (Log-rank, $p<0.05$; **Figure 2.3**). And finally, expression of ZNF671 was also varied widely. As with the previous examples, Kaplan-Meier analysis showed that when patients were stratified based on ZNF671 expression, patients with low expression of ZNF671 in primary tumour tissue (n=84, bottom 17%) showed a significantly decreased overall survival when

ZNF154

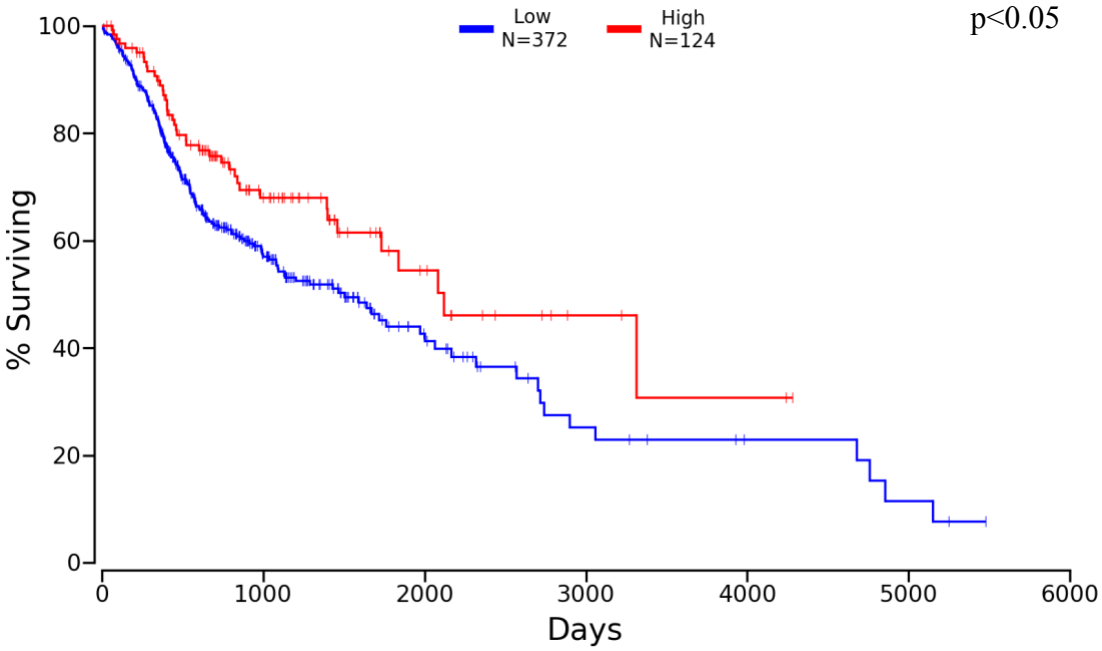

ZNF132

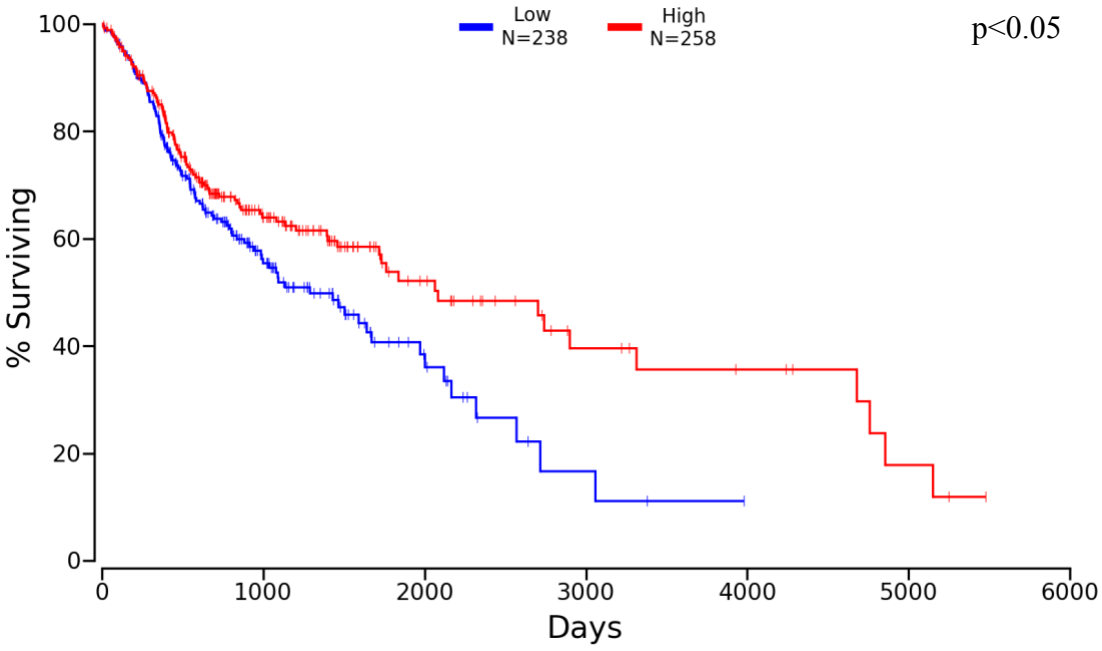

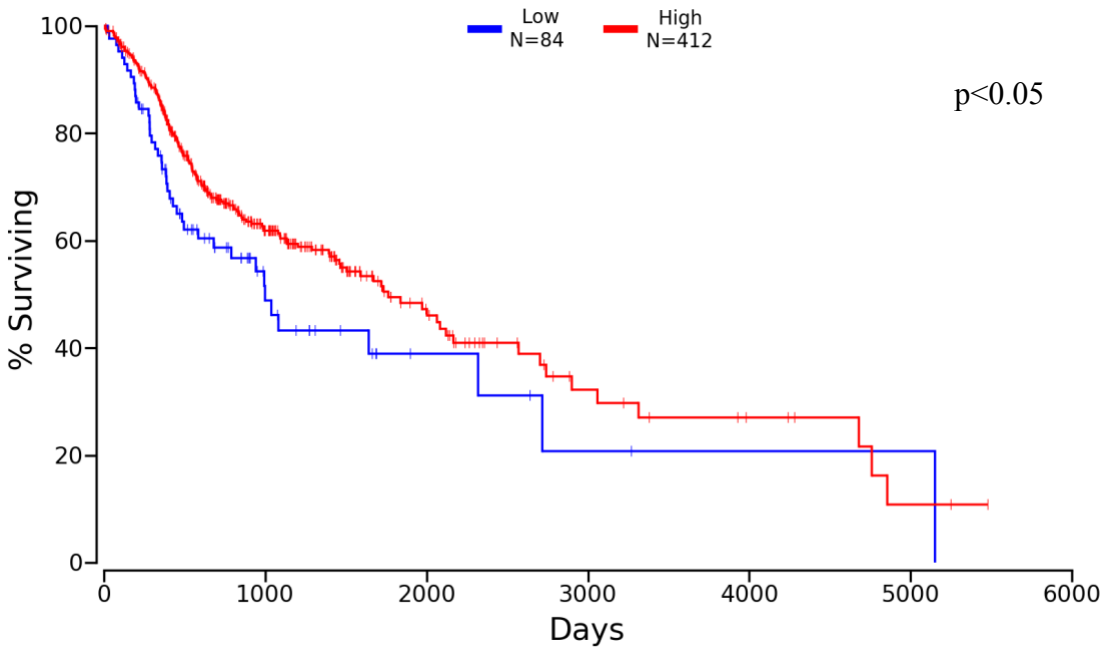

Figure 2.3: Kaplan-Meier Plots of overall survival (OS) for HNSCC patients stratified by ZNF154 expression, HNSCC patients stratified by ZNF132 expression, HNSCC patients stratified by ZNF671 expression.

Kaplan-Meier survival plots for ZNF132, ZNF154, and ZNF671 comparing the percentage of group surviving over a period of time in days. Plots are stratified by high expressors and low expressors, with the red line representing the high expressors and the blue line representing the low expressors. These plots were also shown to be statistically significant.

compared to the remaining patient cohort (Log-rank, $p<0.05$; **Figure 2.3**). These results indicate that the expression of ZNF132, ZNF154, and ZNF671 are significantly associated with disease prognosis, with their expression levels in primary tumours may be useful as potential prognostic markers in this disease.

Section 2.7: Significant gene associations between ZNF132, ZNF154, and ZNF671

KRAB-ZNFs exert their function by acting as transcriptional repressors of target genes, either by binding within the promoter region of a downstream target, or within the coding sequence itself, as in the case of other ZNF target genes (Cassandri *et al*., 2017). We therefore hypothesized that targets of each ZNF gene should show anti-correlative features in the TCGA expression dataset of HNSCC patient primary tumours. We also wanted to evaluate any commonality between genes targeted by these three ZNFs.

A list of genes correlated with both ZNF132 and ZNF154, as well as ZNF132, ZNF154, and ZNF671 were generated from the TCGA HNSCC dataset. In this analysis, a gene is considered to be mutually correlated if it is correlated for all of the listed genes after being cross-referenced. 13,362 genes were significantly mutually correlated with ZNF154, 13,213 genes were significantly mutually correlated with ZNF132, and 17,591 genes were significantly mutually correlated with ZNF671. 10,413 genes were found to be significantly mutually correlated between ZNF132 and ZNF154, while 7,329 genes were found to be significantly mutually correlated between ZNF132, ZNF154, and ZNF671. Of these genes, 4219 were found to be moderately mutually correlated between ZNF132 and ZNF154, and 2552 were found to be moderately mutually correlated between ZNF132, ZNF154, and ZNF671. Finally, 127 genes

were found to be strongly mutually correlated between ZNF132 and ZNF154, while 59 were found to be strongly mutually correlated between ZNF132, ZNF154, and ZNF671 (**Table 2.4A and Table 2.4B).**

DISCUSSION

Data from the TCGA patient dataset indicates that ZNF132 and ZNF154 are significantly altered in expression and methylation between matched HNSCC tumour and non tumour tissue. Additionally, expression levels of ZNF132, ZNF154, and ZNF671 were found to have a significant correlation to overall patient survival. These genes have been shown to be associated with overall survival and clinical outcomes, described in previous studies, in addition to our analysis. (Liu *et al*., 2021; Wiesmueller *et al*., 2018; Zhan *et al*., 2020). ZNF154 methylation has been shown to have potential as a multicancer biomarker (Miller, Petrykowska, and Elnitski, 2021). ZNF154 hypermethylation was seen in early-stage tumours throughout ten different cancers and was not significantly associated with age or sex. By analyzing DNA from patient plasma, these genetic markers hold the potential to identify tumours versus healthy tissue.

A study by Liu *et al.* (2021) displayed that downregulated ZNF132 via promoter hypermethylation could be identified as a risk factor in breast cancer. This could hold promise for use as a diagnostic biomarker. These results are similar to the trends we have seen in ZNF132

Table 2.4A: Genes strongly associated between ZNF132 and ZNF154.

GPRASP1	MICU3	NR2F2	ZIK1	TTC28
CUBN	ZNF677	ZNF333	PWARSN	PKP3
SNED1	CACNB2	ACACB	ZNF568	PPP1R3E
ZNF418	SH3BP5	ZFP82	ZNF253	CACNA1D
ZNF135	FRZB	NOVA1	TRAK2	ADAM22
SPARCL1	ZNF583	ADGRG2	ZNF780B	FAXDC2
CARD8	KCTD7	FAM171A1	ZNF224	ZNF347
TNS2	GUCY1B1	ZNF540	TRIM52	ZNF280B
CMAHP	ZNF610	MGAT3	ARMCX2	ZFP28
NRIP2	TSPAN12	BCL2	ZNF280D	TMEM54
RAI2	SHE	ZNF546	NR2F1	ZFP2
ZNF582	ATM	KL	ZNF445	
ZC3H12B	AFF3	NIPSNAP3B	DPY19L3	
ZNF737	ZNF439	PPM1H	TUBA1C	
CD200	NBEA	VASH2	ZNF302	
NOTCH4	PLPP3	CCPG1	ZFP14	
SEMA3G	INSR	PRKD1	YPEL1	
RGS5	PTCH2	SLAIN1	SUGT1P4-STRA6LP-CCDC180	
ZNF486	ZNF626	ZNF621	ZNF701	
ZCCHC18	HTR2B	TNRC6C	PHLDA2	
ZNF43	NR3C2	PKD2	GPRC5B	
CNTN4	ZNF454	MCF2L	KRBA2	
FAT4	IKZF4	PARM1	ZBED3	
ZMAT1	TMEM150C	ZSCAN18	ZNF829	
KIT	MAP3K12	CADPS2	CBX7	
ZNF578	ZNF471	PDE5A	IL17REL	
ZNF25	ZNF542P	ZNF417	CDC14A	
CD302	ENPP4	CACNB4	SFN	
ZNF415	ZNF667	COL4A4	BANK1	

A table of genes that have a strong association between ZNF132 and ZNF154. A strong association was defined as having a Spearman correlation of greater than 0.400.

Table 2.4B: Genes strongly associated between ZNF132, ZNF154, and ZNF671. A strong correlation is defined as having a Spearman correlation greater than 0.400.

CARD8	**ZNF583**
ZNF582	**KL**
ZCCHC18	**SPARCL1**
ZFP82	**RGS5**
ZNF418	**TNS2**
FRZB	**ZNF439**
ZNF43	**BANK1**
CMAHP	**HTR2B**
ZIK1	**IKZF4**
ZNF135	**MGAT3**
SEMA3G	**ZNF25**
ZNF540	**ZNF677**
AFF3	**ZNF280B**
YPEL1	**ENPP4**
CUBN	**ZNF542P**
SNED1	**CACNB2**
SH3BP5	**ZNF546**
BCL2	**COL4A4**
ZMAT1	**NRIP2**
RAI2	**CADPS2**
ZNF578	**ZNF667**
ZNF737	**ACACB**
PARM1	**NOTCH4**
GPRASP1	**PLPP3**
CD302	**ZNF568**
ZNF626	**KIT**
SHE	**NOVA1**
ZNF610	**ZNF486**
CD200	**ZNF454**
SLAIN1	

A table of genes that have a strong association between ZNF132, ZNF154, and ZNF671. A strong association was defined as having a Spearman correlation of greater than 0.400.

in HNSCC. We saw increased methylation of ZNF132, as well as a decreased expression of ZNF132.

Additionally, research has shown that ZNF132 hypermethylation is indicative of clinicopathological aggressiveness of 'pan-negative' lung adenocarcinomas (Hamada *et al*., 2021). DNA methylation patterns were shown to have effects on gene expression, which may contribute to clinicopathological features, such as tumour aggression (Hamada *et al*., 2021). ZNF132, by methylation, was found to enhance cancer progression in esophageal squamous cell carcinoma (Jiang *et al*., 2018). In that study, ZNF132 was found to have a role as a tumour suppressor, significantly inhibiting cell growth, migration/invasion, and cell tumourigenicity. This supports our findings that ZNF132 appears to be hypermethylated in tumour tissue, compared to normal tissue. This hypermethylation seems to be associated with decreased gene expression. The patients with hypermethylation of ZNF132 in the TCGA data also appeared to display had lower gene expression, and were associated with a lower overall survival rate.

ZNF671 has previously been shown to significantly inhibit cell proliferation and metastasis in non-small-cell lung cancer (Zhan *et al*., 2020). This occurs via the Wnt/β-Catenin pathway, a pathway previously shown to be affected by other ZNFs (Hu *et al*., 2017). The epigenetic downregulation of ZNF671 has also been shown to predict poor prognosis in patients with solid tumours (Zhang *et al*., 2019). The research indicates that ZNF671 could be a useful predictive factor for multiple cancer types including lung adenocarcinoma, breast cancer, head and neck squamous cell carcinoma, among many others.

The prior mentioned research highlights the various findings that ZNF132, ZNF154, and ZNF671 appear to be affecting survival and other pathophysiological factors in cancers (Liu *et al.,* 2021; Miller, Petrykowska, and Elnitski, 2021; Zhan *et al*. 2020). Prior research established

by Hu *et al*. (2017) displayed that ZNF154 had an effect on invasion and metastasis in NPC. Prior research by Lleras, Belbin, *et al.* (2013) identified ZNF132 and ZNF154 as potential targets of interest. The ZNF132 and ZNF154 promoters displayed hypermethylation in human solid epithelial tumours and cancer cell lines. These prior findings formed the basis upon our investigation into the effects of these ZNF132 and ZNF154 in HNSCC.

Our data analysis has shown that ZNF132, ZNF154, and ZNF671 expression is significantly downregulated in HNSCC tumour compared to matched normal tissue (**Figure 2.1**). In addition ZNF132 and ZNF154 has been shown to be significantly hypermethylated in HNSCC tumour tissue, compared to matched normal tissue (**Figure 2.2**). Finally, survival analysis has indicated that low expression of ZNF132, ZNF154, and ZNF671 is associated with worse long-term survival (**Figure 2.3**). These results lead us to believe that specifically ZNF132 and ZNF154 are being hypermethylated in tumours to reduce their expression, as high expression of these genes has been significantly associated with longer survival.

Figures:

Table 2.5: HNSCC Patient characteristics by tumor site (Dr. Tom Belbin).						
	Oral Cavity		**Oropharynx**		**Larynx**	
	N=310		N=82		N=124	
	N	%	N	%	N	%
Gender						
Male	206	66.5	69	84.1	101	81.5
Female	104	33.5	13	15.9	23	18.5
Race						
White	266	85.8	76	92.7	99	79.8
Black or African American	20	6.5	6	7.3	19	15.3
Asian	10	3.2	0	0	1	0.8
American Indian or Alaska Native	1	0.3	0	0	1	0.8
Information not available	13	4.2	0	0	4	3.2
Ethnicity						
Hispanic/Latino	16	5.2	3	3.7	5	4
Non-Hispanic/Latino	269	86.8	76	92.7	109	87.9
Information not available	25	8.1	3	3.7	10	8.1
Smoking						
Ever smoker	215	69.4	56	68.3	113	91.1
Lifelong non-smoker	86	27.7	25	30.5	8	6.5
Information not available	9	2.9	1	1.2	3	2.4
HPV Status						
HPV +	31	10	56	68.3	11	8.9
HPV -	278	89.7	26	31.7	112	90.3
Indeterminate	1	0.3	0	0	1	0.8
Vital Status						
Alive	197	63.5	69	84.1	82	66.1
Deceased	113	36.5	13	15.9	42	33.9
Nodal Status						
Positive	147	47.4	34	41.5	58	46.8
Negative	119	38.4	16	19.5	42	33.9
Information not available	44	14.2	32	39	24	19.4
Pathologic Tumor Stage						
Stage I	19	6.1	4	4.9	2	1.6
Stage II	56	18.1	10	12.2	12	9.7
Stage III	52	16.8	9	11.0	14	11.3
Stage IV	160	51.6	28	34.1	79	63.7
Information not available	23	7.4	31	37.8	17	13.7

Table displaying data from the TCGA dataset of 516 HNSCC patients. It includes information such as, gender, race, ethnicity, HPV status, vital status, and pathologic tumour status compared against HNSCC subsites oral cavity, oropharynx, and larynx.

Table 2.6: Patient characteristics for 50 HNSCC patients with adjacent tumor and non-tumor and samples (Dr. Tom Belbin).			
	Oral Cavity N=32	**Oropharynx** N=2	**Larynx** N=16
Gender			
Male	21	2	15
Female	11	0	1
Race			
White	28	2	12
Black or African American	2	0	4
Information not available	2	0	0
Ethnicity			
Hispanic/Latino	4	0	4
Non-Hispanic/Latino	25	2	12
Information not available	3	0	0
HPV Status			
HPV +	6	0	2
HPV -	26	2	14
Vital Status			
Alive	11	0	7
Deceased	21	2	9
Pathologic Tumor Stage			
Stage II	9	1	1
Stage III	10	1	6
Stage IV	13	0	9

Table displaying data from the TCGA dataset of 50 HNSCC patients with matched tumour and non tumour samples. It includes information such as, gender, race, ethnicity, HPV status, vital status, and pathologic tumour status compared against HNSCC subsites oral cavity, oropharynx, and larynx.

CHAPTER 3: *IN VITRO* OVER-EXPRESSION OF ZNF132 AND ZNF154 IN HUMAN IMMORTALIZED HUMAN EMBRYONIC KIDNEY (HEK-293) CELLS AND ORAL SQUAMOUS CELL CARCINOMA (UM-SCC-1) CELLS

Co-Authorship Statement

As the primary author of this thesis I was responsible for the majority of experiments conducted, analyses completed, and preparing an initial draft of this chapter. I would like to acknowledge and thank my supervisor, Dr. Tom Belbin, and my supervisory committee, Dr. Touati Benoukraf and Michael Leitges, for their invaluable feedback and constructive criticism in improving the initial draft.

Kendra Smith and Elizabeth Chia assisted with cell culture and sample collection, genomic sequencing, Western blot, and genomic PCR imagining in Chapter 3 where credited. Elizabeth Chia completed the Western blot as seen in **Figure 3.4A**. Kendra Smith completed the genomic PCR and genomic sequencing as seen in **Figure 3.4B, Figure 3.5,** and **Figure 3.6B**. I performed all other experiments myself.

INTRODUCTION

Section 3.1: Identifying the Mechanism behind ZNF132 and ZNF154

As shown in the previous chapter, ZNF132 and ZNF154 promoters appear to be hypermethylated, reducing expression of each of these genes. Lower expression of these ZNFs is associated with poorer overall survival rate. A related study by Hu *et al* found that ZNF154 expression was frequently downregulated in NPC cell lines (2017). Promoter methylation of ZNF154 was associated with poor survival in locoregionally advanced NPC. In cells that were transduced with ZNF154, there was an increased expression of epithelial markers, such as E-cadherin, and a decreased expression of mesenchymal markers, such as vimentin. They suggested that ZNF154 is being downregulated in NPC, via promoter methylation, promoting invasion and metastasis (Hu *et al*., 2017). They propose the use of ZNF154 promoter methylation as a candidate biomarker for disease prognosis and a novel therapeutic target for NPC.

While the effects of ZNF154 have been investigated in NPC as seen in the Hu *et al* study, there is a lack of research on the effects of ZNF154 and similar ZNFs, such as ZNF132 in HNSCC (2017). Using the HNSCC cell line UM-SCC1, we wanted to investigate the effects of overexpressing ZNF132 and ZNF154 and how it affects EMT marker expression, cell growth rate, and any potential targets of interest that may arise. From the TCGA data, we have seen the increased methylation of ZNF132 and ZNF154 in HNSCC tumours, as well as a reduced gene expression. Low expression of each gene was associated with a significantly reduced overall survival rate. This data indicates there may be a mechanism by which ZNF132 and ZNF154 promoter methylation is being influenced by HNSCC.

METHODS

Section 3.2: Growth of Cell Lines and Lentiviral Transduction of ZNF132 and ZNF154 expressing Constructs

Growth of Cell Lines

The HNSCC cell line, UM-SCC1, (Cat.# SCC070, Millipore Sigma) was maintained at 37°C, 5% CO_2. UM-SCC-1 cells were cultured in DMEM/F12 (Cat.# SH30023FS, HyClone) supplemented with 10% fetal bovine serum (FBS; Cat.# 081150, Wisent) and non-essential amino acids (Cat.# TMS-001-C, Millipore Sigma). Isolation of total RNA was carried out using the RNeasy total RNA kit (Cat.# 74104, Qiagen). The constitutive overexpression of ZNF132 and ZNF154 via lentiviral transductions in UM-SCC-1 and HEK-293 cells were carried out using the pLenti-C-Myc-DDK-P2A-Puro lentiviral system. Central to this system was the use of a CMV promoter expressing a FLAG-tagged ZNF154 or ZNF132 fusion protein, (Cat.# RC219041L3, RC218278L3, Origene). Transduced clones were selected using 0.25-0.50 μg/mL of puromycin. A negative control for each cell type contained only the empty pLenti-C-Myc-DDK- P2A-Puro vector via transduction (Cat.# PS100092, Origene). Single clones were selected for use in experiments. P-Lenti-50 (PL-50) and P-Lenti-100 (PL-100) represent the samples numbers used in experiments.

Taqman Real-Time PCR

Taqman real-time PCR was used to determine expression of ZNF proteins, as well as the EMT markers vimentin (Hs00985111_m1) and e-cadherin (Hs00170423_m1), at the RNA transcript level, as per the manufacturer's instructions (Thermo Fisher Scientific). The Taqman probes used included the following: ZNF154 (Hs06618628_s1), ZNF132 (Hs01036387_m1),

Vimentin, and E-Cadherin. Isolation of total RNA was carried out using the RNeasy total RNA kit (Cat.# 74104, Qiagen). GAPDH (Thermo Fisher Scientific Cat.# 402869) was used as the control probe. The guidelines for the real time PCR reaction are as follows: a reverse transcription step (50°C, 5 minutes), followed by a RT inactivation/initial denaturation (95°C, 20 seconds), and finally 40 cycles of denaturation (95°C, 5 seconds) and annealing/extension (60°C, 15 seconds).

PCR Expression of Confirmation

The internal vector PCR primers V2 (5'-AGAGCTCGTTTAGTGAA-3') and LR50 (5'-CAGAGGTTGATTATCGATAAG-3') were used for the amplification of viral DNA. Phusion Green Hot Start II High Fidelity PCR master mix was used to conduct PCR reactions (Thermo Fisher, Cat.#F-566S). The guidelines for the PCR reaction are as follows: an initial denaturation (98°C, 30 seconds), followed by 35 cycles of denaturation (98°C, 10 seconds), annealing (56°C, 30 seconds) and extension (72°C, 2 minutes), with a final extension step (72°C, 10 minutes). PCR products were then resolved on a 0.8% agarose gel. The expected amplifier size for ZNF154 is 2340 bp.

Growth Measurements

For growth measurements, cells were grown and harvested in triplicate wells for each cell type. Cells were counted using a haemocytometer and phase contrast microscope; Trypan Blue exclusion was used to assess cell viability. Tumor cell numbers were expressed as mean ± SD. One way ANOVA was conducted using Microsoft Excel 2013 to calculate differences between two independent groups. Doubling time was calculated using the formula as seen in **Figure 3.1A**. A p-value of less than 0.05 was considered to be statistically significant.

$$T_d = t\frac{ln(2)}{ln(1+\frac{r}{100})}$$

Figure 3.1A: Formula for calculating the doubling time of cells, where Td represents the doubling time, t represents the time between plating and harvesting, and r represents the growth rate.

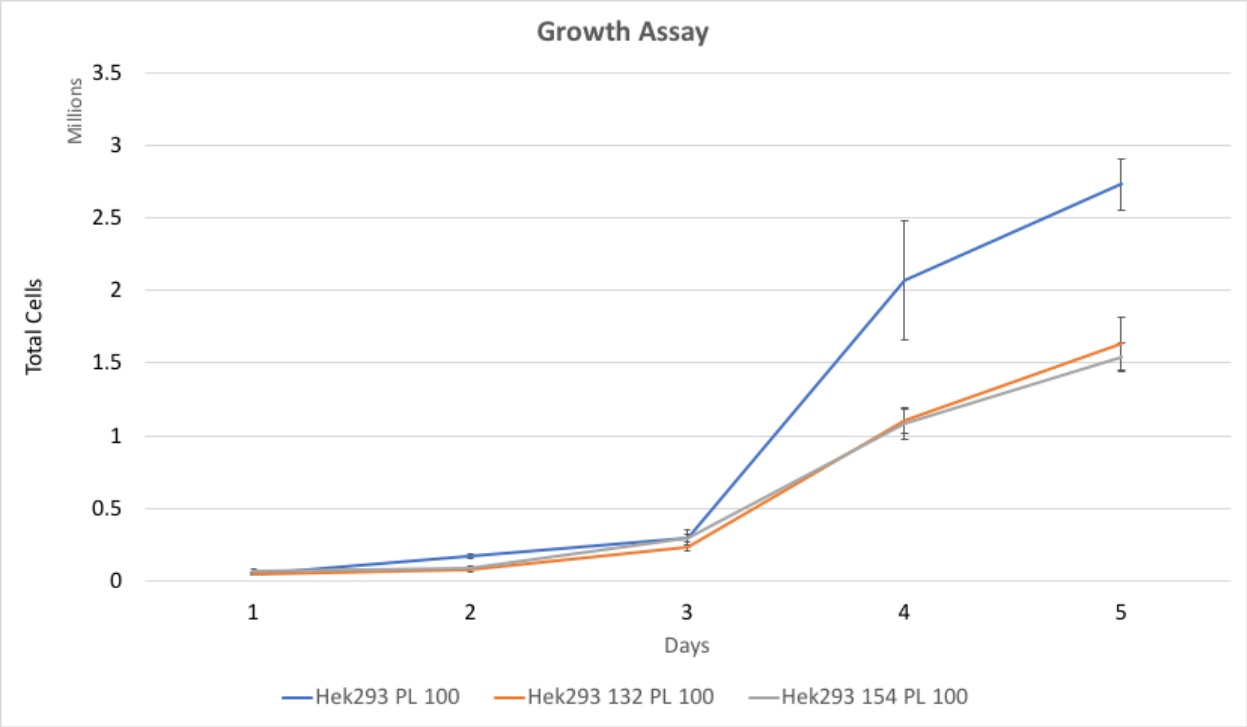

Figure 3.1B: HEK293 cell growth assay over comparing parental HEK293, empty vector, and ZNF154 overexprossors.

A graph comparing the growth times between various HEK293 samples, including HEK293 cells transduced with ZNF132, ZNF154, and empty vector.

Section 3.3: Measurement of FLAG-Tagged Protein Expression

Measurement of ZNF154-FLAG and ZNF132-FLAG fusion protein expression was carried out by Western blot. Cells were plated in six-well plates, washed with ice cold PBS, and lysed with 200µl RIPA buffer (50mM Tris pH7.4, 137mM NaCl, 2.7mM KCl, 11.9mM phosphates, 1% TritonX, 5mM EDTA, 0.5% Deoxycholic Acid, 0.1% SDS, 50mM β-glycerophosphate, 50mM sodium fluoride, 1mM PMSF, 2mM sodium orthovanate, 10µg/ml Aprotinin, 10µg/ml Leupeptin and 10µg/ml Pepstatin). To harvest, cells were scraped from the six well plates using a cell scraper. Cell lysates were removed from the plate surface by cell scraper and passed through a 25-gauge needle. Samples were then centrifuged at 11,000xg for 15 minutes at 4°C to remove cell debris. The Pierce BCA protein assay kit was used to determine protein concentrations (Cat.# 2322S, Thermo Fisher Scientific) as per manufacturer's instructions using a BSA standard curve. 60µg of total protein were loaded onto a 10% SDS-PAGE gel, and resolved proteins were transferred onto a nitrocellulose membrane (Cat.# 1620115, BioRad). Membranes were probed using a FLAG primary antibody (1:2000; Cat.# TA50011, Origene) and secondary antibody (goat anti-mouse HRP (1:5000) (Cat.# 115-035-071, Jackson Immunoresearch). HRP signal was detected using Amersham ECL Select Western Blotting Detection Reagent (RPN2235) and blots were imaged on a Biorad Chemidoc MP Imaging System. The membranes were reprobed for β-actin (1:2000; Cat.# MABT523, Millipore Sigma); secondary antibody goat anti-rabbit HRP (1:10000; Cat.# 65-6120, Invitrogen) as a loading control. SuperSignal West Pico PLUS Chemiluminescent Substrate was used to detect HRP signal (Cat.# 34579, Thermo Fisher Scientific). This was then imaged on a Biorad Chemidoc MP Imaging System. All images were analyzed using Bio-rad Laboratories Image Lab software (version 6.1).

Section 3.4: Screening for Cancer Related Targets of Interest Using Proteome Profiler Antibody Array

Proteome Profiler (R&D Systems, Inc., Minneapolis, MN, USA) antibody array was used to screen HEK293 cells for changes in cancer related targets of interest. Specifically, the Human XL Oncology (Cat.# ARY026) was used to detect differences in 84 cancer-related proteins between samples. Selected capture antibodies were spotted in duplicate on nitrocellulose membranes **(Table 3.2)**. The Human XL Oncology antibody array was used according to the manufacturer's protocol. For each array, 200 μg of protein sample was used. Membranes were blocked in Array Buffer 6 and incubated for an hour on a rocking platform. 0.5 mL of each sample was added to 0.5 mL of Array Buffer 4. Final volume was adjusted to 1.5 mL with Array Buffer 6. This was then incubated overnight at four degrees Celsius on a rocking shaker. After washing each membrane with 1X Wash Buffer, 30 μL of Detection Antibody Cocktail was added to 1.5 mL of 1X Array Buffer 4/6. 1.5 mL of this was added to each well and blots were incubated for one hour on a rocking shaker at room temperature. After incubating and washing, 2 mL of 1X Streptavidin-HRP was added to each well and was incubated for 30 minutes on a rocking shaker at room temperature. 1 mL of Chemi Reagent Mix was added to each well and covered with a plastic sheet protector. This was incubated for one minute, and after excess reagent was squeezed out. This was then imaged on a Biorad Chemidoc MP Imaging System.

The arrays were imaged using the ChemiDoc™ MP (Bio-rad, Hercules, CA, USA) system. Prior to image analysis, image grayscale was inverted. Chemiluminescent spots were measured using ImageJ image processing software and normalized to the array reference spots. Integrated density for each spot was calculated. Statistical significance was determined using one

Table 3.2: 84 Cancer-related proteins on Human XL Oncology Array

AFP	ErbB4	MMP-2
Amphiregulin	FGF basic	MMP-3
Angiopoietin-1	FoxC2	MMP-9
ANGPTL4	FKHR	MSP/MST1
ENPP-2/Autotaxin	Galectin-3	MUC-1
AXL	GM-CSF	Nectin-4
BCL-X	HCG	Osteopontin
CA125/MUC-16	HGF R/c-Met	p27/Kip1
E-Cadherin	HIF-1alpha	p53
VE-Cadherin	HNF-3beta	PDGF-AA
CAP-G	HO-1/HMOX1	CD31/PECAM-1
CA-9	ICAM-1/CD54	Progesterone R
Cathepsin B	CD25/IL-2 R alpha	Progranulin
Cathepsin D	IL-6	Prolactin
Cathepsin S	CXCL8/IL-8	Prostasin
CEACAM-5	IL-18 Bpa	E-Selectin
Decorin	KLK-3/PSA	Maspin
DKK-1	KLK-5	PAI-1/Serpin E1
DLL-1	KLK-6	SNAIL
EGF R/ErbB1	Leptin (OB)	SPARC
Endoglin/CD105	Lumican	Survivin
Endostatin	CCL2/MCP-1	Tenascin-C
Enolase 2	CCL8/MCP-2	THBS-1
eNOS	CCL7/MCP-3	TIE-2
EpCAM	M-CSF	UPA-1

ER-alpha	Mesothelin	VCAM-1
ErbB2	CCL3/MIP-1alpha	VEGF
ErbB3	CCL20/MIP-3alpha	Vimentin

A list of cancer related proteins that were included in the Human XL Oncology Array Kit

way ANOVA and significant results were verified use a post hoc Tukey test. Results are reported as relative expression set as a ratio to a value of one, from one divided by the integrated density.

RESULTS

Section 3.5: Attempts to Overexpress ZNF154 in Head and Neck Squamous Cell Carcinoma Cell Line UM-SCC-1 and its Effect on Markers of Epithelial-Mesenchymal Transition (EMT)

ZNF154 has previously been identified as a candidate gene for investigation based upon its epigenetic silencing in HNSCC (Lleras, Belbin, *et al*., 2013) Our research attempts to elucidate this further in identifying the potential tumour suppressive properties of ZNF154. This was attempted by the overexpression of ZNF154 in the oral cavity cancer cell line UM-SCC1. Overexpression of ZNF154 in this cell line was first investigated by qPCR to identify the effects of how EMT related markers are affected by overexpression. A previous study by Hu *et al*. demonstrated that ZNF154 overexpression in nasopharyngeal cancer cells lines caused a decrease in mesenchymal markers such as vimentin and an increase in epithelial markers such as E-cadherin (2017). These two proteins were chosen as markers of EMT for our investigation of the effects of ZNF154 overexpression in HNSCC cell lines. Real-time qPCR results measuring E-Cadherin and vimentin expression levels compared between empty vector UM-SCC1 cells and ZNF154 overexpressing UM-SCC1 cells identified an increase in vimentin levels in the ZNF154 overexpressors and a decrease in E-cadherin levels in the ZNF154 overexpressors (**Figure 3.3**). We hypothesized that the overexpression of ZNF154 would push the HNSCC cells towards a more epithelial phenotype. However, these results contradict that by indicating a decrease in

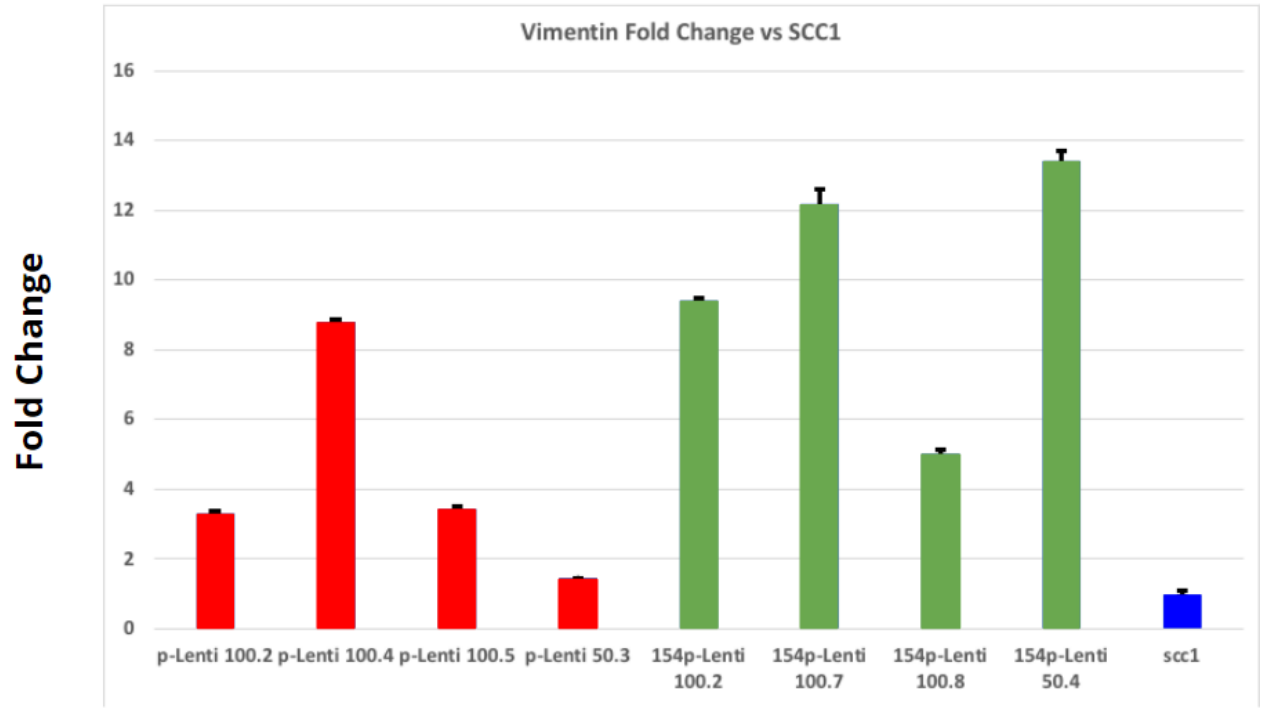

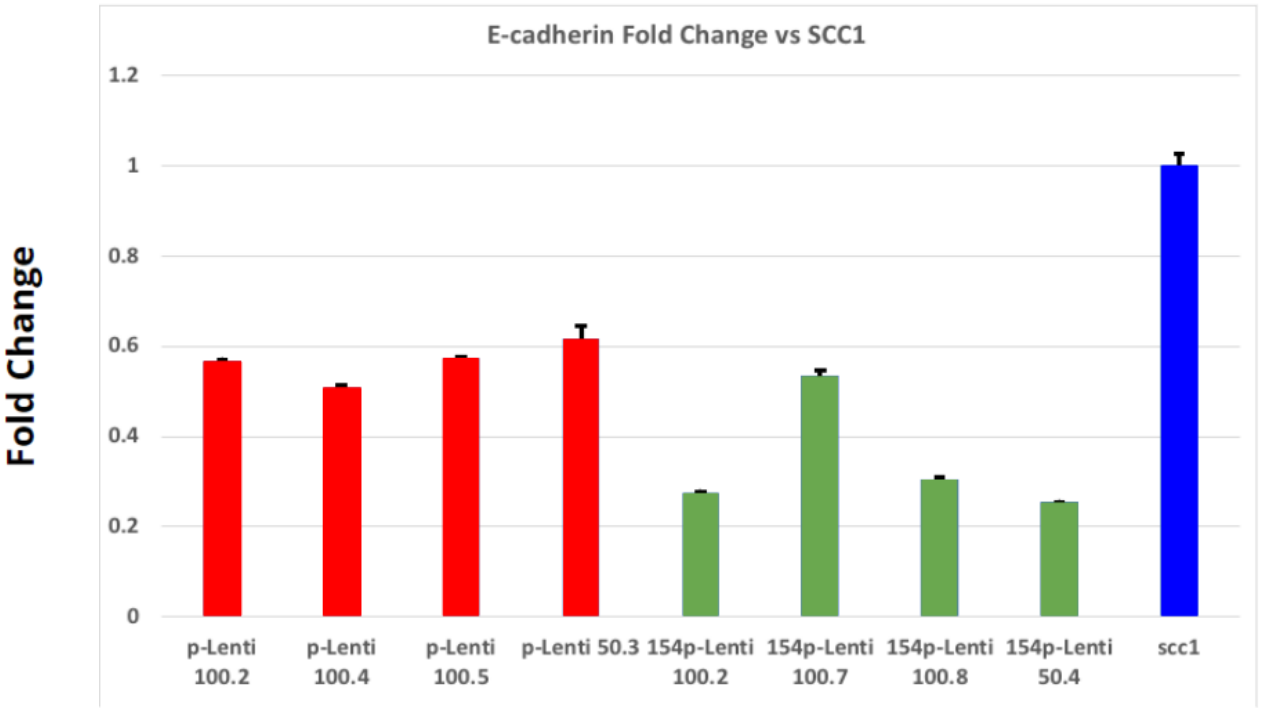

Empty Vector Samples **ZNF154 Overexpressors** **Parental**

Figure 3.3: qPCR of various EMT related markers in UM-SCC1 samples transduced with empty vector and ZNF154

A qPCR was completed of various EMT markers for UM-SCC1 samples transduced with ZNF154 and empty vectors. This graph compares the empty vector samples (in red) to the ZNF154 overexpressors (in green), and parental UM-SCC1 (in blue).

epithelial markers and an increase in mesenchymal markers. In order to further explain these results, ZNF154 expression was investigated at the protein level by Western blot. In this experiment, samples used include ZNF154 overexpressing UM-SCC1 cells as well as UM-SCC1 cells transduced with an empty p-lenti virus. Samples for both were taken at various cellular passages. ZNF154 overexpressing samples contain a FLAG-tag protein tag to enable identification of ZNF154 protein expression. Using this construct, complete ZNF154 protein expression has an expected banding pattern of approximately 57 k. From the western blot results, we see no banding patterns in the empty samples, as expected. However, in the ZNF154 overexpressing samples a banding pattern of approximately 35 k is present **(Figure 3.4A)**. This shorter banding pattern was not expected, and is possibly indicative of the production of a truncated protein. Genomic PCR was then conducted to identify if a full-length gene for ZNF154 is present in the UM-SCC1 overexpressors **(Figure 3.4B)**. A full length ZNF154 gene has an approximate size of 1067 bp. (control lane). Other samples tested include UM-SCC1 cells transduced with an empty p-lenti virus, as well as ZNF154 overexpressing UM-SCC1 cells. The results show that the empty transductions do not display any banding patterns. However, the ZNF154 overexpressors show a smaller than expected genomic PCR product of approximately 900 bp in length. This suggests that an incomplete gene sequence may be present in the ZNF154 overexpressing cells. In order to test this hypothesis, genomic DNA samples from these cells were sequenced to identify any possible alterations in the ZNF154 gene. Sequencing of the ZNF154 overexpressing UM-SCC1 samples in the forward and reverse direction showed that internal sections of the ZNF154 gene had been deleted in these clones **(Figure 3.5)**. We hypothesize that this shortened gene is causing the production of the truncated protein, as seen in the Western blot.

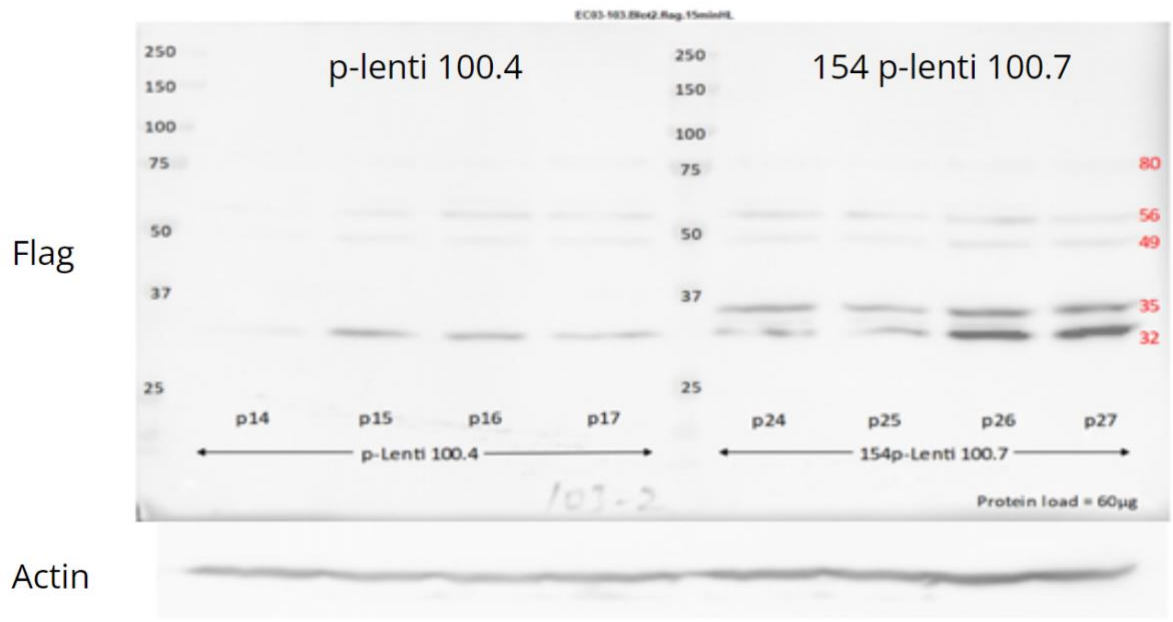

Figure 3.4A: Western Blot displaying UM-SCC1 samples transduced with empty vector and ZNF154, taken at various passages (Elizabeth Chia, 2021).

A western blot comparing UM-SCC1 samples transduced with empty vector and ZNF154. The empty samples are on the left of the blot and the ZNF154 samples are on the right side. The various samples were taken at different passages during cell culturing.

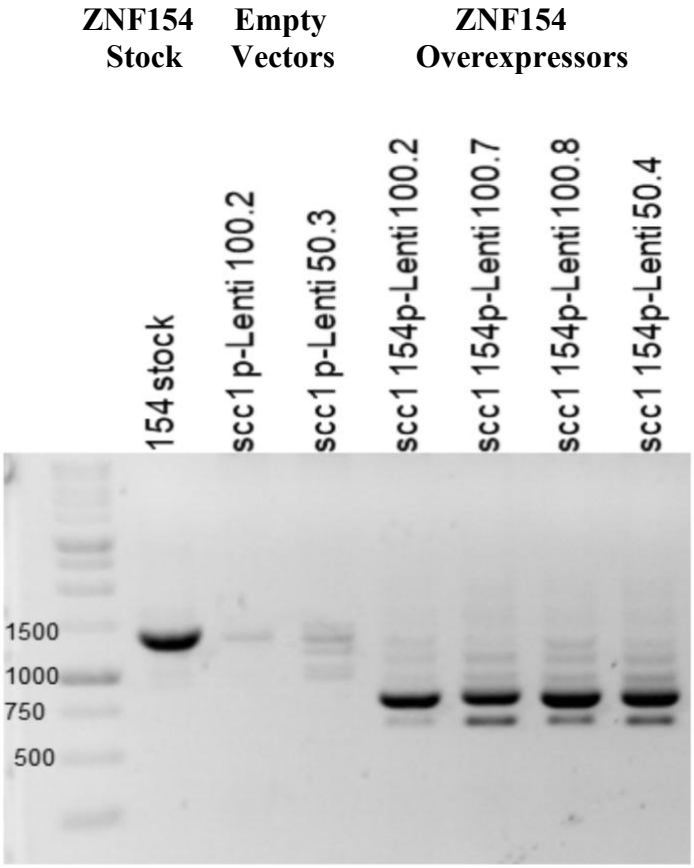

Figure 3.4B: Genomic PCR displaying UM-SCC1 samples transduced with empty vector and ZNF154 (Kendra Smith, 2021).

A genomic PCR comparing stock ZNF154 transcript, UM-SCC1 cells transduced with ZNF154, and UM-SCC1 cells transduced with an empty vector. This PCR is comparing the length of ZNF154 transcript in various samples.

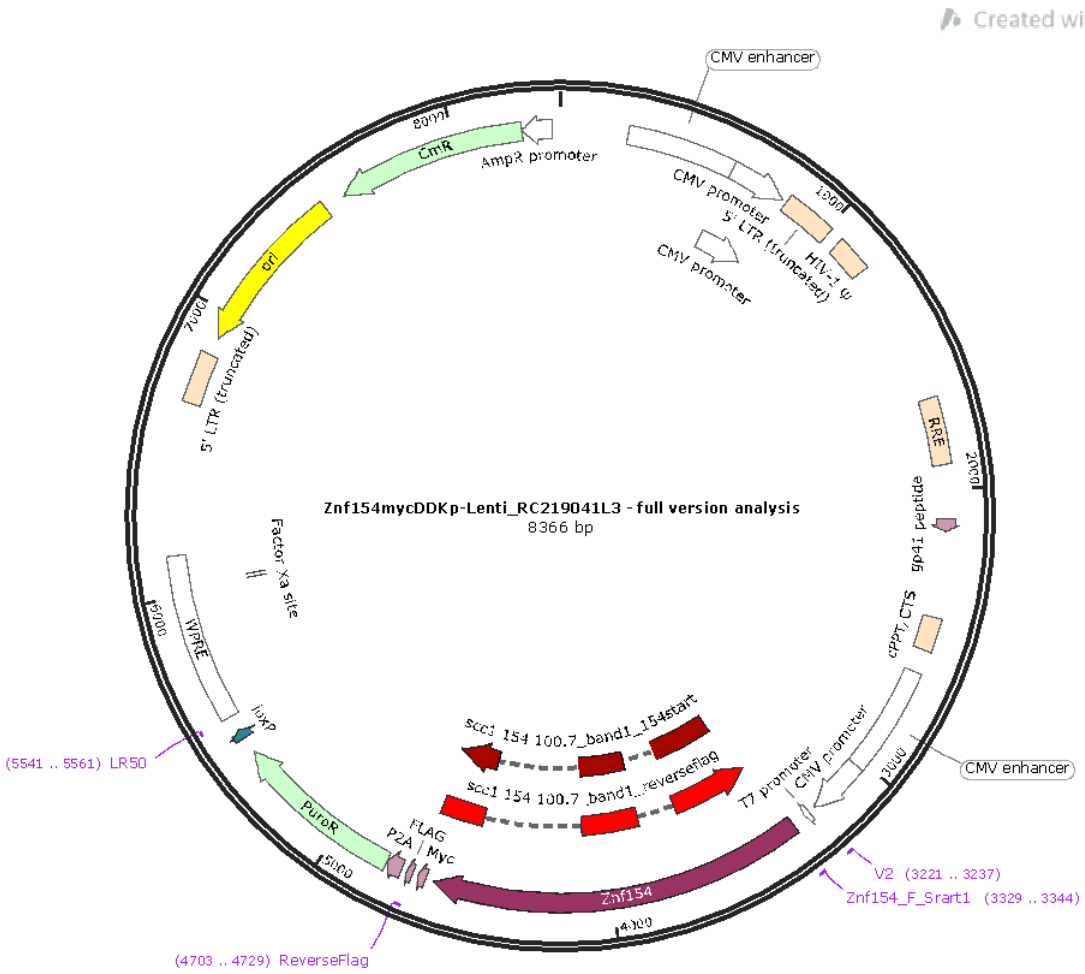

Figure 3.5: Sequencing of a UM-SCC1 sample transduced with ZNF154 (Kendra Smith, 2021).

A genomic sequencing displaying a UM-SCC1 sample transduced with ZNF154. In this figure the missing sections of ZNF154 can be seen having been sequenced in the forward and reverse directions.

Section 3.6: Overexpression of ZNF154 in Non-HNSCC Cell Line HEK293 Results in Full Length Protein with Growth Suppressive Phenotype

To test the effect of ZNF154 overexpression on a non-HNSCC cell line, HEK293 cells were transduced with ZNF154. The overexpression of ZNF154 was confirmed by qPCR as well as Western blot (**Figure 3.6A)**. HEK293 cells overexpressing ZNF154, as well as HEK293 cells transduced with an empty p-lenti virus, were measured by qPCR. The results indicate that there is ZNF154 expression in the overexpressing cells, but not in the empty vector controls. Additionally, Western blot analysis identified a 57 k protein in the overexpressing cells which is not present in the empty vector controls, consistent with the molecular weight of ZNF154. This suggests that the HEK293 ZNF154 overexpressing cells are capable of expressing a full length ZNF154 protein. Genomic PCR was also performed to identify whether a complete ZNF154 gene was present in the HEK293 overexpressing cells **(Figure 3.6B)**. PCR amplification of this genomic DNA product containing both the ZNF154 gene and adjacent vector product would produce a fragment of 1067 bp. ZNF154 overexpressing cells showed a PCR product of approximately 1067 for the complete gene. These results indicates that HEK293 cells were able to express full length ZNF154 product.

A growth assay was conducted on HEK293 cells transduced with an empty p-lenti virus, cells overexpressing ZNF154, and cells overexpressing ZNF132 **(Figure 3.1B)**. Cell counts were completed over a period of five days for all cell types. While the difference in growth rates between the samples were not statistically significant, the ZNF132 and ZNF154 overexpressors trended towards an increase in doubling time, compared to the empty transductions. Statistical analyses for cell growth were completed using one way ANOVA, however a post hoc Tukey

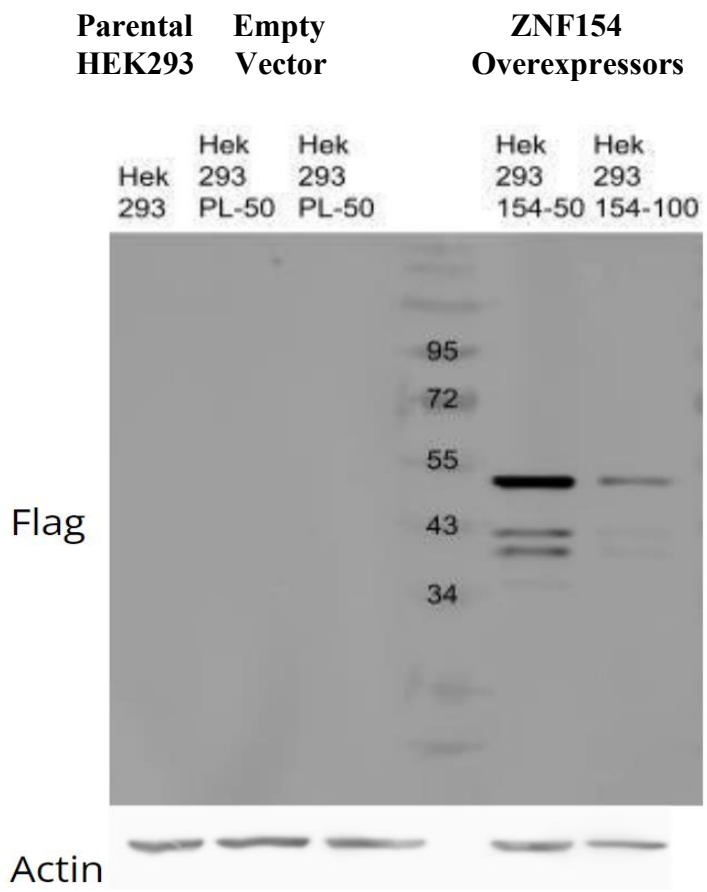

Figure 3.6A: Western blot displaying HEK293 samples transduced with empty vector and ZNF154.

A western blot displaying parental HEK293 and HEK293 cells transduced with an empty vector and ZNF154. This graph shows the expected banding pattern for ZNF154.

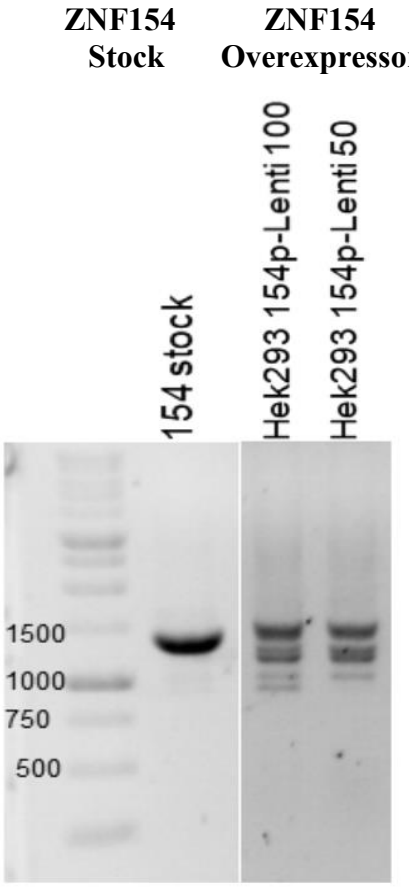

Figure 3.6B: Genomic PCR displaying UM-SCC1 samples transduced with ZNF154 and a stock ZNF154 control (Kendra Smith, 2021).

A genomic PCR comparing HEK293 samples transduced ZNF154 and the stock genomic ZNF154 control . The ZNF154 overexpressors are notably showing the expected banding pattern of a full length ZNF154 transcript.

is not required as the result was not statistically significant. **Figure 3.1A** represents the formula used to calculate doubling time.

Section 3.7: ZNF154 Overexpression may Target P53 and FOXO1 Expression in HEK293 Cells

Knowing that HEK293 cells are capable of expressing a complete ZNF154 protein, we wanted to identify any changes that may occur to target markers of interest. This was achieved using the Human XL Oncology Array Kit, which identifies changes related to various EMT markers **(Table 3.7, Figure 3.8)**. Duplicate arrays for samples of ZNF154 overexpressors, as well as parental HEK293 cells, were completed and analyzed via single factor ANOVA and confirmed with a post hoc Tukey test. The results indicate that FOXO1 and p53 are significantly down regulated in the ZNF154 overexpressors, compared to parentals.

DISCUSSION

The experiments show ZNF154 appears to produce a truncated gene and proteins when transduced into the HNSCC cell line UM-SCC1. However, this does not appear to occur with the cell line HEK293. This suggests that there is a mechanism preventing the expression of a complete ZNF154 gene in the HNSCC cell line. There appears to be an inability of the virus to insert a complete ZNF154 gene into the genome. The PCR and genomic sequencing highlight deletions of the ZNF154 gene where the lentivirus inserted the gene into the genome. A possible candidate mechanism to explain this phenomenon is KAP1 regulating the ZNF154 gene (Cassandri *et al*, 2017). KAP1 is a transcriptional repressor

Table 3.7: Table of Adjusted Integrated Density Measured from Antibody Arrays

	HEK293	HEK293	HEK293-ZNF154	HEK293-ZNF154
Marker Names	**Adjusted Integrated Density**			
Reference Spots	81	97	118	92
	111	90	109	90
α-Fetoprotein	310	292	318	294
	314	296	328	298
Amphiregulin	315	298	330	300
	315	298	330	300
Angiopoietin-1	316	298	331	300
	316	299	331	300
Angiopoietin-like 4	316	298	330	300
	315	299	330	300
ENPP-2/Autotaxin	312	295	326	296
	312	295	327	296
Axl	315	298	330	298
	315	298	330	298
BCL-x	315	299	331	300
	315	299	331	300
CA125/MUC16	317	300	332	302
	317	300	332	302

E-Cadherin	314	297	329	299
	313	297	330	299
VE-Cadherin	308	292	325	295
	304	287	323	291
Reference Spots	113	95	109	94
	106	89	104	94
CapG	310	291	328	297
	311	293	329	298
Carbonic Anhydrase IX	315	297	330	300
	315	297	331	300
Cathepsin B	310	292	328	297
	310	292	328	297
Cathepsin D	300	281	322	292
	301	281	322	292
Cathepsin S	313	296	328	298
	313	296	329	298
CEACAM-5	316	300	332	301
	316	300	331	300
Decorin	314	297	328	298
	313	296	328	298

Dkk-1	313	297	328	298
	313	297	328	298
DLL1	311	295	329	298
	311	295	329	298
EGF R/ErbB1	278	261	311	281
	277	261	310	281
Endoglin/CD105	315	298	330	300
	315	298	331	300
Endostatin	312	293	331	300
	311	292	331	300
Enolase 2	247	220	289	257
	250	218	288	258
eNOS	315	298	331	300
	315	298	331	300
EpCAM/TROP1	316	299	331	301
	316	299	331	301
Erα/NR3A1	317	300	333	302
	317	300	332	301
ErbB2	305	289	324	293
	305	289	325	292
ErbB3/Her3	315	299	331	300

	315	298	330	300
ErbB4	311	295	329	299
	311	295	329	299
FGF basic	298	283	324	294
	297	282	324	294
FoxC2	313	294	329	298
	312	293	328	297
FoxO1/FKHR	271	246	306	275
	272	247	309	274
Galectin-3	181	151	223	186
	179	155	217	186
GM-CSF	306	290	321	294
	311	295	326	298
CG α/β (HCG)	310	292	327	297
	310	293	327	297
HGF R/c-Met	305	289	325	295
	305	289	325	295
HIF-1α	313	297	329	299
	313	298	330	299
HNF-3β	311	294	327	296

	311	294	327	296
HO-1/HMOX1	306	287	326	295
	305	287	326	295
ICAM-1/CD54	316	299	331	301
	316	299	331	301
IL-2 Rα	315	300	331	300
	315	299	330	300
IL-6	313	297	328	298
	313	297	328	298
CXCL8/IL-8	308	290	325	295
	308	290	325	295
IL-18 Bpa	312	297	329	298
	313	297	329	298
Kallikrein 3/PSA	313	297	326	296
	313	297	326	296
Kallikrein 5	314	300	331	300
	315	300	331	301
Kallikrein 6	315	298	330	300
	314	298	330	300
Leptin	314	298	329	299
	314	298	329	300

Lumican	318	301	333	303
	318	302	333	303
CCL2/MCP-1	316	300	332	301
	317	300	332	301
CCL8/MCP-2	315	298	330	300
	315	298	330	300
CCL7/MCP-3	317	300	332	302
	316	300	332	302
M-CSF	310	293	328	297
	310	294	327	297
Mesothelin	310	294	325	295
	310	294	325	295
CCL3/MIP-1α	317	300	331	301
	316	299	332	301
CCL20/MIP-3α	313	296	330	299
	313	296	330	299
MMP-2	309	293	325	294
	308	293	325	294
MMP-3	308	293	325	293
	309	293	326	294

MMP-9	317	300	332	302
	317	301	332	302
MSP/MST1	315	299	330	300
	315	299	330	300
MUC-1	316	299	331	301
	316	299	331	301
Nectin-4	316	299	331	301
	316	299	331	300
Osteopontin (OPN)	303	287	318	287
	303	287	318	287
p27/Kip1	303	286	327	297
	300	285	327	297
p53	237	202	282	251
	229	196	280	245
PDGF-AA	312	295	328	301
	313	297	330	301
CD31/PECAM-1	316	299	331	299
	316	299	331	299
Progesterone R/NR3C3	314	297	329	276
	314	297	330	275
Progranulin	263	245	304	298

	265	245	305	299
Prolactin	313	296	329	300
	314	297	330	301
Prostasin/Prss8	316	299	331	302
	316	299	331	302
E-Selectin/CD62E	317	300	332	302
	317	301	332	302
Serpin B5/Maspin	317	301	332	298
	317	301	332	299
Serpin E1/PAI-1	313	297	329	298
	314	297	329	298
Snail	312	295	329	295
	311	294	329	295
SPARC	307	291	326	257
	306	291	326	252
Survivin	250	222	290	300
	245	212	287	301
Tenascin C	313	297	329	299
	314	299	331	298
Thrombospondin-1	313	295	329	297

	314	295	328	296
Tie-2	313	296	328	298
	313	297	329	298
u-Plasminogen Activator/Urokinase	316	299	331	301
	316	299	331	301
VCAM-1/CD106	316	300	332	301
	316	300	332	301
VEGF	317	300	332	302
	317	300	332	302
Vimentin	303	283	323	293
	304	285	323	293
Reference Spots	100	91	122	101
	107	91	117	105

This table displays a list of all 84 cancer related proteins on the Human XL Oncology Array Kit. The integrated density has been captured as a method of measuring the difference between the control array (HEK293) and the test array (HEK293 ZNF154). The integrated density has been adjusted for background noise to ensure consistency between the arrays and is presented in this chart as Adjusted Integrated Density. Each measurement was done in duplicate.

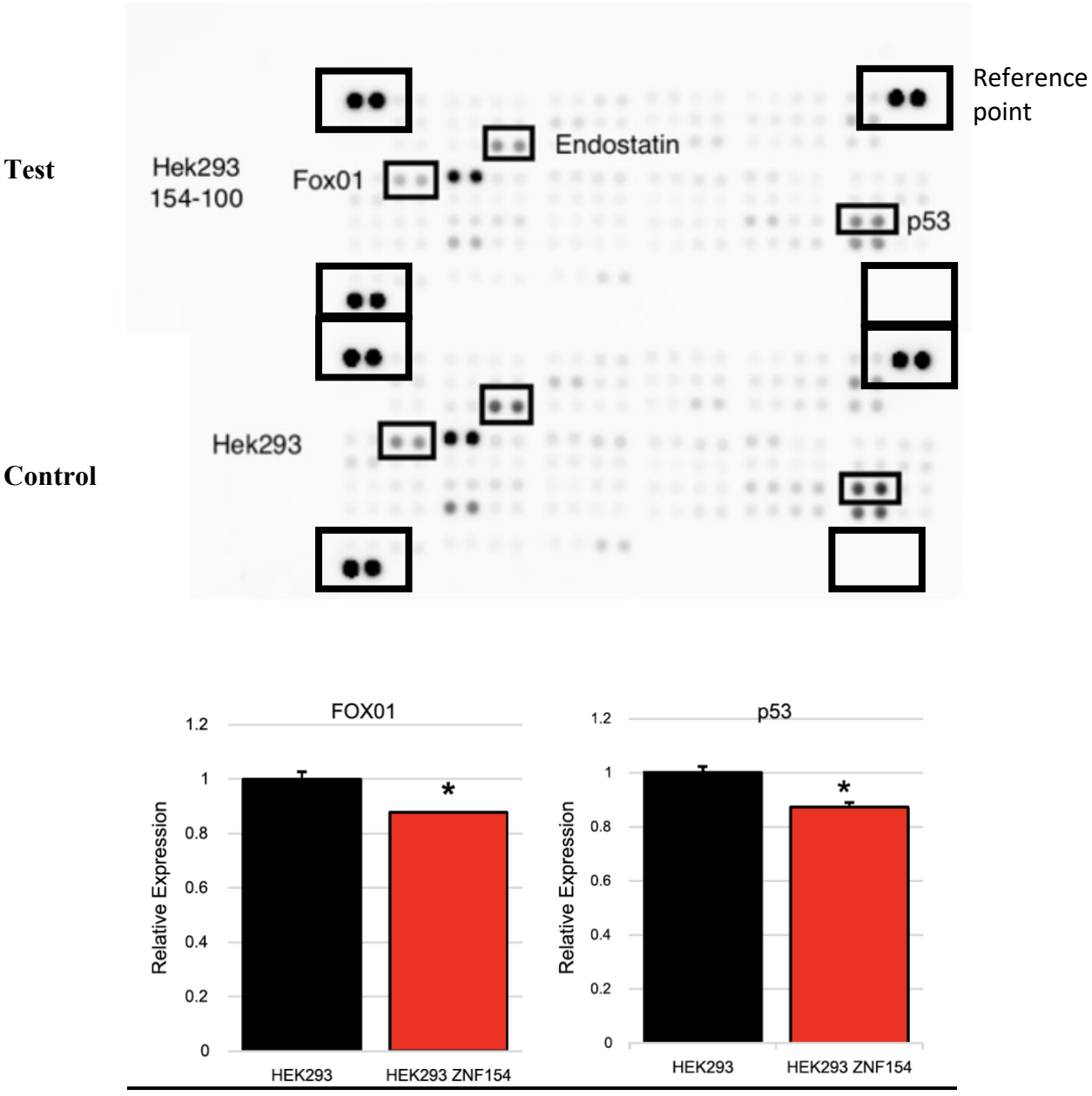

Figure 3.8: Human XL Oncology Array Kit comparing HEK293 transduced with ZNF154 and parental HEK293. Bar graphs highlight the statistical significance of FOX01 and p53, two targets of interest.

that typically interacts with KRAB-ZNFs via the KRAB domain. However, in some circumstances, instead of regulating ZNFs via the KRAB domain, it can bind downstream in the coding region of a gene (**Figure 3.9**; O'Green *et al*, 2007). We believe this is what is occurring with ZNF154 in the UM-SCC1 cell line. The UM-SCC1 samples transduced with ZNF154 have been sequenced in the forward and reverse directions. This has revealed possible KAP1 binding sites within the coding region of ZNF154 (**Figure 3.5**). These are possible regions where KAP1 is binding and regulating ZNF154 causing an incomplete gene to be produced. The inability of UM-SCC1 cells to express a complete ZNF154 transcript highlights a possible role of ZNF154 in oral cancer cell death. FoxO1 was significantly downregulated in the ZNF154 HEK293 overexpressors.

As seen in **Figure 3.8**, there was a significant decrease in FoxO1 and p53 expression in ZNF154 overexpressing HEK293 cells, compared to parental HEK293. FoxO1 has been shown to have a role in the epithelial mesenchymal transition (Remadevi *et al*., 2021). In the Remadevi study, increased expression of FoxO1 was associated with an increase in epithelial markers in HNSCC. Additionally, frequent mutations to the p53 gene have been associated with a shorter survival period in HNSCC (Zhou *et al*., 2016). The status of p53 and the rate at which it is mutated may show promise for the gene as a biomarker. These examples further highlight potential relations between our markers of interest, FoxO1 and p53, and HNSCC.

Expression of ZNF154 has been linked to worse prognosis in multiple types of cancer (He *et al*., 2022). Specifically, in a study be He *et al.,* low expression of ZNF154 was significantly associated with poor prognosis in gastric cancer. The demethylation of the ZNF154 promoter region was associated with increased ZNF154 expression and decreased growth and migration of esophageal squamous cell carcinoma (He *et al*., 2022). Further supporting its role in cancer,

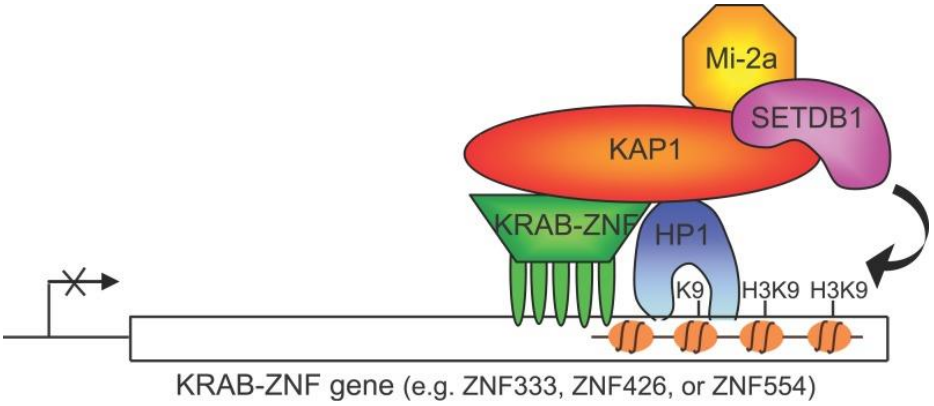

Figure 3.9: Diagram of KAP1 binding within the coding region of a KRAB-ZNF gene (O'Green *et al*., 2007). Creative Commons license.

A diagram showing the ability of KAP1 to bind within the coding region of a gene.

when overexpressed in HEK293 cells, a non-oral cancer cell line, a complete ZNF154 gene and protein are seen, unlike with the HNSCC cell line UM-SCC1 (**Figure 3.6A**). This further supports the hypothesis of ZNF154 having a role in oral cancer cell death. The process by which KAP1 may be regulating the ZNF154 coding region is unknown. It is possible that a different ZNF gene may be acting as an intermediary in the KAP1. HEK293 cells incorporated the whole ZNF154 gene, despite also expressing KAP1, however only one clone of UM-SCC1 was analyzed. It is possible this is an artifact of selecting a single aberrant clone that had defective integration. In future studies, other UM-SCC1 clones could be tested to verify that this cell line alters the lenti-virus integration into the genome.

CHAPTER 4: EFFECTS OF KAP1 KNOCKDOWN ON EXPRESSION OF ZNF132 AND ZNF154 IN HUMAN EPITHELIAL KERATINOCYTES

Co-Authorship Statement

As the primary author of this thesis I was responsible for all experiments conducted, analyses completed, and preparing an initial draft of this chapter. I would like to acknowledge and thank my supervisor, Dr. Tom Belbin, my supervisory committee, Dr. Touati Benoukraf and Michael Leitges for their invaluable feedback and constructive criticism in improving the initial draft.

Introduction

Section 4.1: Using Keratinocytes to Elucidate the Effects of KAP1 on ZNFs

Genomic sequencing of UM-SCC1 cells transduced with ZNF154 p-lenti virus reveal that there are deletions within the ZNF154 gene. This indicates a possible inability of the virus to insert itself in the cell genomes. KAP1 may be upregulated in UM-SCC1 cells, as they are a cancer cell line (Ferlier and Coulouarn, 2022). Cancer cell lines can show dysregulation in gene expression and signaling pathways. This same issue may not be present in keratinocytes cells as they are a non-cancerous epithelial cell line (Ścieżyńska *et al.*, 2019). This may allow for observations that were not possible when using the UM-SCC1 cell line. As an epithelial cell line, keratinocytes are especially relevant in the study of HNSCC.

Keratinocytes will be cultured with the application of a KAP1 inhibiting siRNA in an effort to knockdown the gene. This will allow us to test for the relative expression of KAP1, ZNF132, and ZNF154 in comparison to control keratinocytes treated with only transfection reagent. This experiment, if successful, will allow us to examine the effects of KAP1 on ZNFs of interest.

Section 4.2: Experiment Methods

Growth and Culturing of Human Epithelial Keratinocytes and UM-SCC1 Cells

Keratinocyte cells were obtained from Thermofisher (Cat.#C005CC) and were cultured in Complete Keratinocyte Media. These cells were validated by STR genotyping. Isolation of total RNA was carried out using the RNeasy total RNA kit (Cat.# 74104, Qiagen). A concentration of 50 nM of siRNA were used for the knockdowns, in addition to 1uL of Dharmafect Reagent #4 (Cat. T-2004-02, Fisher). siRNA concentration was based upon previous work completed by Nilita Sood. Taqman real-time PCR was used to confirm whether there is an

effect of mRNA expression at the transcript level, as per the manufacturer's instructions (Thermo Fisher Scientific).

UM-SCC1 cells were transfected with the KAP1 knockdown siRNA by itself, a sample that combined KAP1 siRNA and 5-azacytidine, and a sample that used solely 5-azacytidine. In addition, a non-targeting siRNA as well as mock transfection were used as controls. The treatments were added to the cells, which were then left to grow and harvested after a period of two to three days for RNA. Culturing and plating techniques are the same as described in **Section 3.2**. Keratinocyte cells used in knockdowns followed the same protocol, but were transfected with KAP1 siRNA. The Taqman probes used included the following: ZNF132 (ACCTCACTTGGTTCTTGGCATGGAG), ZNF154 (CTCTTTTAACCTCTCTAGATGTTCA), and KAP1. GAPDH was used as an endogenous control to normalize expression.

One way ANOVA was conducted using Microsoft Excel 2013 to calculate differences between two independent groups and confirmed with a post hoc Tukey test. A p-value of less than 0.05 was considered to be statistically significant.

Section 4.3: Results

qPCR analysis revealed that neither the KAP1 siRNA knockdown, 5-azacytidine treatment, or a combination of both were sufficient to re-express ZNF154 or ZNF132 in the UM-SCC1 cells. ZNF132 and ZNF154 expression was not detected over any of these conditions. Additionally, when the keratinocyte cells were knocked down with KAP1 siRNA ZNF132 expression was not marginally different. However, ZNF154 expression increased by 45% compared to NTC control (**Figure 4.1**). This was statistically significant and confirmed with a post hoc Tukey test.

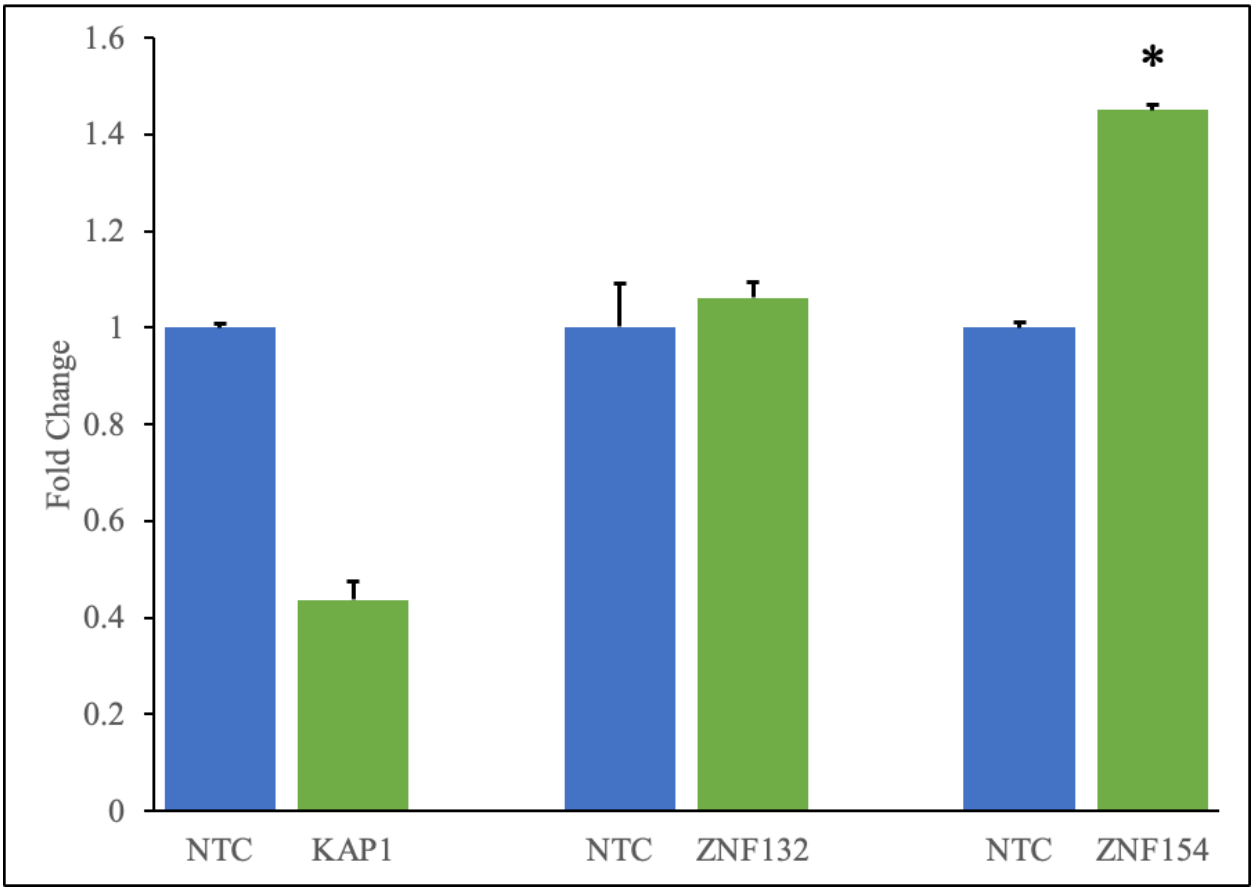

Figure 4.1: Fold change comparing KAP1 siRNA knockdown in keratinocyte cells relative to NTC.

Graphs comparing the fold change between keratinocyte cells knocked down with KAP1 siRNA. The graph in blue represents samples knocked down with an NTC siRNA and the graph in green represents cells knocked down with KAP1.

Section 4.4: Discussion

We hypothesized that KAP1 may be having a regulatory effect in the UM-SCC1 cell line, so we wanted to conduct a siRNA knockdown of KAP1 in the UM-SCC1 samples. In addition, we wanted to also use the demethylating agent 5-azacytidine because methylation may have also had a role in regulating ZNF132 and ZNF154 reexpression in the samples. The samples were tested for ZNF132 and ZNF154 expression using qPCR analysis. Parental UM-SCC1 cells have little, if any, expression of these genes. The qPCR analysis revealed that neither the siRNA knockdown, 5-azacytidine treatment, or a combination of both were sufficient to re-express either gene. This suggests there may be additional mechanisms beyond KAP1 regulation and DNA methylation that are suppressing the expression of these two genes.

Next, we wanted to test the effects of gene knockdowns on epithelial keratinocytes with some expression of ZNF132 and ZNF154. These cells were treated with siRNA to knockdown expression of ZNF132, ZNF154, ZNF671, and KAP1 under the conditions as described in **Section 4.2**. qPCR analysis revealed that KAP1 knockdown caused a significant increase in ZNF154 expression by 45%, compared to NTC (**Figure 4.1)**. This suggests that KAP1 may have a function in the co-regulation of ZNF genes. However, the mechanism that may be underlying this is unknown.

Our prior experiments indicated the presence of an incomplete ZNF154 gene in the UM-SCC1 cells, whereas the HEK293 cells displayed a complete ZNF154 gene(**Figure 3.4B, Figure 3.6 B**). For these cells to have grown, the puromycin gene must have been retained. While the entire construct was present in the HEK293 cells, the gene became truncated in the UM-SCC1 cells. We believe that the UM-SCC1 cells truncate ZNF154 as a survival mechanism, possibly through transcriptional repression. KAP1's role as a transcriptional regulator may contribute to

the ZNF154 becoming truncated in the UM-SCC1 cells. Another possible explanation is that aberrant splicing is causing a portion of the ZNF154 gene to be excluded, while retaining the puromycin resistance. A truncated mRNA transcript could alter the function of the ZNF154 gene, which may normally be lethal to the UM-SCC1 cells. Finally, another possibility is that the transgene may have undergone degradation or recombination during integration. This could allow the cell to retain the puromycin resistance gene, but alter the ZNF154 gene due to selective pressure. Future research could focus on the elucidation of this mechanism and how KAP1 affects ZNF genes.

A previous study by Tie et al (2018) has indicated that KAP1 represses endogenous retroviruses and ZNF genes. A loss of KAP1 caused a reduction of H3K9me3 enrichment at endogenous retroviruses and ZNF genes in the study. Retroviruses such as HERV-T and HERV-S and ZNF genes were shown to overlap with KAP1 binding sites and H3K9me3 in multiple cell types (Tie *et al*., 2018). H3K9me3 is essential for chromatin repression and genome stability. This indicates that the KAP1-KZNF pathway has a role in genome stability. Our results also indicate a potential connection between KAP1 and ZNF genes. Our results also indicate a potential connection between KAP1 and ZNF genes. In our results we see an increase in ZNF154 expression of approximately 40%. This signifies that there may be a connection between KAP1 expression and its ability to inhibit ZNF genes.

We acknowledge that our research in this area is some of the first of its kind. The effects of ZNF154 and its relation to KAP1 in HNSCC has not been investigated as explored in our research. As a result, it is difficult to draw comparisons between our work and what exists currently in the literature. We hope that our contributions on this topic will engage future investigations into the role of KAP1 in its interactions with ZNFs. Our lab is continuing research

on some promising ZNF targets in HNSCC that may be able to build upon the data presented in this thesis.

CHAPTER 5: CONCLUSION

Co-Authorship Statement

As the primary author of this thesis I was responsible for preparing an initial draft of this chapter. I would like to acknowledge and thank my supervisor, Dr. Tom Belbin, and my supervisory committee, Dr. Touati Benoukraf and Michael Leitges, for their invaluable feedback and constructive criticism in improving the initial draft.

Conclusion

In conclusion, my research focused on identifying the tumour suppressive properties of ZNF154 in HNSCC. A study by Lleras and Belbin in 2013 previously found that ZNF154 was frequently methylated and had decreased gene expression in HNSCC tumour tissue, compared to adjacent normal tissue. They identified ZNF154 as a candidate for future study because of its effects in HNSCC and reported tumour suppressive properties in other cancers. For example, a study by Hu *et al.* in 2017 identified ZNF154 as significantly affecting EMT markers, cell invasion, and other factors in nasopharynx cell lines (Hu *et al*., 2017). These and other studies provided the basis and reasoning for investigating ZNF154 and its effects in an HNSCC cell line.

First, we utilized HNSCC patient data from the Cancer Genome Atlas (TCGA) to assess the expression of both ZNF132 and ZNF154 and their associations with patient clinical and pathologic variables. From this, we observed that HNSCC patients with lower levels of ZNF132 and ZNF154 expression had significantly decreased overall survival rate compared to those with higher expression (**Figure 2.3**). Additionally, the tumour tissue has increased ZNF132 and ZNF154 methylation, as well as decreased gene expression, when compared to matched non-tumour tissue from the same patient. ZNF132 gene hypermethylation has also been associated with worse overall survival in lung adenocarcinoma (Hamada *et al*., 2021) HPV status can be associated with hypermethylation because HPV can be associated with global methylation (Camuzi *et al*., 2021).

Initial qPCR experiments to identify the effects of ZNF154 overexpression in UM-SCC1 oral cancer cells revealed increased expression of the mesenchymal marker vimentin and decreased expression of the epithelial marker E-cadherin in UM-SCC-1 cells overexpressing ZNF154. This was not our hypothesized result, as we expected the ZNF154 overexpressors to

push the cells toward an epithelial phenotype. A Western blot and genomic PCR appeared to indicate the production of a truncated protein as well as an incomplete ZNF154 genomic transcript. The same PCR products were sequenced in the forward and reverse directions, displaying missing internal segments of the ZNF154 gene. The missing ZNF154 gene segments appeared to overlap with KAP1 binding sites, indicating a possible explanation for the shortened gene, and a possible mechanism of transcriptional suppression of ZNF154 by the chromatin regulator KAP1 whereby it prevents the insertion of a complete ZNF154 gene into the genome.

Given the difficulties in expressing ZNF154 in cancer cells, we wanted to identify whether a non-HNSCC cell could express a complete ZNF154 gene. HEK293 cells overexpressing ZNF154 were investigated in the same manner as the UM-SCC1 samples. Western blot and genomic PCR appeared to indicate that there was complete protein expression, as well as a complete ZNF154 genomic transcript present. Having confirmed ZNF154 overexpression in the HEK293 cells, we wanted to identify what effects the overexpression of ZNF154 would have on EMT markers. To do this we used the Human XL Oncology antibody array kit which contains various cancer related markers. p53 and FOXO1 were found to be significantly expressed in the ZNF154 overexpressors. Growth assays conducted with the HEK293 ZNF132 and ZNF154 overexpressors displayed that the doubling time was not significantly different in overexpressors compared to control, but they trended towards significance. FOXO1 has been shown to have significant implications on invasion and the epithelial mesenchymal transition (Remadevi *et al*., 2021). Increased FOXO1 expression was associated with increased expression of epithelial markers. p53 mutations have been associated with shorter survival in HNSCC, and has been argued to be a useful biomarker for HNSCC (Zhou *et al*., 2016).

Finally, siRNA knockdowns were conducted on UM-SCC1 cells using both a KAP1 siRNA and the demethylating agent, 5-azacytidine. Neither of these treatments were sufficient in enabling ZNF154 or ZNF132 expression in parental UM-SCC1 samples. Furthermore, a similar knockdown was attempted with human epithelial keratinocyte (HEKn) cells. This included the use of ZNF132, ZNF154, ZNF671, and KAP1 siRNA's. When expression of ZNF154 was knocked down by siRNA treatment, there was a significant increase in KAP1 expression. This may support our theory of KAP1 being involved in the mechanism causing the insertion of an incomplete ZNF154 gene. It may also support a mechanism by which ZNF154 plays a role in regulating KAP1 itself. KAP1 typically binds within the promoter region of a gene, but with ZNF genes it can sometimes bind downstream in the coding region of the gene. Under the selective pressure of puromycin selection, we hypothesize that the ZNF genes are integrated without the presence of this KAP1 binding site so as to permit expression of the polycistronic transcript which includes puromycin resistance gene. This is what we believe is occurring with ZNF154. However, the mechanism that may be causing this is unknown.

Limitations and Future Directions

Limitations of the research include the inability to express a full length gene of ZNF154 in an HNSCC cell line. However, expression of full length ZNF154 was possible in HEK-293 cells as a means to identify effects of ZNF154 overexpression on EMT markers. The changes in EMT related markers may be different in an HNSCC cell line. The TCGA dataset is heterogenous, meaning tumour samples can contain normal cells as well as immune-infiltrated cells. This can introduce noise into the RNA-seq data. Another limitation of our study included the possibility of another ZNF interacting with ZNF132 and ZNF154 in relation to our

hypothesis. We believe that KAP1 is binding within the coding region of these ZNFs, but there is also a possibility that an unknown ZNF is having a role in transcription regulation. This could prove difficult to isolate if this is the case. Finally, the overexpression of ZNF132 and ZNF154 could affect cell viability differently when expressed in different cell lines. This could affect the surviving cells in culture due to culture induced selection bias. This could affect results from testing done on these cell lines.

Future studies related to this topic could also focus on identifying the mechanism causing the production of an incomplete ZNF154 gene in HNSCC cell lines. Another ZNF may be acting as an intermediary in KAP1 binding to the coding region of ZNF154. If this is true, isolating and identifying that ZNF gene may be important to understanding the role of ZNF proteins in HNSCC cells, and the potential role of ZNF154 in target gene regulation. Further research could also use gene editing to induce a mutation or deletion within the suspected KAP1 binding site. This could then be assessed to determine the effect on gene expression of the ZNFs. This could be especially useful in helping to identify the reason we are not able to fully express ZNF154 in UM-SCC1 cells. If we are able to fully express ZNF154 in the UM-SCC1 cells, we could compare gene expression, profiles between cells able to express the gene, and those that are not. This could allow us to identify downstream targets and pathways that are influenced by the repression of ZNF154. Additionally, research is currently being undertaken by other lab members within our group to expand upon the results of the research presented in the thesis. This includes identifying other candidate ZNFs of similar interest to HNSCC, and determining how they are affected by KAP1 binding. The goal is to determine whether other ZNFs are being repressed by KAP1, and if able to be expressed, what are their effects in HSCC.

References

Alsahafi, E., Begg, K., Amelio, I., Raulf, N., Lucarelli, P., Sauter, T., & Tavassoli, M. (2019). Clinical update on head and neck cancer: molecular biology and ongoing challenges. *Cell death & disease, 10*(8), 540. https://doi.org/10.1038/s41419-019-1769-9

Asheer, J., Jensen, J. S., Grønhøj, C., Jakobsen, K. K., & Buchwald, C. V. (2020). Rate of locoregional recurrence among patients with oropharyngeal squamous cell carcinoma with known HPV status: a systematic review. *Acta oncologica (Stockholm, Sweden)*, *59*(9), 1131–1136. https://doi.org/10.1080/0284186X.2020.1759822

Aupérin, A. (2020). Epidemiology of head and neck cancers: an update. *Current opinion in oncology, 32*, 3, 178-186. doi:10.1097/CCO.0000000000000629

Baur, M., Kienzer, H.-R., Schweiger, J., DeSantis, M., Gerber, E., Pont, J., Hudec, M., Schratter Sehn, A. U., Wicke, W., & Dittrich, C. (2002). Docetaxel/cisplatin as first-line chemotherapy in patients with head and neck carcinoma: A phase II trial. *Cancer*, *94*(11), 2953–2958. https://doi.org/10.1002/cncr.10574

Bonner, J. A., Harari, P. M., Giralt, J., Azarnia, N., Shin, D. M., Cohen, R. B., Jones, C. U., Sur, R., Raben, D., Jassem, J., Ove, R., Kies, M. S., Baselga, J., Youssoufian, H., Amellal, N., Rowinsky, E. K., & Ang, K. K. (2006). Radiotherapy plus cetuximab for squamous-cell carcinoma of the head and neck. *The New England journal of medicine*, *354*(6), 567–578. https://doi.org/10.1056/NEJMoa053422

Brenner, D. R. , Weir, H. K., Demers, A. A, Ellison, L. F., Louzado, C., Shaw, A., . . . Smith, L. M. (2020). *Projected estimates of cancer in Canada in 2020. Canadian Medical Association Journal (CMAJ), 192*(9), E199-E205.

Cadoni, G., Giraldi, L., Petrelli, L., Pandolfini, M., Giuliani, M., Paludetti, G., Pastorino, R., Leoncini, E., Arzani, D., Almadori, G., & Boccia, S. (2017). Prognostic factors in head and neck cancer: a 10-year retrospective analysis in a single-institution in Italy. Fattori prognostici del tumore testa-collo: un'analisi retrospettiva monocentrica di 10 anni. *Acta otorhinolaryngologica Italica : organo ufficiale della Societa italiana di otorinolaringologia e chirurgia cervico-facciale*, *37*(6), 458–466. https://doi.org/10.14639/0392-100X-1246

Camuzi, D., Buexm, L. A., Lourenço, S. Q. C., Esposti, D. D., Cuenin, C., Lopes, M. S. A., Manara, F., Talukdar, F. R., Herceg, Z., Ribeiro Pinto, L. F., & Soares-Lima, S. C. (2021). HPV Infection Leaves a DNA Methylation Signature in Oropharyngeal Cancer Affecting Both Coding Genes and Transposable Elements. *Cancers*, *13*(14), 3621. https://doi.org/10.3390/cancers13143621

Canadian Cancer Society. Cancer-specific stats 2020. Available at https://www.cancer.ca/~/media/cancer.ca/CW/cancer%20information/cancer%20101/Ca n adian%20cancer%20statistics%20supplementary%20information/2020/2020_cancer specific-stats.pdf?la=en

Caponigro, F., Massa, E., Rosati, G., Biglietto, M., De Lucia, L., Sguotti, C., Sganga, P., Avallone, A., Comella, P., Mantovani, G., & Comella, G. (2001). Docetaxel and cisplatin in locally advanced or metastatic squamous-cell carcinoma of the head and neck: A phase II study of the Southern Italy Cooperative Oncology Group (SICOG). *Annals of Oncology*, *12*(2), 199–202. https://doi.org/10.1023/A:1008322415335

Cassandri, M., Smirnov, A., Novelli, F., Pitolli, C., Agostini, M., Malewicz, M., Melino, G., & Raschellà, G. (2017). Zinc-finger proteins in health and disease. *Cell death discovery,*

3, 17071. https://doi.org/10.1038/cddiscovery.2017.71

Chang, J. H., Wu, C. C., Yuan, K. S., Wu, A., & Wu, S. Y. (2017). Locoregionally recurrent head and neck squamous cell carcinoma: incidence, survival, prognostic factors, and treatment outcomes. *Oncotarget*, *8*(33), 55600–55612. https://doi.org/10.18632/oncotarget.16340

Cohen, E. E. W., Bell, R. B., Bifulco, C. B., Burtness, B., Gillison, M. L., Harrington, K. J., Le, Q.-T., Lee, N. Y., Leidner, R., Lewis, R. L., Licitra, L., Mehanna, H., Mell, L. K., Raben, A., Sikora, A. G., Uppaluri, R., Whitworth, F., Zandberg, D. P., & Ferris, R. L. (2019). The Society for Immunotherapy of Cancer consensus statement on immunotherapy for the treatment of squamous cell carcinoma of the head and neck (HNSCC). *Journal for Immunotherapy of Cancer*, *7*(1), 184–184. https://doi.org/10.1186/s40425-019-0662-5

Cramer, J. D., Burtness, B., Le, Q. T., & Ferris, R. L. (2019). The changing therapeutic landscape of head and neck cancer. *Nature reviews. Clinical oncology, 16*(11), 669–683. https://doi.org/10.1038/s41571-019-0227-z

Cury, S. S., Miranda, P. M. de, Marchi, F. A., Canto, L. M. do, Chulam, T. C., Petersen, A. H., Aagaard, M. M., Pinto, C. A. L., Kowalski, L. P., & Rogatto, S. R. (2021). Germline variants in DNA repair genes are associated with young-onset head and neck cancer. *Oral Oncology*, *122*, 105545–105545. https://doi.org/10.1016/j.oraloncology.2021.105545

Descamps, G., Karaca, Y., Lechien, J. R., Kindt, N., Decaestecker, C., Remmelink, M., Larsimont, D., Andry, G., Hassid, S., Rodriguez, A., Khalife, M., Journe, F., & Saussez, S. (2016). Classical risk factors, but not HPV status, predict survival after chemoradiotherapy in advanced head and Neck Cancer patients. *Journal of Cancer Research and Clinical Oncology, 142*(10), 2185–2196.

https://doi.org/10.1007/s00432- 016-2203-7

Eisa, M., & Omer, E. (2022). Cetuximab-Induced Small Intestine Stricture in Metastatic Squamous Cell Carcinoma of the Oral Cavity. *ACG case reports journal*, *9*(6), e00784. https://doi.org/10.14309/crj.0000000000000784

Elrefaey, S., Massaro, M. A., Chiocca, S., Chiesa, F., & Ansarin, M. (2014). HPV in oropharyngeal cancer: the basics to know in clinical practice. *Acta otorhinolaryngologica Italica : organo ufficiale della Societa italiana di otorinolaringologia e chirurgia cervico-facciale, 34*(5), 299–309.

Errazquin, R., Sieiro, E., Moreno, P., Ramirez, M. J., Lorz, C., Peral, J., Ortiz, J., Casado, J. A., Roman-Rodriguez, F. J., Hanenberg, H., Río, P., Surralles, J., Segrelles, C., & Garcia-Escudero, R. (2021). Generating new FANCA-deficient HNSCC cell lines by genomic editing recapitulates the cellular phenotypes of Fanconi anemia. *Genes, 12*(4), 548. https://doi.org/10.3390/genes12040548

Fares, J., Fares, M. Y., Khachfe, H. H., Salhab, H. A., & Fares, Y. (2020). Molecular principles of metastasis: a hallmark of cancer revisited. *Signal Transduction and Targeted Therapy*, *5*(1), 28–28. https://doi.org/10.1038/s41392-020-0134-x

Ferlier, T., & Coulouarn, C. (2022). Regulation of Gene Expression in Cancer-An Overview. *Cells (Basel, Switzerland)*, *11*(24), 4058-. https://doi.org/10.3390/cells11244058

Ferris R. L. (2015). Immunology and Immunotherapy of Head and Neck Cancer. *Journal of clinical oncology : official journal of the American Society of Clinical Oncology*, *33*(29), 3293–3304. https://doi.org/10.1200/JCO.2015.61.1509

Ghosh, N., Tiongson, M. D., Stewart, C., Chan, K. K., Jivanelli, B., Cappelli, L., & Bass, A. R. (2021). Checkpoint Inhibitor-Associated Arthritis: A Systematic Review of Case Reports and Case Series. *Journal of clinical rheumatology : practical reports on*

rheumatic & musculoskeletal diseases, *27*(8), e317–e322. https://doi.org/10.1097/RHU.0000000000001370

Glisson, B. S., Murphy, B. A., Frenette, G., Khuri, F. R., & Forastiere, A. A. (2002). Phase II Trial of Docetaxel and Cisplatin Combination Chemotherapy in Patients With Squamous Cell Carcinoma of the Head and Neck. *Journal of Clinical Oncology*, *20*(6), 1593–1599. https://doi.org/10.1200/JCO.20.6.1593

Goel, B., Tiwari, A. K., Pandey, R. K., Singh, A. P., Kumar, S., Sinha, A., Jain, S. K., & Khattri, A. (2022). Therapeutic approaches for the treatment of head and neck squamous cell carcinoma-An update on clinical trials. *Translational oncology*, *21*, 101426. https://doi.org/10.1016/j.tranon.2022.101426

Graham, K., & Unger, E. (2018). Overcoming tumor hypoxia as a barrier to radiotherapy, chemotherapy and immunotherapy in cancer treatment. *International journal of nanomedicine*, *13*, 6049–6058. https://doi.org/10.2147/IJN.S140462

Hamada, K., Tian, Y., Fujimoto, M., Takahashi, Y., Kohno, T., Tsuta, K., Watanabe, S., Yoshida, T., Asamura, H., Kanai, Y., & Arai, E. (2021). DNA hypermethylation of the ZNF132 gene participates in the clinicopathological aggressiveness of "pan-negative"-type lung adenocarcinomas. *Carcinogenesis (New York)*, *42*(2), 169–179.

He, J., Huang, J., Tang, G., Wang, P., He, M., & Wei, S. (2022). Low Expression of ZNF154 is Related to Poor Prognosis in Gastric Cancer. *Cancer Management and Research*, *14*, 659–672.

Head and neck cancer - types of treatment. Cancer.Net. (2021, July 21). Retrieved September 15, 2021, from https://www.cancer.net/cancer-types/head-and-neck-cancer/types-

treatment.

Hu, Y., Qi, M. F., Xu, Q. L., Kong, X. Y., Cai, R., Chen, Q. Q., Tang, H. Y., & Jiang, W. (2017). Candidate tumor suppressor ZNF154 suppresses invasion and metastasis in NPC by inhibiting the EMT via Wnt/β-catenin signalling. *Oncotarget, 8*(49), 85749–85758. https://doi.org/10.18632/oncotarget.20479

Iyengar, S., Ivanov, A. V., Jin, V. X., Rauscher, F. J., 3rd, & Farnham, P. J. (2011). Functional analysis of KAP1 genomic recruitment. *Molecular and cellular biology*, *31*(9), 1833–1847. https://doi.org/10.1128/MCB.01331-10

Johnson, D.E., Burtness, B., Leemans, C.R. *et al*. Head and neck squamous cell carcinoma. *Nat Rev Dis Primers 6*, 92 (2020). https://doi.org/10.1038/s41572-020-00224-3

Journal of Cancer Diagnosis Open Access. Journal of Cancer Diagnosis- Open Access Journals. (n.d.). https://www.omicsonline.org/cancer-diagnosis.php.

Kitamura, N., Sento, S., Yoshizawa, Y., Sasabe, E., Kudo, Y., & Yamamoto, T. (2021). Current trends and future prospects of molecular targeted therapy in head and neck squamous cell
carcinoma. *International Journal of Molecular Sciences*, *22*(1), 1–13. https://doi.org/10.3390/ijms22010240

Lee, Y.-G., Kang, E. J., Keam, B., Choi, J.-H., Kim, J.-S., Park, K. U., Lee, K. E., Kwon, J. H., Lee, K.-W., Kim, M. K., Ahn, H. K., Shin, S. H., Kim, H. R., Kim, S.-B., & Yun, H. J. (2020). Treatment strategy and outcomes in locally advanced head and neck squamous cell carcinoma: a nationwide retrospective cohort study (KCSG HN13-01). *BMC Cancer, 20*(1), 813–819. https://doi.org/10.1186/s12885-020-07297-z

Lleras, R. A., Smith, R. V., Adrien, L. R., Schlecht, N. F., Burk, R. D., Harris, T. M., Childs, G., Prystowsky, M. B., & Belbin, T. J. (2013). Unique DNA methylation loci distinguish anatomic site and HPV status in head and neck squamous cell carcinoma. *Clinical cancer research : an official journal of the American Association for Cancer Research, 19*(19), 5444–5455. https://doi.org/10.1158/1078-0432.CCR-12-3280

Mahmutović, L., Bilajac, E., & Hromić-Jahjefendić, A. (2021). Meet the Insidious Players: Review of Viral Infections in Head and Neck Cancer Etiology with an Update on Clinical Trials. *Microorganisms*, *9*(5), 1001.

Margolin, G., Petrykowska, H. M., Jameel, N., Bell, D. W., Young, A. C., & Elnitski, L. (2016). Robust Detection of DNA Hypermethylation of ZNF154 as a Pan-Cancer Locus with in Silico Modeling for Blood-Based Diagnostic Development. *The Journal of molecular diagnostics : JMD, 18*(2), 283–298. https://doi.org/10.1016/j.jmoldx.2015.11.004

Mundi, N., Ghasemi, F., Zeng, P. Y. F., Prokopec, S. D., Patel, K., Kim, H. A. J., . . . Nichols, A. C. (2020). Sex disparities in head & neck cancer driver genes: An analysis of the TCGA dataset. *Oral Oncology, 104*, 104614.

NCI dictionary of Cancer TERMS. National Cancer Institute. (n.d.). Retrieved September 15, 2021, from https://www.cancer.gov/publications/dictionaries/cancer-terms/def/immune checkpoint-inhibitor.

Niu, Y.-M., Du, X.-Y., Cai, H.-X., Zhang, C., Yuan, R.-X., Zeng, X.-T., & Luo, J. (2015). Increased risks between interleukin-10 gene polymorphisms and haplotype and head and neck cancer: A meta-analysis. *Scientific Reports, 5*(1). https://doi.org/10.1038/srep17149

O'Geen, H., Squazzo, S. L., Iyengar, S., Blahnik, K., Rinn, J. L., Chang, H. Y., Green, R., & Farnham, P. J. (2007). Genome-wide analysis of KAP1 binding suggests autoregulation

of KRAB-ZNFs. *PLoS Genetics*, *3*(6), e89–e89.

Oosting, S. F., & Haddad, R. I. (2019). Best Practice in Systemic Therapy for Head and Neck Squamous Cell Carcinoma. *Frontiers in oncology*, *9*, 815. https://doi.org/10.3389/fonc.2019.00815

Oral and Oropharyngeal Cancer - Stages and Grades. Cancer.Net. (2021, May 5). https://www.cancer.net/cancer-types/oral-and-oropharyngeal-cancer/stages-and-grades.

Oral Cavity and Oropharyngeal Cancer Stages. American Cancer Society. (n.d.). https://www.cancer.org/cancer/oral-cavity-and-oropharyngeal-cancer/detection-diagnosis staging/staging.html.

Pestana, R. C., Becnel, M., Rubin, M. L., Torman, D. K., Crespo, J., Phan, J., Hanna, E., Bell, D., Glisson, B. S., Johnson, J. M., Lee, J. J., & Ferrarotto, R. (2020). Response rates and survival to systemic therapy after immune checkpoint inhibitor failure in recurrent/metastatic head and neck squamous cell carcinoma. *Oral oncology*, *101*, 104523. https://doi.org/10.1016/j.oraloncology.2019.104523

Pisani, P., Airoldi, M., Allais, A., Aluffi Valletti, P., Battista, M., Benazzo, M., Briatore, R., Cacciola, S., Cocuzza, S., Colombo, A., Conti, B., Costanzo, A., Della Vecchia, L., Denaro, N., Fantozzi, C., Galizia, D., Garzaro, M., Genta, I., Iasi, G. A., Krengli, M., … Zigliani, A. (2020). Metastatic disease in head & neck oncology. *Acta otorhinolaryngologica Italica : organo ufficiale della Societa italiana di otorinolaringologia e chirurgia cervico-facciale*, *40*(SUPPL. 1), S1–S86. https://doi.org/10.14639/0392-100X-suppl.1-40-2020

Plavc, G., & Strojan, P. (2020). Combining radiotherapy and immunotherapy in definitive treatment of head and neck squamous cell carcinoma: review of current clinical trials. *Radiology and oncology*, *54*(4), 377–393. https://doi.org/10.2478/raon-2020-0060

Remadevi, V., Muraleedharan, P., & Sreeja, S. (2021). FOXO1: a pivotal pioneer factor in oral squamous cell carcinoma. *American journal of cancer research*, *11*(10), 4700–4710.

Stoyanov, G. S., Kitanova, M., Dzhenkov, D. L., Ghenev, P., & Sapundzhiev, N. (2017). Demographics of Head and Neck Cancer Patients: A Single Institution Experience. *Cureus, 9*(7), e1418. https://doi.org/10.7759/cureus.1418

Su, Y.-Y., Chien, C.-Y., Luo, S.-D., Huang, T.-L., Lin, W.-C., Fang, F.-M., Chiu, T.-J., Chen, Y.-H., Lai, C.-C., Hsu, C.-M., & Li, S.-H. (2016). Betel nut chewing history is an independent prognosticator for smoking patients with locally advanced stage IV head and neck squamous cell carcinoma receiving induction chemotherapy with docetaxel, cisplatin, and Fluorouracil. *World Journal of Surgical Oncology, 14*(1). https://doi.org/10.1186/s12957-016-0844-2

UICC. (2021). How to use the TNM Classification.

Van der Kamp, M. F., Muntinghe, F. O., Iepsma, R. S., Plaat, B. E., van der Laan, B. F., Algassab, A., Steenbakkers, R. J., Witjes, M. J., van Dijk, B. A., de Bock, G. H., & Halmos, G. B. (2020). Predictors for distant metastasis in head and neck cancer, with emphasis on age. *European Archives of Oto-Rhino-Laryngology*, *278*(1), 181–190. https://doi.org/10.1007/s00405-020-06118-0

Wolf, G., Greenberg, D., & Macfarlan, T. S. (2015). Spotting the enemy within: Targeted

silencing of foreign DNA in mammalian genomes by the Krüppel-associated box zinc finger protein family. *Mobile DNA*, *6*(1), 17–17. https://doi.org/10.1186/s13100-015-0050-8

Xu, W., Xu, M., Wang, L., Zhou, W., Xiang, R., Shi, Y., Zhang, Y., & Piao, Y. (2019). Integrative analysis of DNA methylation and gene expression identified cervical cancer-specific diagnostic biomarkers. *Signal Transduction and Targeted Therapy*, *4*(1), 55–11. https://doi.org/10.1038/s41392-019-0081-6

Zhan, W., Li, Y., Liu, X., Zheng, C., & Fu, Y. (2020). ZNF671 Inhibits the Proliferation and Metastasis of NSCLC via the Wnt/β-Catenin Pathway. *Cancer Management and Research*, *12*, 599–610. https://doi.org/10.2147/CMAR.S235933

Zhou, G., Liu, Z., & Myers, J. N. (2016). TP53 Mutations in Head and Neck Squamous Cell Carcinoma and Their Impact on Disease Progression and Treatment Response. *Journal of Cellular Biochemistry*, *117*(12), 2682

Appendix A: Kruppel-family zinc finger proteins as emerging epigenetic biomarkers in head and neck squamous cell carcinoma

Appendix A is a published paper for which I am a primary co-author, using data I completed over the course of my Master's degree. The paper is published in the Journal of Otolaryngology – Head and Neck Surgery.

Authors

Patrick Pearson, Kendra Smith, Nilita Sood, Elizabeth Chia, Alicia Follett, Michael B. Prystowsky, Simon Kirby & Thomas J. Belbin

Contributions

KS, EC and AF designed and carried out experiments to overexpress ZNF proteins in UM-SCC-1 and HEK-293 cells. PP and NS analyzed and interpreted patient data regarding association between ZNF protein methylation and expression, and patient clinical parameters. PP and KS carried out phenotypic experiments on HEK-293 and UM-SCC-1 cells. PP carried out antibody arrays to identify potential targets of ZNF154. PP, KLS, and TJB contributed to the writing of the manuscript. MBP, SK and TJB contributed insights into the clinical associations associated with ZNF protein expression, and edited the final version of the manuscript for publication. All authors read and approved the final manuscript.

Journal of Otolaryngology - Head & Neck Surgery

ORIGINAL RESEARCH ARTICLE

Open Access

Kruppel-family zinc finger proteins as emerging epigenetic biomarkers in head and neck squamous cell carcinoma

Patrick Pearson[1†], Kendra Smith[1,2†], Nilita Sood[2], Elizabeth Chia[1,2], Alicia Follett[1], Michael B. Prystowsky[4], Simon Kirby[3] and Thomas J. Belbin[1,2,4*]

Abstract

Background Krüppel-type zinc finger protein genes located on chromosome 19q13 are aberrantly hypermethylated with high frequency in all anatomic sub-sites of head and neck cancers as well as other epithelial tumours resulting in decreased expression.

Methods We examined prognostic significance of ZNF154 and ZNF132 expression and DNA methylation in independent patient cohort of about 500 head and neck cancer patients in the Cancer Genome Atlas (TCGA). We also overexpressed these genes in HEK-293 cells, as well as the oral cancer cell line UM-SCC-1.

Results In 20 patients from the TCGA cohort of HNSCC patients where ZNF154 and ZNF132 DNA methylation and RNA expression could be compared in tumor and adjacent normal tissue, there was increased DNA methylation and decreased expression of both ZNF154 and ZNF132 in primary tumours. Low ZNF154 and low ZNF132 expression were associated with shorter overall survival in both head and neck squamous cell carcinoma (HNSCC) and lung adenocarcinoma (LUAC patients). While expression of these proteins in HEK-293 cells produced full-length protein, only truncated copies could be expressed in head and neck cancer cells (UM-SCC-1). The truncated version of ZNF154 protein increased doubling time and reduced cell migration in UM-SCC-1 cancer cells.

Conclusions Both ZNF132 and ZNF154 represent novel clinically significant biomarkers in head and neck cancer with potential tumour suppressive properties. Future studies will address the underlying molecular mechanisms by which ZNF154 expression in HNSCC contributes to the control of cell growth and migration.

Keywords ZNF, Oral cavity, Squamous, Carcinoma

†Patrick Pearson and Kendra Smith contributed equally to the manuscript.

*Correspondence:
Thomas J. Belbin
tbelbin@mun.ca
Full list of author information is available at the end of the article

Graphical abstract

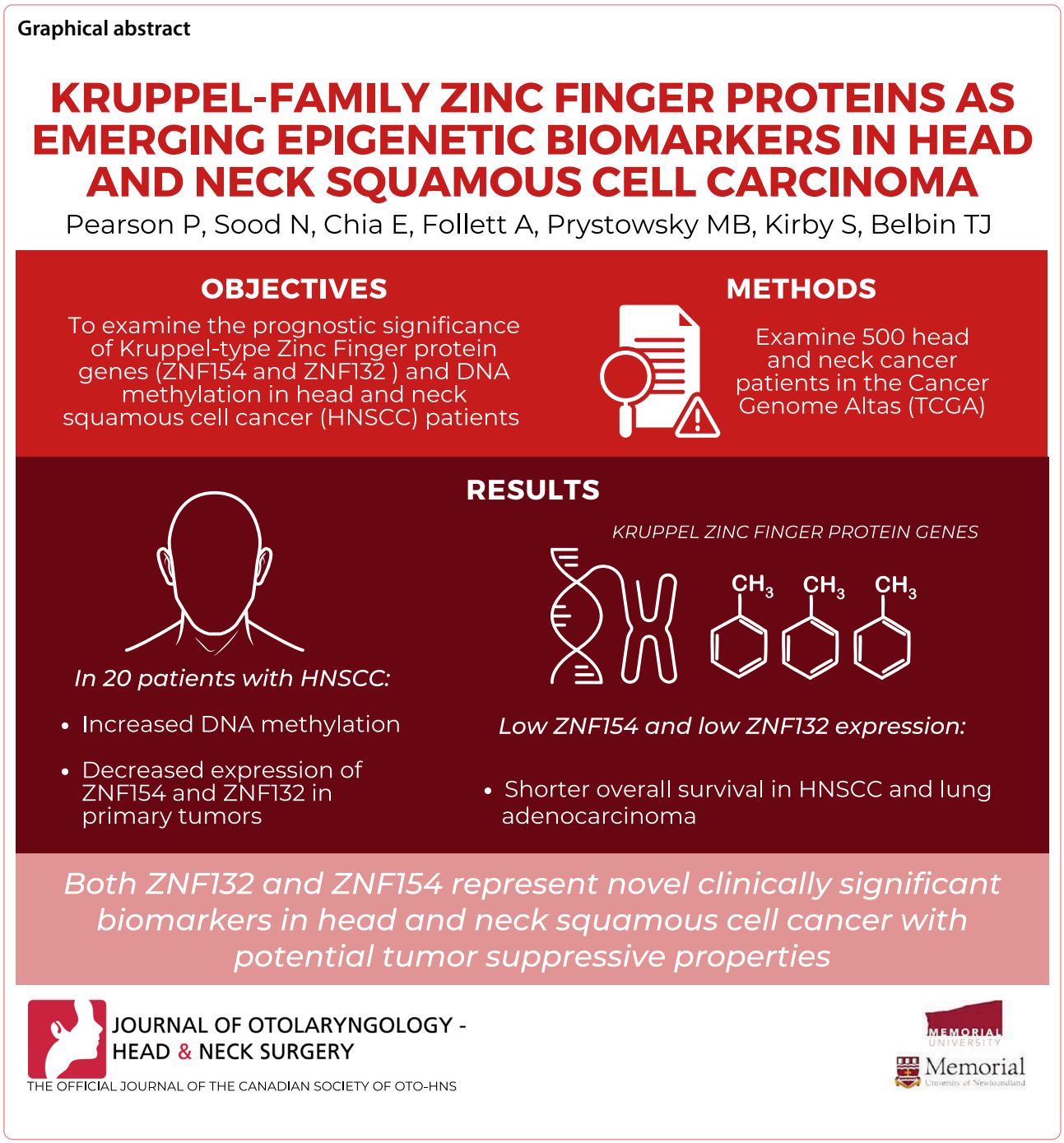

Introduction

Head and neck squamous cell carcinomas (HNSCCs) rank among the 10 most common malignancies in men and women worldwide. All have in common an etiological association with tobacco and/or alcohol exposure [1]. Overall, 5-year survival rates are approximately 50%, but there is substantial variability in response to treatment and long-term prognosis that cannot be predicted based on standard histopathology. That 5-year survival rate has improved only marginally over the past several decades. Although treatment paradigms have evolved significantly over time, there has been little change in 5-year survival since the 1970's. Conventional treatment will usually employ surgery and adjuvant radiation therapy, with or without chemotherapy depending upon pathologic results. Any of these costly therapies can, and do,

produce significant morbidities affecting speech, swallowing, and overall quality of life. Despite these interventions, recurrence of the disease is observed in about 50% of patients with high rates of associated mortality.

The identification of genes specifically affected by DNA methylation represent a way forward to the identification of genes with relevance as potential clinical biomarkers. In HNSCC, promoter methylation of tumour suppressor genes appears to be a common mechanism of transcriptional silencing. Numerous studies have identified promoter methylation of CDKN2A (p16), DAP kinase (DAPK), and DNA repair genes MGMT and MLH1 [2, 3]. Based on these and other studies, the identification of epigenetically silenced genes has become an important tool for identifying potential new tumour suppressors and understanding their mechanisms of action.

With the potential for novel gene discovery in mind, our group previously completed a genome-wide scan of aberrant DNA methylation in DNA samples from 118 HNSCCs [4]. We hoped to identify novel genes affected by aberrant DNA methylation that may play a role in head and neck tumourigenesis but have not been previously identified in this disease. From these studies and others, we identified a cluster of novel Krüppel-type zinc finger protein (ZNF) genes located on chromosome 19q13 that are aberrantly hypermethylated with high frequency in all anatomic sub-sites of HNSCC as well as other epithelial tumours [4, 5]. These genes also showed a significant reduction in gene expression in the primary tumour compared to adjacent mucosa. Two interesting examples of epigenetic silencing in primary HNSCC tumours were the Kruppel family zinc finger proteins ZNF132 and ZNF154 which showed both elevated DNA hypermethylation as well as reduced gene expression with high frequency in HNSCC tumours compared to matching adjacent mucosa from the same patient [5].

Here, we examine the expression of these genes in independent patient cohorts of the Cancer Genome Atlas (TCGA). We also describe our attempts to re-express these proteins in HEK293 cells, as well as an HNSCC cell line (UM-SCC-1). Our results shed some light on possible downstream targets of ZNF154 expression, as well as on additional mechanisms of silencing of these proteins by the chromatin regulator TRIM28 in this disease.

Materials and methods

Analysis of global gene expression and DNA methylation data from the Cancer Genome Atlas (TCGA)

Global gene expression, DNA methylation, clinical characteristics, and overall survival data, current as of December 2020, for 530 primary HNSCC patients was downloaded from TCGA database [6]. Overall survival was defined as the time between the date of surgery, and the date of death or the last follow-up date. In addition, within the TCGA dataset, gene expression and methylation data for primary tumour and adjacent non-tumor tissue samples were available for 50 primary HNSCC patients. The HNSCC tumours were categorized based on site into three categories—oral cavity (alveolar ridge, buccal mucosa, floor of mouth, hard palate, and oral tongue); oropharynx (base of tongue, uvula, soft palate, and tonsil); and larynx (hypopharynx, and larynx). Tobacco smoking status was classified as 'Ever smoker' or 'Lifelong non-smoker'. In addition to HNSCC, gene expression data was also downloaded for 492 primary lung adenocarcinoma (LUAD) patients from the TCGA.

Data is presented as Mean ± SD, unless otherwise stated. Analyses were conducted using R3.2.1. GraphPad Prism5 (GraphPad, San Diego, CA, USA) and R scripts and Microsoft Excel were used to construct figures. Measurements of gene expression and DNA methylation profiles were represented as continuous variables, whereas clinical data are represented as categorical variables. Comparisons between HNSCC based on primary tumour site were performed using one-way analysis of variance (ANOVA) with post-hoc Bonferroni correction. Comparisons between HNSCC primary tumour and adjacent non-tumor tissue samples were performed using paired t-test, or the Wilcoxon signed-rank test, as appropriate. Overall survival curves for these patient cohorts were assessed using Kaplan–Meier analysis and the log-rank test to assess differences between curves. The association between ZNF154 or ZNF132 gene expression and clinical characteristics were analyzed using the Chi-square test. In all cases, a threshold p-value of $p < 0.05$ was accepted as statistically significant.

Growth of cell lines and lentiviral transduction of ZNF154 and ZNF132 expressing constructs

Head and neck squamous cell carcinoma (HNSCC) cell line UM-SCC-1 (Cat# SCC070, Millipore Sigma) was maintained at 37 °C, 5%CO_2. UM-SCC-1 cells were cultured in DMEM/F12 (Cat# SH30023FS, HyClone) supplemented with 10% fetal bovine serum (FBS) (Cat# 081150, Wisent) and non-essential amino acids (Cat# TMS-001-C, Millipore Sigma). Isolation of total RNA was carried out using the RNeasy total RNA kit (Cat# 74104, Qiagen).

Stable constitutive overexpression of ZNF154 and ZNF132 protein in UM-SCC-1 and HEK-293 cells was carried out by lentiviral transduction using the pLenti-C-Myc-DDK-P2A-Puro vector expressing either the tagged ZNF154 or ZNF132 fusion protein under the control of the CMV promoter (Origene Cat# RC219041L3, RC218278L3), followed by selection of transduced clones using 0.25–0.50 μg/mL of puromycin. Transduction

using the empty pLenti-C-Myc-DDK-P2A-Puro vector was used as a negative control for each cell type (Origene Cat# PS100092). Expression of ZNF proteins were confirmed at the RNA transcript level by Taqman real-time PCR using the protocol as described by the manufacturer (Thermo Fisher Scientific). Taqman probes for measurement of gene expression were as follows: ZNF154 (Hs06618628_s1) and ZNF132 (Hs01036387_m1). PCR amplification of integrated viral DNA was carried out using internal vector primers V2 (5′-AGAGCTCGTTTA GTGAA-3′) and LR50 (5′-CAGAGGTTGATTATCGAT AAG-3′). PCR reactions were carried out using the Phusion Green Hot Start II High Fidelity PCR master mix (Thermo Fisher, Cat#F-566S). PCR parameters included an initial denaturation (98 °C, 30 s), followed by 35 cycles of denaturation (98 °C, 10 s), annealing (56 °C, 30 s) and extension (72 °C, 2 min), with a final extension (72 °C, 10 min). PCR products were then resolved on a 0.8% agarose gel.

For measurements of cell growth, cells were plated and triplicate wells were harvested every 48 h. Cells counts were obtained using a haemocytometer and phase contrast microscope; cell viability was confirmed by Trypan Blue exclusion. All tumor cell numbers were expressed as mean ± SD. Differences between two independent groups were assessed by single factor AVOVA using Microsoft Excel 2013. A p-value of less than 0.05 was considered as the threshold for statistical significance.

Measurement of FLAG-tagged protein expression

Expression of ZNF154 and ZNF132 protein in lentiviral transductants was determined through quantification of Flag fusion-proteins by Western blot. Transduced cells plated in six well plates were washed with cold phosphate buffered saline and lysed with 200 µl RIPA buffer (50 mM Tris pH7.4, 137 mM NaCl, 2.7 mM KCl, 11.9 mM phosphates, 1% TritonX, 5 mM EDTA, 0.5% deoxycholic acid, 0.1% SDS, 50 mM β-glycerophosphate, 50 mM sodium fluoride, 1 mM PMSF, 2 mM sodium orthovanate, 10 µg/ml Aprotinin, 10 µg/ml Leupeptin and 10 µg/ml Pepstatin) and removed from the plate surface by cell scraper. Lysates were passed through a 25 gauge needle and sonicated three times for 30 s with 30 s incubation intervals on ice. Samples were then centrifuged at 11,000 × g for 15 min at 4 °C to remove cell debris. Protein concentrations were measured using the Pierce BCA protein assay kit (Cat# 2322S, Thermo Fisher Scientific) as per manufacturer's instructions. Equal amounts of total protein (60 µg) were loaded onto a 10% SDS-PAGE gel, and resolved proteins were transferred onto a nitrocellulose membrane (Cat# 1620115, BioRad). Membranes were probed using a Flag primary antibody (1:2000) (Cat# TA50011, Origene) and secondary antibody (goat anti-mouse HRP (1:5000) (Cat# 115-035-071, Jackson Immunoresearch). HRP signal was detected using Amersham ECL Select Western Blotting Detection Reagent (RPN2235) and imaged on a Biorad Chemidoc MP Imaging System. The membranes were reprobed for β-actin (1:2000) (Cat# MABT523, Millipore Sigma) in the presence of 0.05% sodium azide; secondary antibody was goat anti-rabbit HRP (1:10,000) (Cat# 65-6120, Invitrogen). HRP signal was detected using SuperSignal West Pico PLUS Chemiluminescent Substrate (Cat# 34579, Thermo Fisher Scientific) and imaged on a Biorad Chemidoc MP Imaging System. All images were analyzed using Bio-rad Laboratories Image Lab software (version 6.1).

Measurement of tumor cell migration

Cell migration was measured using the Radius 96-well cell migration assay (Cat# CBA-126, Cell Biolabs). Culture wells were pre-incubated with gel pre-treatment solution at room temperature for 20 min. Cells were harvested and incubated in assay wells at 37 °C, 5% CO_2 until gel free area reached 90% confluence. Cells were then starved with serum free media (1% FBS) for an additional 24 h, the gel was removed using gel removal solution. Cells were then washed three times with serum free media (1% FBS). Images of cell migration were captured at 0, 24 and 48 h post gel removal. Cell free area was measured using Adobe Photoshop (version 23.2.2.325).

Screening of ZNF154 targets using antibody arrays

Changes in response to ZNF154 expression in HEK-293 cells were screened using the Human XL Oncology antibody array according to the manufacturer's recommended protocol using 200 µg of total protein extract. An integrated density was measured using ImageJ image processing software, and signals were normalized to array reference spots on each array in the experiment. Results were presented as relative expression as compared to the parental HEK-293 cells.

Results

Epigenetic downregulation of ZNF154 and ZNF132 expression occurs with high frequency in HNSCC tumours

Our first objective was to validate the previous findings that ZNF154 and ZNF132 were epigenetically silenced in HNSCC tumors, and to test whether their expression might be prognostically relevant in this disease. From the original downloaded data for 530 HNSCC patients, we excluded 11 patients that did not have any clinical data available. We also excluded patients with primary tumours originating from the lip (n = 3), bringing our cohort to 516 HNSCC patients. The characteristics of our overall cohort of 516 HNSCC patients are presented in Table 1. Characteristics of the 50 HNSCC patients with

Table 1 HNSCC patient characteristics by tumor site

	Oral cavity N = 310		Oropharynx N = 82		Larynx N = 124	
	N	%	N	%	N	%
Gender						
Male	206	66.5	69	84.1	101	81.5
Female	104	33.5	13	15.9	23	18.5
Race						
White	266	85.8	76	92.7	99	79.8
Black or African American	20	6.5	6	7.3	19	15.3
Asian	10	3.2	0	0	1	0.8
American Indian or Alaska Native	1	0.3	0	0	1	0.8
Information not available	13	4.2	0	0	4	3.2
Ethnicity						
Hispanic/Latino	16	5.2	3	3.7	5	4
Non-Hispanic/Latino	269	86.8	76	92.7	109	87.9
Information not available	25	8.1	3	3.7	10	8.1
Smoking						
Ever smoker	215	69.4	56	68.3	113	91.1
Lifelong non-smoker	86	27.7	25	30.5	8	6.5
Information not available	9	2.9	1	1.2	3	2.4
HPV status						
HPV +	31	10	56	68.3	11	8.9
HPV −	278	89.7	26	31.7	112	90.3
Indeterminate	1	0.3	0	0	1	0.8
Vital status						
Alive	197	63.5	69	84.1	82	66.1
Deceased	113	36.5	13	15.9	42	33.9
Nodal status						
Positive	147	47.4	34	41.5	58	46.8
Negative	119	38.4	16	19.5	42	33.9
Information not available	44	14.2	32	39	24	19.4
Pathologic tumor stage						
Stage I	19	6.1	4	4.9	2	1.6
Stage II	56	18.1	10	12.2	12	9.7
Stage III	52	16.8	9	11.0	14	11.3
Stage IV	160	51.6	28	34.1	79	63.7
Information not available	23	7.4	31	37.8	17	13.7

matched primary tumour and adjacent non-tumour tissue samples are presented in Table 2. Unfortunately, ZNF154 and ZNF132 expression data was not available for 30 non-tumour tissue samples, so those samples were excluded from our analysis. An overview of the remaining 20 patients are shown in Additional file 1: Table S3.

RNA sequencing data obtained from the TCGA confirmed that ZNF154 expression was significantly downregulated in HNSCC tumors compared with matching non-tumour tissue from the same patient (tumour 13.80 ± 17.46 versus non-tumour 25.16 ± 20.75, $p < 0.05$) (Fig. 1A). This reduced gene expression in primary tumors was also observed for ZNF132 (tumour 26.38 ± 122.76 versus non-tumour 88.89 ± 43.65, $p < 0.001$). We also obtained data on DNA methylation measurements using the Illumina HumanMethylation450k beadchip. Measurements of DNA methylation (M-values) of two CpG loci located within the ZNF154 promoter CpG island showed significantly increased DNA methylation in HNSCC tumours compared with matching non-tumour tissue from the same patient (cg08668790: 1.02 ± 0.92 (tumor) versus -2.22 ± 0.90 (non-tumour) $p < 0.001$, and cg21790626: 0.38 ± 0.83 (tumour) versus -4.18 ± 1.29 (non-tumour) $p < 0.001$) (Fig. 1B). In the case of ZNF132,

Table 2 Patient characteristics for 50 HNSCC patients with adjacent tumor and non-tumor samples

	Oral cavity N = 32	Oropharynx N = 2	Larynx N = 16
Gender			
Male	21	2	15
Female	11	0	1
Race			
White	28	2	12
Black or African American	2	0	4
Information not available	2	0	0
Ethnicity			
Hispanic/Latino	4	0	4
Non-Hispanic/Latino	25	2	12
Information not available	3	0	0
HPV status			
HPV +	6	0	2
HPV −	26	2	14
Vital status			
Alive	11	0	7
Deceased	21	2	9
Pathologic tumor stage			
Stage II	9	1	1
Stage III	10	1	6
Stage IV	13	0	9

methylation of two promoter CpG loci also showed significantly increased DNA methylation in HNSCC tumors compared with matching non-tumour tissue from the same patient (cg13877915: 0.80 ± 1.38 (tumour) versus -1.72 ± 1.20 (non-tumour), $p < 0.001$), and cg19776201: -0.93 ± 1.18 (tumour) versus -3.73 ± 0.67 (non-tumour), $p < 0.001$). Taken together, the results confirm our initial findings of epigenetic downregulation of both ZNF132 and ZNF154 in a separate cohort of HNSCC patients.

Low expression of ZNF154 and ZNF132 proteins are associated with a worse prognosis in both HNSCC and LUAD patient cohorts

Not all HNSCC tumours showed epigenetic silencing of ZNF154 or ZNF132 expression. We therefore tested whether ZNF154 or ZNF132 expression might have prognostic significance in this disease. Utilizing our TCGA cohort of 516 HNSCC patients, we excluded eight HNSCC patients for which gene expression data was not available. In the case of ZNF154, we identified a subgroup of HNSCC patients (n = 127, 25% of cohort) where ZNF154 expression in their primary tumour was not silenced, and was comparable to that observed in non-tumor adjacent tissue. Survival analysis stratifying patients based on this criterion demonstrated that patients whose primary tumours had higher ZNF154 expression showed a significantly better overall survival when compared to the remaining cohort (Fig. 2A, Log-rank, $p < 0.05$). Given the increased range of expression levels for ZNF132 in our patient cohort, we decided to stratify these patients to identify a subgroup with low ZNF132 gene expression (n = 173, 33% of cohort). Survival analysis demonstrated that those HNSCC patients with low ZNF132 expression had a significantly worse overall survival compared to the rest of the patient cohort (Fig. 2B). The patient characteristics of the ZNF154 and ZNF132 subgroupings are shown in Additional file 1: Tables S1 and S2. Expression of ZNF154 was significantly associated with primary tumour site (Chi-square test, $p < 0.05$), while expression of ZNF132 was significantly associated with primary tumour site (Chi-square test, $p < 0.001$), gender (Chi-square test, $p = 0.016$), HPV status (Chi-square test, $p = 0.005$), and pathologic T stage (Chi-square test, $p = 0.001$). There appeared to be a statistically significant association between low ZNF132 expression and HPV positivity. However, the nature of HPV detection in the cohort leaves some uncertainty as to whether this was accompanied by active expression of E6 and E7 oncoproteins. In order to assess the influence of HPV-positivity as a confounding variable, we also removed the HPV DNA positive cases from the cohort and re-assessed the survival analysis using only HPV negative cases. The significant association between high ZNF154 expression and improved overall survival remained; interestingly, the difference in overall survival between ZNF132 low expressors versus the remaining cohort was no longer significant (Additional file 2: Fig. S1). This implies that in the case of ZNF132, HPV-positivity may be a confounding variable in the association between patient survival and ZNF132 expression. The association of high ZNF154 expression with improved overall survival was also validated in a cohort of 53 laryngeal squamous cell carcinoma patients undergoing treatment with curative intent as part of the earlier Albert Einstein College of Medicine Head and Neck Cancer cohort (Log-rank, $p < 0.05$) (Additional file 2: Fig. S2). Unfortunately, we were unable to validate the association of overall survival to ZNF132 expression in this cohort. This may have been due to the much smaller size of this patient cohort when compared to the TCGA.

The prognostic value of ZNF154 and ZNF132 expression was similarly observed in patients from the lung adenocarcinoma (LUAD) TCGA patient cohort. Using the same stratification criteria described above but applied to a cohort of 492 LUAD patients, we found that patients whose primary tumours expressed higher ZNF154 levels (n = 123, 25% of cohort) also had significantly better overall survival compared to the

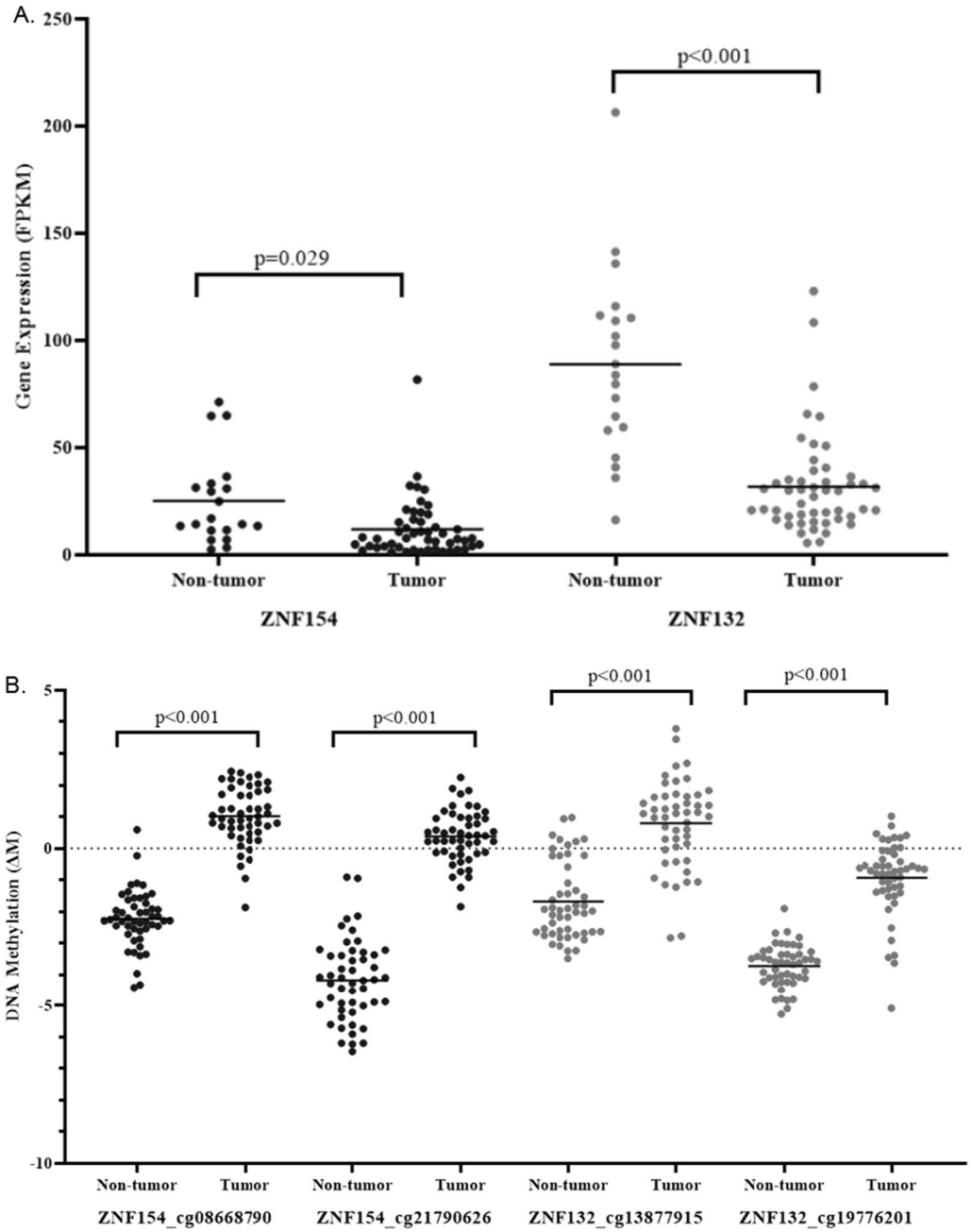

Fig. 1 **A** Gene expression and **B** DNA methylation analysis of ZNF154 (black) and ZNF132 (grey) in HNSCC tumor and adjacent non-tumor tissue samples. Specific CpG loci corresponding to each ZNF gene are shown on the x-axis label

remaining patient cohort (Fig. 2C, Log-rank, $p < 0.05$). And in the case of ZNF132, patients whose primary tumours expressed low levels of ZNF132 (n = 162, 33%) showed a significantly decreased overall survival when compared to the remaining cohort (Fig. 2D, Log-rank, $p < 0.05$). These observations were consistent with those of the HNSCC patient cohort, and support a prognostic role for ZNF154 and ZNF132 expression as a possible prognostic biomarker in both lung and upper aerodigestive malignancies.

Overexpression of ZNF154 and ZNF132 proteins in HEK-293 and head and neck squamous cell carcinoma cell line UM-SCC-1

To investigate the possible tumour suppressive properties of ZNF154 and ZNF132 proteins in head and neck

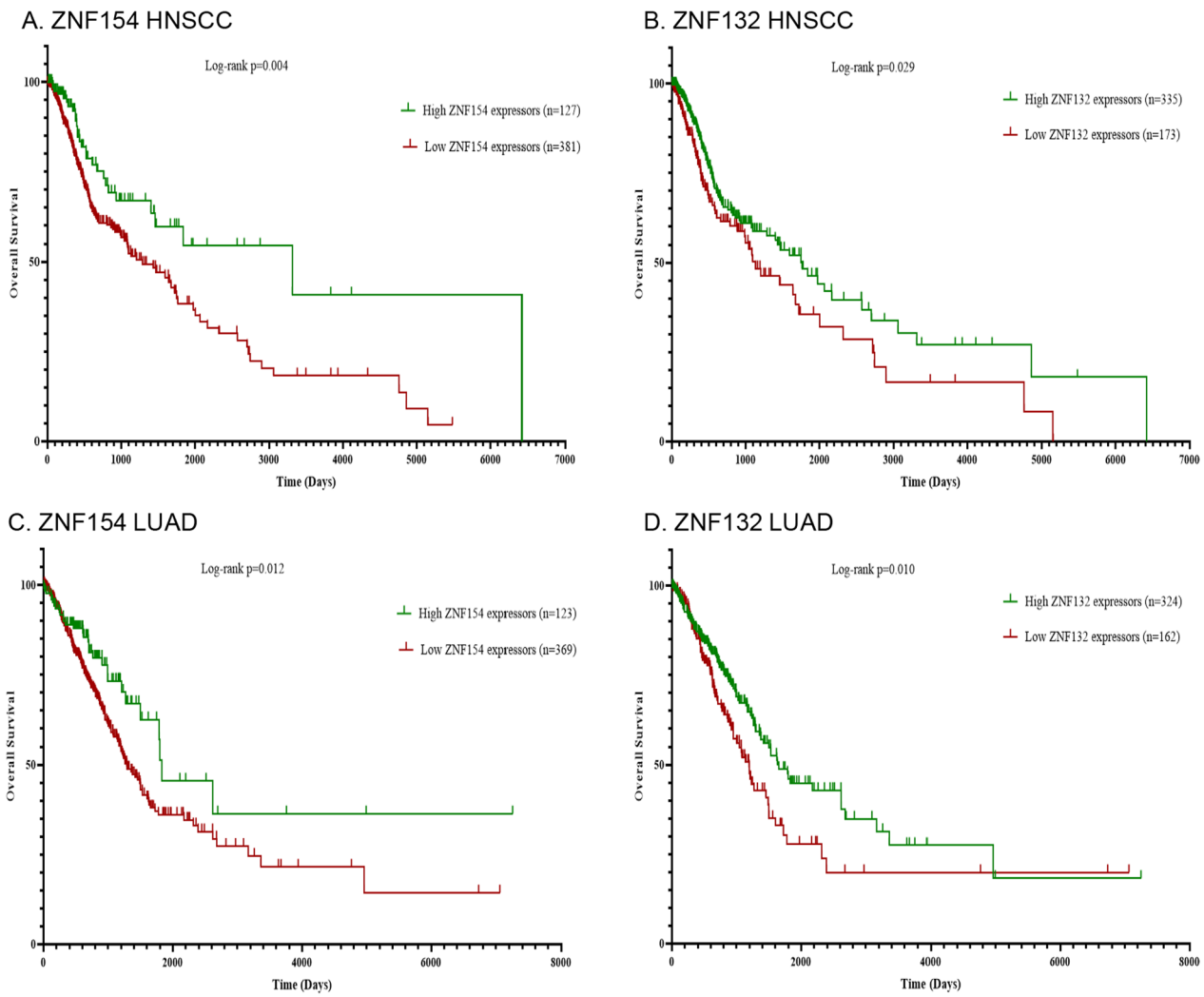

Fig. 2 Kaplan–Meier Plots of overall survival (OS) for **A** HNSCC patients stratified by ZNF154 expression, **B** HNSCC patients stratified by ZNF132 expression, **C** LUAD patients stratified by ZNF154 expression, **D** LUAD patients stratified by ZNF132 expression. The red lines indicate low expressors; the green lines indicate high expressors. Difference in survival between patient groups were assessed by Log-rank statistic

cancer, we attempted to overexpress these proteins in a head and neck squamous cell carcinoma cell line (UM-SCC-1) by lentiviral transduction of a C-terminal Flag-tagged fusion protein construct under the control of a CMV promoter. As a control to confirm functionality of the vector constructs for stable overexpression, we also overexpressed both ZNF fusion proteins using the same lentiviral constructs in the human embryonic kidney 293 cell line (HEK-293).

We initially confirmed overexpression of the Flag-tagged ZNF154 and ZNF132 fusion-constructs by both real-time quantitative PCR (qPCR) and at the protein level by Western blot. In HEK-293 cells, quantitation of RNA transcripts by Taqman quantitative real-time PCR (qPCR) revealed significant increase in transcript abundance for ZNF154 and ZNF132 in the transduced HEK-293 clones when compared to the empty vector control (Fig. 3A). Similarly, significant expression of both ZNF transcripts were observed in UM-SCC-1 cancer cells that were both undetectable in empty vector UM-SCC-1 control cells. At the protein level, Western blot analysis demonstrated a similar over-expression of both Flag-tagged ZNF proteins in HEK-293 cells, with molecular weights of 50 kDa (ZNF154) and 82 kDa (ZNF132) (Fig. 3B). These proteins were absent in the empty vector control cells. While overexpression of Flag-tagged fusion proteins were observed in UM-SCC-1 cancer cells, both proteins were smaller in size then the expected molecular weights, with molecular weights of approximately 34 kDa in both transductants.

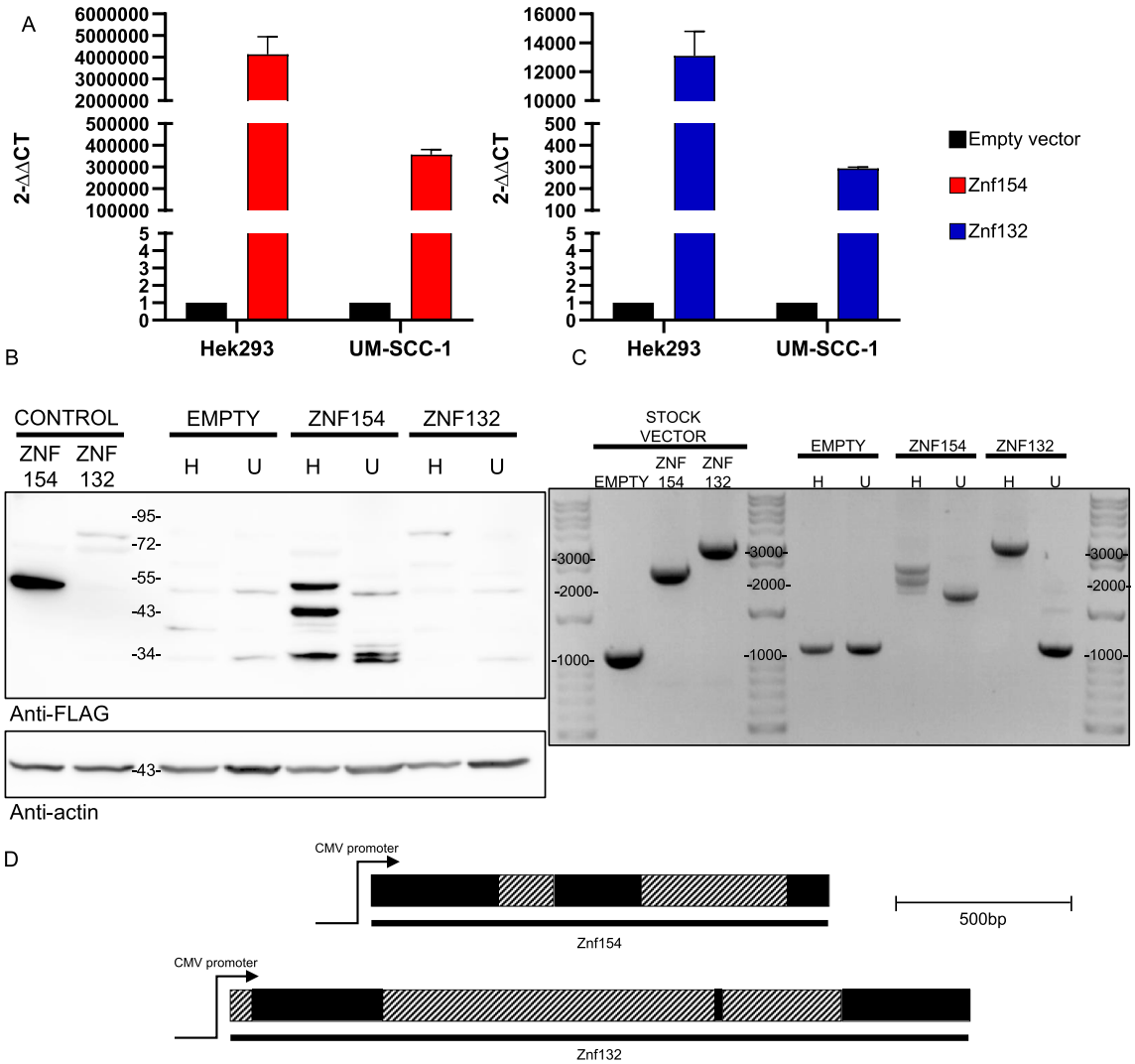

Fig. 3 **A** Assessment of ZNF154 and ZNF132 transcripts in HEK-293 and UM-SCC-1 transductant cells and empty vector controls by real-time PCR. RNA transcript measurements are expressed as ΔΔCt values using GAPDH as a measurement control. **B** Western blot assessment of the same lentiviral transductants overexpressing ZNF154 or ZNF132 as probed using a Flag antibody. Also shown are empty vector controls for HEK-293 (H) and UM-SCC-1 (U). β-actin is used as a loading control. **C** PCR amplification of integrated vector DNA constructs for ZNF154-Flag, ZNF132-Flag, and empty vector control in both HEK-293 (H) and UM-SCC-1 cells (U). Stock vector DNA and a water blank were used as PCR positive and negative controls, respectively. **D** Schematic diagram showing locations of deleted internal coding sequences for each ZNF gene in UM-SCC-1 transductants as determined by sequencing of genomic DNA PCR products

In order to establish the basis for the reduced protein sizes at the gene level, we checked whether complete ZNF gene sequences were successfully integrated into the host genomic DNA. PCR amplification using primers internal to the vector sequence at each end of the ZNF gene insert should produce PCR products of 2340 bp (ZNF154), 3147 bp (ZNF132) and 1067 bp (empty vector control). PCR amplification from host cell genomic DNA showed that all lentiviral transduction of HEK-293 cells resulted in stably integrated DNA sequences corresponding to the expected sizes of 2340 bp (ZNF154), 3147 bp (ZNF132) and 1067 bp (empty vector control) (Fig. 3C). In contrast, transduction of the same constructs into UM-SCC-1 cells resulted in stably integrated DNA sequences of a length that was shorter than expected. All empty vector controls produced PCR products of the expected size (1067 bp). This same trend was observed in all isolated clones. Sequencing of these truncated PCR products from UM-SCC-1 cells for each construct revealed a deletion of internal coding sequences for both ZNF genes (Fig. 3D). From this, we suspect that other regulatory mechanisms, in addition to aberrant promoter

DNA hypermethylation, may play a role in the transcriptional silencing of these genes in oral cancer cells that are not a factor in HEK-293 cells.

Overexpression of partial ZNF154 construct affects HNSCC tumor cell phenotypes

In spite of the fact that the HNSCC cell line produced truncated ZNF154 and ZNF132 proteins, we wanted to examine what effects these partial proteins might have on tumor cell phenotype. We also wanted to test any effects of the full-length ZNF proteins on HEK-293 growth. In the case of HEK-293 cells, we measured growth of cells overexpressing either the ZNF154 or ZNF132 protein and compared each to cells containing the empty vector construct. In both cases, overexpression of either the ZNF154 protein or ZNF132 protein resulted in a slight increase in doubling time (23.5 and 23.8 h, respectively) when compared to the empty vector control (19.9 h) (Fig. 4A). For comparison, we also measured growth of UM-SCC-1 cells expressing the truncated ZNF154 and ZNF132 proteins (Fig. 4B). In this case, expression of the truncated ZNF154 construct resulted in a significant increase in UM-SCC-1 doubling time (40.4 h) when compared to the empty vector control (33.4 h). This reduction was not observed for cells overexpressing the ZNF132 partial construct (33.1 h). From these results, we concluded that even when expressed as a partial sequence, ZNF154 peptide reduced doubling time for UM-SCC-1 cancer cells while neither full length ZNF protein had significant effect on growth of HEK-293 cells.

In addition to growth, migration of UM-SCC-1 cancer cells was measured using the Radius 96-well cell migration assay. As with the growth assay, overexpression of the truncated ZNF154 protein resulted in a significant decrease in tumor cell migration when compared to the empty vector control cells (Fig. 5A, B). However, this decrease in cell migration was not observed in UM-SCC-1 cells overexpressing the truncated ZNF132 protein. From these and the previous results, it appeared that even the truncated version of ZNF154 retained some biological activity resulting in the reduction in both growth and tumor cell migration. However, the truncated version of ZNF132 appeared to have neither a growth of migratory effect in vitro, a result inconsistent with the survival associations in Fig. 2.

We wanted to test whether we could identify potential downstream targets of ZNF154 in its full-length form. To do this, we compared total protein extracts from parental HEK-293 cells to those overexpressing the full-length ZNF154 protein using the Proteome Profiler Human XL Oncology Antibody Array. This array compares relative expression levels of 84 human cancer-related proteins in a single experiment (Fig. 6). Comparisons of protein extracts revealed a significant reduction in both the levels of p53 and Forkhead box protein FOXO1 in cells overexpressing ZNF154 protein compared to the parent HEK-293 cells. However, the relevance of these changes to head and neck cancer cells is still not clear.

Discussion

Inactivation of tumour suppressor genes due to promoter DNA hypermethylation is thought to be one of the most common transcriptional gene silencing mechanisms in human malignancies. In this current study, we found in genomic datasets obtained from the TCGA that both ZNF154 and ZNF132 were silenced and hypermethylated

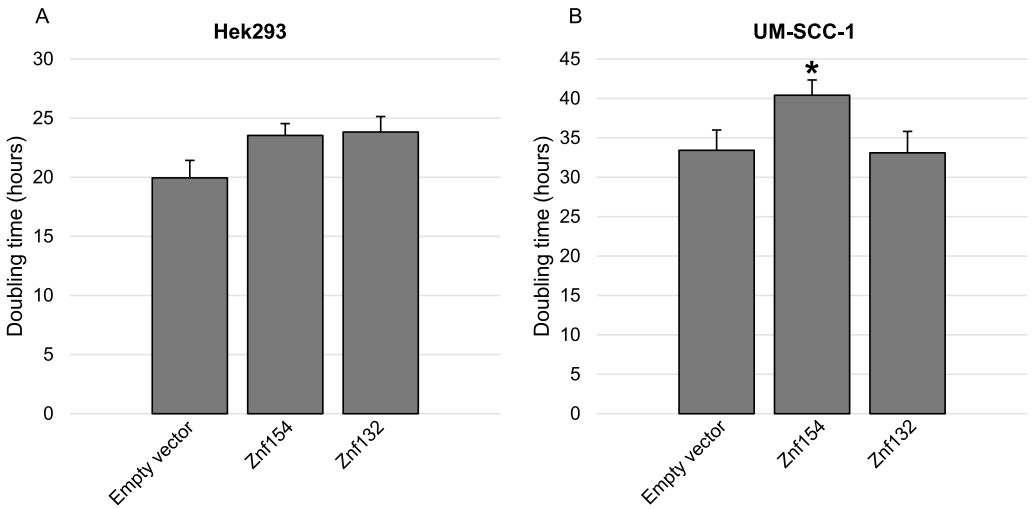

Fig. 4 **A** Comparison of doubling times for HEK-293 transductants expressing full length ZNF154, ZNF132 or the empty vector control. **B** Comparison of doubling times for UM-SCC-1 transductants expressing partial length ZNF154, ZNF132 or the empty vector control

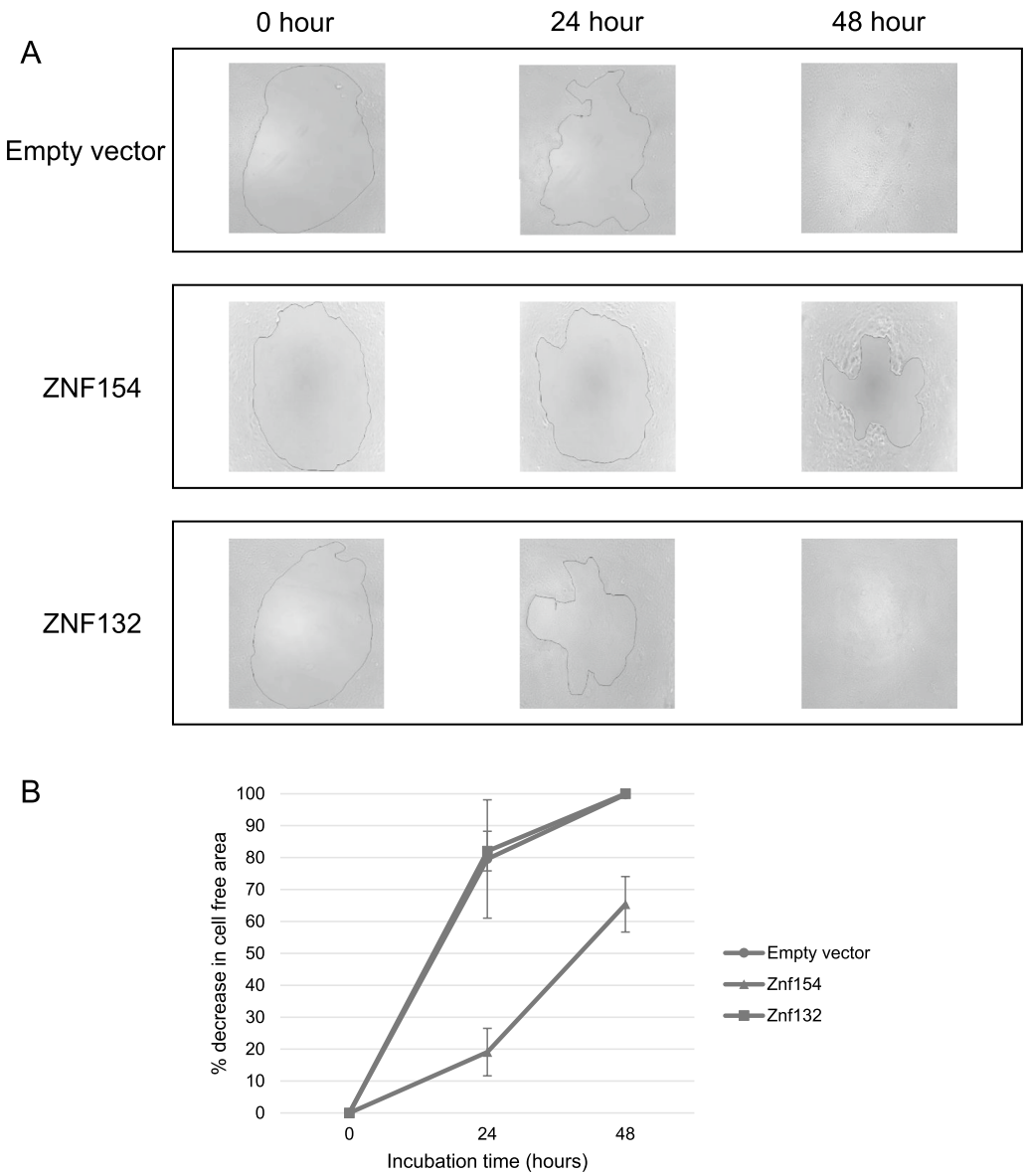

Fig. 5 **A** Representative images of wound healing assay comparing cell mobility of HNSCC cancer UM-SCC-1 cells containing empty vector, ZNF154 construct, or ZNF132 construct. Images were taken at 0, 24 and 48 h. **B** Mobility was quantified as a reduction in the percentage of cell free area after 24 and 48 h

in a significant number of HNSCC primary tumour samples when compared to adjacent non-tumor samples from the same patient. Our research group previously identified six novel KRAB-ZNF genes (ZNF154, ZNF132, ZNF542, ZNF545/ZFP82 and ZNF781) that were hypermethylated with high frequency in HNSCC tissue samples [4]. ZNF154 and ZNF132 were also observed to be hypermethylated in a previous dataset of oral cavity SCC cases [7].

The epigenetic silencing of ZNF154 and ZNF132 were not confined to head and neck cancers. In 2013, Sánchez-Vega and coworkers found ZNF154 hypermethylation and downregulation to be one of the most common epigenetic changes in ovarian and endometrial cancers, and subsequently, across 15 distinct solid cancer types from the TCGA [8]. The importance of ZNF154 in cancer is further highlighted by recurring reports of its hypermethylation in several other malignancies, including bladder [9], breast [10], lung [11], ovarian [12], renal [13] and prostate [14]. Hypermethylation of ZNF154 has also been identified in hepatocellular carcinoma, and as part of a panel of early detection biomarkers in DNA

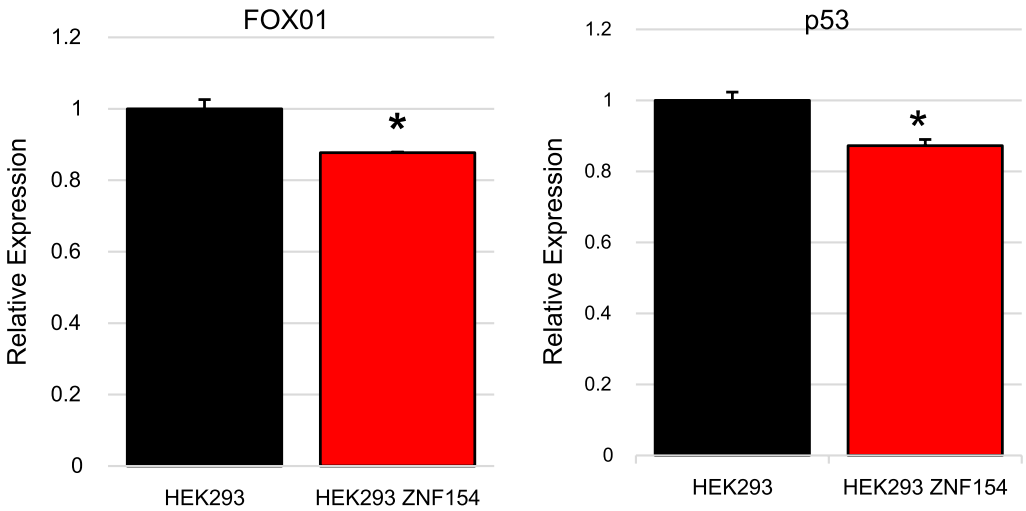

Fig. 6 Measurement of FOXO1 and P53 protein as determined by the antibody array in HEK293 cells overexpressing ZNF154 compared to the HEK293 empty vector control

from voided urine of bladder cancer patients [9, 15]. ZNF154 methylation has most recently been documented in plasma samples from early-stage cancer patients, suggesting it as a promising target in liquid biopsy [16]. That same study demonstrated that ZNF154 circulating-free DNA (cfDNA) methylation discriminated cases from healthy donor plasma samples and outperformed KRAS mutation frequency as a biomarker in pancreatic cancer. In the case of ZNF132, it was observed to be downregulated in prostate cancer [17], breast cancer [18] and esophageal squamous cell carcinomas [19].

Epigenetic regulation of ZNF154 and ZNF132 may also have prognostic relevance for both HNSCC and LUAD patients. Consistent with their roles as tumor suppressors, we found that low expression of either ZNF154 or ZNF132 were significantly associated with a worse overall survival in 508 HNSCC patients. Those associations were also observed in 492 LUAD patients with gene expression data from the TCGA database. Consistent with our observations, Kaplan–Meier analysis also showed that hypermethylation of the ZNF154 promoter was associated with significantly poorer disease-free survival ($p=0.032$) and distant metastasis-free survival ($p=0.040$) among patients with locoregionally advanced nasopharyngeal carcinoma (NPC) [20]. Kaplan–Meier analysis has also shown that ZNF154 methylation level was associated with biochemical recurrence (BCR) ($p=0.005$) in prostate cancer, and that ZNF154 could be an independent factor for BCR prediction by using univariate and multivariate Cox regression analysis ($p=0.035$, HR = 8.218) [21]. This association was observed despite the fact that these cancers represent differing cancer biologies. Curiously, an opposite association was observed in pancreatic cancer patients who had undergone a pancreatic resection, where a silenced ZNF154 gene was actually associated with a better patient survival [22]. The reason for this is unclear, but the investigators suggest that silencing of ZNF154 might foster the growth of more stable, less aggressive tumor clones [22]. In the case of ZNF132, low protein expression was associated with a higher Gleason score and advanced T stage in prostate cancer patients, indicating more a aggressive and progressive disease phenotype [17].

While we were able to express full-length ZNF154 and ZNF132 constructs in HEK-293 cells without issue, attempts to express these same constructs in head and neck UM-SCC-1 cancer cells resulted in truncated proteins lacking partial internal amino acid sequences. In another HNSCC cell line (SCC-25), similarly transduced cells showed no expression of either ZNF154 or ZNF132 despite their selection for puromycin-resistance (data not shown). One explanation for this is the observation that global chromatin regulator TRIM28 can suppress transcription of some ZNF genes via binding to the internal coding sequence of the gene, in a mechanism that itself utilizes other ZNF proteins [23]. The absence of internal sequences within the ZNF154 and ZNF132 constructs of UM-SCC-1 supports this as a possible mechanism of silencing that is in addition to promoter DNA hypermethylation. However, this mechanism is poorly understood, and we have not yet identified a ZNF protein that may involved in this specific silencing mechanism. Moreover, it is unclear why this mechanism differs between HEK-293 and UM-SCC-1 cells. Experiments to knockdown TRIM28 expression by siRNA, or inhibit DNA methylation using 5-aza-cytidine, seemed to have little

effect on ZNF154 or ZNF132 re-expression in parental UM-SCC-1 cells (data not shown).

In HEK-293 cells, overexpression of ZNF154 resulted in significant downregulation of tumor protein p53 and Forkhead box protein FOXO1. FOXO1 has previously been identified as a possible tumour suppressor in prostate cancer cells and glioma cells by upregulating proapoptotic factors [24]. In keratinocytes, nuclear localization of FOXO1 has been shown to enhance the wound healing process by encouraging migration of keratinocytes [25]. Other studies with hypopharynx cancers suggest that ZNF154 has tumour-suppressive action by inhibiting the Wnt/β-catenin signalling pathway activation and suppressing epithelial-mesenchymal transition [20]. And most recently, expression of ZNF154 in MGC-803 gastric cancer cells reduced cell proliferation, viability, migration and invasion, and enhanced cell apoptosis and arrested cell cycle in G2 phase [26]. This overexpression of ZNF154 was associated with an increase in the expression of B-cell lymphoma-2 (Bcl-2), matrix metalloproteinase 1 (MMP-1), hepatocyte growth factor (HGF), vascular endothelial growth factor-A/C (VEGF-A/C). Little is known about potential targets of ZNF132. However, in analysis of breast cancer datasets, ZNF132 has been identified by computational approaches as a potential transcriptional master regulator of several transcriptional processes that are well-known hallmarks of cancer [27].

The study as described suffers from several limitations. First, it was not possible to express a full length ZNF154 or ZNF132 construct within oral cancer UM-SCC-1 cells in order to identify possible downstream targets of these proteins in the cancer cell environment. This is despite the fact that the expression system is fully functional within HEK-293 cells. Moreover, our observations are derived from a single HNSCC cell line. UM-SCC-1 cells were the only cell line identified to date that would produce ZNF154 or ZNF132, albeit in a truncated form. We hypothesize that the global chromatin regulator TRIM28 can suppress transcription of ZNF154 and ZNF132 via binding to the internal coding sequence of each gene. Expression was not possible in SCC-25 or SCC-15 oral cancer cells despite several attempts (data not shown). We continue to screen HNSCC cell lines to identify those that might express these as full length proteins. We have expressed another KRAB-ZNF protein (ZNF671) in UM-SCC-1 cells, but also found it was not possible to express ZNF671 protein within other oral cancer cell lines such as SCC-25 and SCC-15 (data not shown). The exact mechanisms responsible for this selective expression is unknown but likely will have significance in head and neck and other cancers. It is also not known what effect these proteins would have on tumor cell phenotype in vivo. However, a recent support supporting a tumour suppressive role for ZNF154 included data showing that targeted expression of ZNF154 inhibited expression of esophageal squamous cell carcinoma cells in vivo [28]. Our future studies include plans to evaluate in vivo effects of ZNF overexpression in a floor of mouth mouse model.

In conclusion, aberrant hypermethylation of ZNF154 and ZNF132 mediated their silencing in primary HNSCC tumor tissue samples. Low ZNF154 and low ZNF132 expression were associated with shorter overall survival in both HNSCC and LUAD patients. Future studies are needed to address the underlying molecular mechanisms regulating ZNF154 and ZNF132 expression in HNSCC and other malignancies, their potential as diagnostic and prognostic markers, and the downstream genes that are possible targets for their suppression.

Abbreviations

ANOVA	Analysis of variance
BCR	Biochemical recurrence
Bcl-2	B-cell lymphoma-2
cfDNA	Circulating free DNA
CMV	Cytomegalovirus
DAPK	DAP kinase
DNA	Deoxyribonucleic acid
FBS	Fetal bovine serum
HEK-293	Human embryonic kidney-293
HGF	Hepatocyte growth factor
HNSCC	Head and neck squamous cell carcinoma
HPV	Human papillomavirus
HRP	Horse radish peroxidase
KCl	Potassium chloride
KRAB-ZNF	Krüppel-type zinc finger protein
LUAD	Lung adenocarcinoma
MMP	Matrix metalloproteinase
NaCl	Sodium chloride
PCR	Polymerase chain reaction
RNA	Ribonucleic acid
SD	Standard deviation
TCGA	The Cancer Genome Atlas

Supplementary Information

The online version contains supplementary material available at https://doi.org/10.1186/s40463-023-00640-x.

Additional file 1: Table S1. Clinical association between ZNF154 expression and clinicopathological variables. **Table S2.** Clinical association between ZNF132 expression and clinicopathological variables. **Table S3.** Patient characteristics for 20 HNSCC patients with adjacent tumor and non-tumor samples. **Table S4.** Summary of 53 larynx squamous cell carcinoma cases obtained from the Albert Einstein College of Medicine Head and Neck Cancer Database.

Additional file 2: Figure S1. Kaplan–Meier Plots of overall survivalfor **A** HPV-negative HNSCC patients stratified by ZNF154 expression, **B** HPV-negative HNSCC patients stratified by ZNF132 expression. The red lines indicate low expressors; the green lines indicate high expressors. Difference in survival between patient groups were assessed by Log-rank statistic. **Figure S2.** Kaplan–Meier Plots of overall survivalfor 53 larynx cancer cases derived from the Albert Einstein College of Medicine Head and Neck Cancer database. Stratified by ZNF154 expression, HPV-negative HNSCC patients stratified by ZNF132 expression. The red line indicate low ZNF154

expressors; the teal line indicate high ZNF154 expressors. Difference in survival between patient groups was assessed by Log-rank statistic.

Acknowledgements
Not applicable.

Author contributions
KS, EC and AF designed and carried out experiments to overexpress ZNF proteins in UM-SCC-1 and HEK-293 cells. PP and NS analyzed and interpreted patient data regarding association between ZNF protein methylation and expression, and patient clinical parameters. PP and KS carried out phenotypic experiments on HEK-293 and UM-SCC-1 cells. PP carried out antibody arrays to identify potential targets of ZNF154. PP, KLS, and TJB contributed to the writing of the manuscript. MBP, SK and TJB contributed insights into the clinical associations associated with ZNF protein expression, and edited the final version of the manuscript for publication. All authors read and approved the final manuscript.

Funding
The design of the study and collection, analysis, and interpretation of data and writing of the manuscript was supported by funds from a Canadian Institutes of Health Research (CIHR): GlaxoSmithKline Partnered Operating Grant, a grant from InnovateNL, and funds from Memorial University of Newfoundland and Labrador's Faculty of Medicine. Patrick Pearson was a trainee in the Cancer Research Training Program of the Beatrice Hunter Cancer Research Institute (BHCRI), with funds provided by the Canadian Cancer Society's JD Irving, Limited—Excellence in Cancer Research Fund.

Availability of data and materials
The datasets analysed during the current study are available in the TCGA repository, (https://www.cbioportal.org/study/summary?id=hnsc_tcga) [6].

Declarations

Ethics approval and consent to participate
The results shown here are in whole or part based upon data generated by the TCGA Research Network: https://www.cancer.gov/tcga.

Consent for publication
Not applicable.

Competing interests
The authors declare that they have no competing interests.

Author details
[1]Division of Biomedical Sciences, Faculty of Medicine, Memorial University of Newfoundland, St. John's, NL A1B 3V6, Canada. [2]Discipline of Oncology, Faculty of Medicine, Memorial University of Newfoundland, St. John's, NL A1B 3V6, Canada. [3]Discipline of Laboratory Medicine, Faculty of Medicine, Memorial University of Newfoundland, St. John's, NL A1B 3V6, Canada. [4]Department of Pathology, Albert Einstein College of Medicine, 1300 Morris Park Avenue, Bronx, NY 10461, USA.

Received: 23 September 2022 Accepted: 4 April 2023
Published online: 30 May 2023

References

1. Maier H, Dietz A, Gewelke U, Heller WD, Weidauer H. Tobacco and alcohol and the risk of head and neck cancer. Clin Investig. 1992;70(3–4):320–7.
2. Maruya S, Issa JPJ, Weber RS, Rosenthal DI, Haviland JC, Lotan R, et al. Differential methylation status of tumor-associated genes in head and neck squamous carcinoma: incidence and potential implications. Clin Cancer Res. 2004;10(11):3825–30.
3. Rosas SL, Koch W, da Costa Carvalho MG, Wu L, Califano J, Westra W, et al. Promoter hypermethylation patterns of p16, O6-methylguanine-DNA-methyltransferase, and death-associated protein kinase in tumors and saliva of head and neck cancer patients. Cancer Res. 2001;61(3):939–42.
4. Lleras RA, Smith RV, Adrien LR, Schlecht NF, Burk RD, Harris TM, et al. Unique DNA methylation loci distinguish anatomic site and HPV status in head and neck squamous cell carcinoma. Clin Cancer Res. 2013;19(19):5444–55.
5. Lleras RA, Adrien LR, Smith RV, Brown B, Jivraj N, Keller C, et al. Hypermethylation of a cluster of Krüppel-type zinc finger protein genes on chromosome 19q13 in oropharyngeal squamous cell carcinoma. Am J Pathol. 2011;178(5):1965–74.
6. Network CGA. Comprehensive genomic characterization of head and neck squamous cell carcinomas. Nature. 2015;517(7536):576–82.
7. Guerrero-Preston R, Soudry E, Acero J, Orera M, Moreno-López L, Macía-Colón G, et al. NID2 and HOXA9 promoter hypermethylation as biomarkers for prevention and early detection in oral cavity squamous cell carcinoma tissues and saliva. Cancer Prev Res (Phila). 2011;4(7):1061–72.
8. Sánchez-Vega F, Gotea V, Petrykowska HM, Margolin G, Krivak TC, DeLoia JA, et al. Recurrent patterns of DNA methylation in the ZNF154, CASP8, and VHL promoters across a wide spectrum of human solid epithelial tumors and cancer cell lines. Epigenetics. 2013;8(12):1355–72.
9. Reinert T, Modin C, Castano FM, Lamy P, Wojdacz TK, Hansen LL, et al. Comprehensive genome methylation analysis in bladder cancer: identification and validation of novel methylated genes and application of these as urinary tumor markers. Clin Cancer Res. 2011;17(17):5582–92.
10. Hill VK, Ricketts C, Bieche I, Vacher S, Gentle D, Lewis C, et al. Genome-wide DNA methylation profiling of CpG islands in breast cancer identifies novel genes associated with tumorigenicity. Cancer Res. 2011;71(8):2988–99.
11. Cancer Genome Atlas Research Network. Comprehensive genomic characterization of squamous cell lung cancers. Nature. 2012;489(7417):519–25.
12. Okamoto T. Methylated-mediated repression of ZNF154 in ovarian cancer is associated with poor overall survival. In: Proceedings of the 103rd annual meeting of the American association for cancer research 2012 [Internet]. Available from: http://cancerres.aacrjournals.org/cgi/content/short/72/8_MeetingAbstracts/LB-87?rss=1.
13. Arai E, Chiku S, Mori T, Gotoh M, Nakagawa T, Fujimoto H, et al. Single-CpG-resolution methylome analysis identifies clinicopathologically aggressive CpG island methylator phenotype clear cell renal cell carcinomas. Carcinogenesis. 2012;33(8):1487–93.
14. Mahapatra S, Klee EW, Young CYF, Sun Z, Jimenez RE, Klee GG, et al. Global methylation profiling for risk prediction of prostate cancer. Clin Cancer Res. 2012;18(10):2882–95.
15. Yamada N, Yasui K, Dohi O, Gen Y, Tomie A, Kitaichi T, et al. Genome-wide DNA methylation analysis in hepatocellular carcinoma. Oncol Rep. 2016;35(4):2228–36.
16. Miller BF, Petrykowska HM, Elnitski L. Assessing ZNF154 methylation in patient plasma as a multicancer marker in liquid biopsies from colon, liver, ovarian and pancreatic cancer patients. Sci Rep. 2021;11(1):221.
17. Abildgaard MO, Borre M, Mortensen MM, Ulhøi BP, Tørring N, Wild P, et al. Downregulation of zinc finger protein 132 in prostate cancer is associated with aberrant promoter hypermethylation and poor prognosis. Int J Cancer. 2012;130(4):885–95.
18. Liu Z, Liu J, Liu R, Xue M, Zhang W, Zhao X, et al. Downregulated ZNF132 predicts unfavorable outcomes in breast cancer via Hypermethylation modification. BMC Cancer. 2021;21(1):1–12.
19. Jiang D, He Z, Wang C, Zhou Y, Li F, Pu W, et al. Epigenetic silencing of ZNF132 mediated by methylation-sensitive Sp1 binding promotes cancer progression in esophageal squamous cell carcinoma. Cell Death Dis [Internet]. 2018 Dec 18 [cited 2020 Sep 2];10(1). Available from: https://www.ncbi.nlm.nih.gov/pmc/articles/PMC6315024/.
20. Hu Y, Qi MF, Xu QL, Kong XY, Cai R, Chen QQ, et al. Candidate tumor suppressor ZNF154 suppresses invasion and metastasis in NPC by inhibiting the EMT via Wnt/β-catenin signalling. Oncotarget. 2017;8(49):85749–58.
21. Zhang W, Shu P, Wang S, Song J, Liu K, Wang C, et al. ZNF154 is a promising diagnosis biomarker and predicts biochemical recurrence in prostate cancer. Gene. 2018;675:136–43.
22. Wiesmueller F, Kopke J, Aust D, Roy J, Dahl A, Pilarsky C, et al. Silenced ZNF154 is associated with longer survival in resectable pancreatic cancer. Int J Mol Sci. 2019;20(21):E5437.

23. Tie CH, Fernandes L, Conde L, Robbez-Masson L, Sumner RP, Peacock T, et al. KAP1 regulates endogenous retroviruses in adult human cells and contributes to innate immune control. EMBO Rep. 2018;19(10): e45000.
24. Wang Y, Zhou Y, Graves DT. FOXO transcription factors: their clinical significance and regulation. Biomed Res Int. 2014;2014: 925350.
25. Xiao E, Graves DT. Impact of diabetes on the protective role of FOXO1 in wound healing. J Dent Res. 2015;94(8):1025–6.
26. He J, Huang J, Tang G, Wang P, He M, Wei S. Low expression of ZNF154 is related to poor prognosis in gastric cancer. Cancer Manag Res. 2022;14:659–72.
27. Tovar H, García-Herrera R, Espinal-Enríquez J, Hernández-Lemus E. Transcriptional master regulator analysis in breast cancer genetic networks. Comput Biol Chem. 2015;59 Pt B:67–77.
28. He W, Lin S, Guo Y, Wu Y, Zhang LL, Deng Q, et al. Targeted demethylation at ZNF154 promotor upregulates ZNF154 expression and inhibits the proliferation and migration of Esophageal Squamous Carcinoma cells. Oncogene. 2022;41(40):4537–46.

Publisher's Note